

DESIGN OF OPTIMAL VARIABLE STRUCTURE CONTROLLERS:
APPLICATIONS TO POWER SYSTEM DYNAMICS

By

NAJI A. AL-MUSABI

A Thesis Presented to the
DEANSHIP OF GRADUATE STUDIES

In Partial Fulfillment of the Requirements

for the degree

MASTER OF SCIENCE

IN

ELECTRICAL ENGINEERING

KING FAHD UNIVERSITY OF PETROLEUM AND MINERALS

Dhahran, Saudia Arabia

JUNE 2004

Dedication

For my family,
who offered me unconditional love
and
support throughout the course of this thesis

Acknowledgment

All praise and glory is to almighty Allah subhanho wa ta'la who gave me the courage and patience to carry out this work, and peace and blessings of Allah be upon his last prophet Mohammed.

Acknowledgement is due to King Fahd University of Petroleum and Minerals for supporting this research. I am grateful to all faculty of Electrical engineering department, some of them: Prof. Ibrahim El-amin (he was first to receive me and advice me on courses), Prof. Asrar Haq Sheikh (I took the first EE course with him), Prof. Adur-Rahim (Power dynamics course), Dr. Samir Al-Baiyat (for all his help and suggestion of this subject for thesis research), Dr. Sharif Iqbal Sheik (Microwave course), Prof. Yousef AbdulMagid (academic advisor). Furthermore, I would like to express my deep appreciation to Prof. Abdullah Al-Shehri who assisted me in applying for the M.Sc program at KFUPM.

Moreover, I would like to express my deep gratitude to my thesis advisor Dr. Zakariya Al-Hamouz and to my thesis co-advisor Dr. Hussain Al-Duwaish for their unconditional help, their encouragement, and their valuable suggestions during the preparation of my thesis. They were very kind and understanding. They were patient with me and didn't hesitate in helping me by all means. Their critical views helped me in forming a strong research perspective. Working with them was enjoyable. I would

also like thank my committee members Prof. Ibrahim El-amin, Dr. Samir Al-Baiyat, and Dr. Abdel AalMantawy for there encouragement and cooperation and for spending their time reading my thesis and for their constructive suggestions and comments.

I am so indebted to my family, especially my parents. I appreciate the warm support of the General Manager of National Marine Dredging Company (NMDC), Sheikh Al-Musa'aban tribe, Mr. Ahmed Naji Alawi, my dear father. I thank him for the religious and scientific foundation he gave me. Warm gratitude also to my dear mother and for the prayers she made for me. May Allah bless them and give them a long life with all good deeds.

Lastly but not least, I would like to express my appreciation to my colleagues and to people who gave me support in technical issues and to those who provided the atmosphere for success. I would like to end this acknowledgement by mentioning some of them: Wael Saleh, Nofal, Dr. Nasser Qaddoumi, Dr. El-Keib, Bader Al-Dohan, Abul-Aziz Al-Harhi, Wael Al-Musabi, Mr. Shaker, Mohammed Al-Zahrani, Abdul-Wahab Bentrchia, Waleed Saif, Sajid Khan, Mouin, Saad Azher, Samer Sharife, Hassan El-Morra, Maher, Saleh Bamasak, Ali Awami, Kamran Arshad, Ahmed Bamugabel, Shiraz Amjad, Abdullah Shwehneh, Osama Fares, Firas Tuffaha, Syahrul, Irman Hermadi , Bambang Sharife, Aa'wad (may Allah bless him and enter him paradise), Khalid Ahmed Al-Musabi, Yousef Aina, Kassim, Abu-Baker, Musa otaru, Mansoor Al-Harbi and more.

TABLE OF CONTENTS

Dedication	iii
Acknowledgment	iv
TABLE OF CONTENTS	vi
LIST OF TABLES	ix
LIST OF FIGURES	x
Thesis Abstract	xv
?????? ??	xvi
1. INTRODCUTION AND LITERATURE SURVEY	1
1.1 Load Frequency control	5
1.2 Supplementary excitation control of Synchronous machines	7
1.3 Thesis Contribution	11
1.4 Thesis Structure	12
2. PROPOSED COMBINED VSC/ITERATIVE HEURISTIC ALGORITHMS	
OPTIMAL DESIGN	14
2.1 Basic Concepts of VSC	14
2.2 Merits and Demerits of VSC	20
2.3 Reported Methods for Reducing Chattering	21
2.4 Iterative heuristic optimization algorithms	24
2.4.1 Genetic Algorithms (GA)	24

2.4.2 Particle Swarm Optimization (PSO)	27
2.4.3 Tabu Search Algorithm (TS).....	30
2.5 Proposed design method of VSC	34
3. APPLICATION OF THE PROPOSED VSC DESIGN TO THE LOAD	
FREQUENCY CONTROL PROBLEM	42
3.1 Introduction.....	42
3.2 Proposed VSC Design for a Single area Power system	44
3.2.1 Linear and Nonlinear Models of a single area LFC system.....	44
3.2.2. Proposed VSC design for a single area LFC system excluding nonlinearities	49
3.2.3 Proposed VSC design for a single area LFC with nonlinearities included in the model.....	56
3.3 Two area Interconnected Power system areas.....	63
3.3.1 The Proposed design of VSC applied to Two Interconnected LFC areas excluding nonlinearities	64
3.3.1.1 Design of an optimal feedback gains with fixed switching surface controller	65
3.3.1.2 Design of an optimal switching vector values with fixed feedback gains controller	69
3.3.1.3 Design of a full switching surface and feedback gains controller.....	72

3.3.2 Interconnected LFC areas with nonlinearities.....	80
3.3.2.1 Proposed Centralized VSC controller	81
3.3.2.2 Proposed VSC controller with scaled feedback gains.....	92
3.3.2.3 Proposed Decentralized VSC controller	96
3.3.2.4 The effect of governor dead band on the design of decentralized VSC.....	101
4. POWER SYSTEM STABILITY OF SINGLE MACHINE	111
4.1 Introduction.....	111
4.2 Comparison with Conventional PSS	112
4.3 Comparison with other VSC methods.....	120
4.4 Nonlinear model of the synchronous machine	122
5. CONCLUSIONS AND FUTURE DIRECTIONS	134
Appendix A	138
References	142
Vita	158

LIST OF TABLES

Table 3-1: (a) Performance indices and weighting coefficients for different designs (b) Switching vectors, C^T , and feedback gains, a of VSC designs. Design number 1 was obtained from [14]. Designs number 2 and 3 were obtained from [20]	51
Table 3-2: Comparison between the three algorithms for VSC design applied to interconnected LFC areas excluding nonlinearities.....	77
Table 3-3: Comparison of the three algorithms for VSC design applied to two interconnected LFC areas with nonlinearities.....	91
Table 3-4: Comparison between the performances of different controllers. The VSC controllers designed by TS are chosen for this comparison	100
Table 3-5: Data of the three area power system.....	107
Table 4-1: Comparison between the algorithms used in the proposed VSC design applied to a single machine infinite bus system.....	115
Table 4-2: Comparison between the three algorithms used in the proposed VSC design applied to a nonlinear model of a synchronous machine infinite bus system.....	129

LIST OF FIGURES

Figure 1-1: Power System Control elements: Overview. Shaded parts indicate parts considered in this study.....	2
Figure 2-1: (a) Block diagram of VSC (b) Regions divided by the switching lines.....	17
Figure 2-2: Phase trajectories (a) System equation (2-2) (b) System equation (2-3) (c) Overall system.....	19
Figure 2-3: Flow chart of GA algorithm	26
Figure 2-4: Flow chart of TS algorithm.....	33
Figure 2-5: Block diagram of variable structure controller	35
Figure 2-6: Flow chart of the proposed optimal design of VSC using iterative heuristic optimization algorithms	39
Figure 2-7: Power system dynamic problems tackled in this thesis using the proposed VSC optimal design	41
Figure 3-1: Single area LFC system (a) Excluding nonlinearities (b) with Generation rate constraint (GRC) (c) with GRC and governor dead band backlash.....	47
Figure 3-2: Effect of Dead band on a given input	48
Figure 3-3: (a) Convergence of objective function (b) Frequency deviation for designs no. 1-4 (c) Frequency deviation for designs 5-8 (d) Change in generated power for designs 4-8 (e) Control effort for designs 3, 5, 6, and 8	54

Figure 3-4: (a) Robustness against change in load disturbance (Design no. 4) (b-d) Scaling of switching feedback gains (b) Convergence of deviation of the performance index (b) Frequency deviation (c) Control effort.....55

Figure 3-5: (a) Convergence of performance index (b) Frequency deviation (c) Change in generated power (d) Control effort57

Figure 3-6: (a)-(b) Robustness of the system with the proposed VSC design for 25% change in $1/T_p$, $1/T_g$, $1/RT_g$, $1/T_t$, and K_p/T_p (c)-(d) Effect of varying the GRC on the controller robustness58

Figure 3-7: Proposed VSC design with accessible states only: (a) Frequency deviation (b) Change in generated power (c) Robustness of frequency deviation (d) Robustness of change in generated power (e) Convergence of performance index (f) Control effort60

Figure 3-8: (a) Convergence of performance index (b) Frequency deviation (c) Control effort (d) Robustness of the proposed design62

Figure 3-9: Two area interconnected LFC system with nonlinearities64

Figure 3-10: (a) Convergence of performance index (b)-(f) Dynamic behavior of the interconnected system for a 0.03 p.u. load disturbance in area 1 (... [17])68

Figure 3-11: (a) Control effort in area 1 (b) Control effort 269

Figure 3-12: (a)-(e) Dynamic response of two area LFC system for 0.03 p.u. load disturbance in area 1 (f) Convergence of performance index value (...[17])71

Figure 3-13: (a) Control signal to area 1 (b) Control signal to area 272

Figure 3-14: (a) Convergence of the objective functions (b)-(f) Dynamical behavior of the interconnected system following a disturbance of 0.03 p.u. in area 1 (...--- [17])74

Figure 3-15: (a) Control signal 1 (b) Control signal 275

Figure 3-16: (a) Convergence of performance index (b)-(f) Dynamic behavior of the system following a 0.03 p.u. disturbance in area 1 (...---[17]).....79

Figure 3-17: (a) Control effort 1 (b) Control effort 280

Figure 3-18: (a) Convergence of objective functions(b)-(d) Dynamic response of the system for a 0.01 p.u. load disturbance in area 1 (e) Control signal 1 (f) Control signal 284

Figure 3-19: (a) Convergence of objective functions (b)-(d) Dynamic behavior when subjected to a 0.01 p.u. load disturbance in area1 (e)-(f) Frequency deviation: Accessible states VSC (g) Control effort 1 (h) Control effort 287

Figure 3-20: (a) Frequency deviation in area 1 (b) Frequency deviation in area 2 for a 25% change in T_g , T_i , and K_p of both areas88

Figure 3-21: (a) Convergence of performance index (b)-(d) Dynamic response of the after a 0.01 p.u. load disturbance (e) Control 1 (f) Control 290

Figure 3-22: (a)-(c) Comparison between the dynamical behavior of the system designed with different heuristic algorithms. Objective function, J_I , is considered in this case.....91

LIST OF FIGURES

Figure 3-23: Scaled feedback gains design: (a) Convergence of the performance index (b)-(d) Dynamical behavior of the system after a 0.01 p.u. load disturbance; comparison of different designs (e) Control signals for area 1 (f) Control signals for area 2	95
Figure 3-24: Proposed decentralized VSC controllers applied to interconnected LFC areas	96
Figure 3-25: (a) Convergence of performance index (b)-(d) Dynamical behavior of the system with decentralized VSC (e) Control signal 1 (f) Control signal 2	99
Figure 3-26: (a) PSO: Comparison between centralized and decentralized VSC designs (b) TS: Comparison between centralized and decentralized VSC designs.....	100
Figure 3-27: The effect of governor dead band backlash on the dynamical behavior of the LQR design [105].....	101
Figure 3-28: (a) Convergence of performance index (b)-(d) Dynamic behavior of the interconnected system after a 0.01 load disturbance (e) and (f) Control signal for areas 1 and 2	103
Figure 3-29: Schematic diagram of power system with three areas	104
Figure 3-30: Three area interconnected LFC system.....	105
Figure 3-31: Block diagram representing Boiler dynamics.....	106

Figure 3-32: (a) Convergence of objective function (b) Frequency deviation area 1 (c) Frequency deviation area 2 (d) Frequency deviation area 3 (e)-(g) Tie line power between: (e) areas 1 and 2 (f) areas 2 and 3 (g) areas 3 and 1109

Figure 4-1: (a) Single machine infinite bus power system [26] (b) Linearized model (c) Conventional PSS114

Figure 4-2: (a)-(b) Damping of frequency oscillation (c) Control signal (d) Frequency deviation of the system with the proposed VSC when operating point is changed for PSO design. Nominal operating point: $P = 1$ p.u. $Q = 0.015$ p.u.116

Figure 4-3: (a) Damping of frequency oscillations (b) Control signal (c) Robustness of the system with the proposed scaled gains VSC when operating point is varied. Nominal operating point: $P=1$ p.u. $Q= 0.015$ p.u.119

Figure 4-4: (a) Damping of frequency oscillations (b) Control effort122

Figure 4-5: Synchronous machine infinite bus power system.....123

Figure 4-6: GA design (a) Performance of system with the proposed VSC (--without controller) (b) Convergence of performance index.....130

Figure 4-7: PSO design (a) Dynamical performance of the system (--without controller) (b) Convergence of the performance index.....131

Figure 4-8: TS design (a) Dynamical behavior of the system and control signals (--without controller) (b) Convergence of performance index132

Thesis Abstract

Name: NAJI AHMED AL-MUSABI

Title: DESIGN OF OPTIMAL VARIABLE STRUCTURE CONTROLLERS:
APPLICATIONS TO POWER SYSTEM DYNAMICS

Degree: MASTER OF SCIENCE

Major field: ELECTRICAL ENGINEERING

Date of degree: JUNE 2004

In this thesis, optimal design of variable structure controllers applied to different power system dynamic problems is explored. Iterative heuristics algorithms namely: Particle Swarm optimization, Tabu Search algorithm, and Genetic Algorithms are utilized in the optimal design of the controllers. Two important power system problems (Load frequency control and Power system dynamic stability) are studied in this thesis. The proposed design of VSC was applied to single area, two areas, and three areas Load frequency control systems both with and without nonlinearities and to a single machine infinite bus-bar system.

The variable structure controller parameters are tuned optimally to minimize certain performance indices that reflect the objectives of the design. These objectives include both improved dynamic behavior and reduced chattering in the control signal. Scaling of the feedback gains in the VSC on convergence of the performance index or the square of the error in the signal further reduced the chattering while preserving the improved dynamic behavior of the system. Comparison with conventional design methods for both problems using the new design procedure is also included in the study. The study shows that the proposed optimal design procedure provides a simple systematic way of arriving at the settings of the VSC with improved dynamic behavior and reduced chattering. This method allows with ease the inclusion of nonlinearities into the studied systems to realize an optimally designed controller. The robustness of the proposed controller against system parameters variations had been studied. It has been found that the proposed controllers are very little sensitive to these variations.

Keywords: Variable Structure control, Load frequency control, Power system stability, iterative heuristic optimization algorithms.

Master of Science Degree
King Fahd University of Petroleum and Minerals
Dhahran, Saudi Arabia
June, 2004

CHAPTER 1

INTRODCUTION AND LITERATURE SURVEY

Power system stability and control methods are one of the most important subjects in the operation of contemporary electric utilities. It is a topic of broad history and extensive research has been done in this field. Power systems are rapidly expanding and are in continuous need for control methods in order to maintain both stable behavior and reliable operation. This involves meeting the load demands at all the time and sustaining constant frequency and voltages for the system. The control of power systems is composed of many elements. The categorization of these elements differs from one source to another; but they all incorporate the same concepts. Figure 1, shows an overview of power system controls, emphasizing the areas studied in this thesis [1].

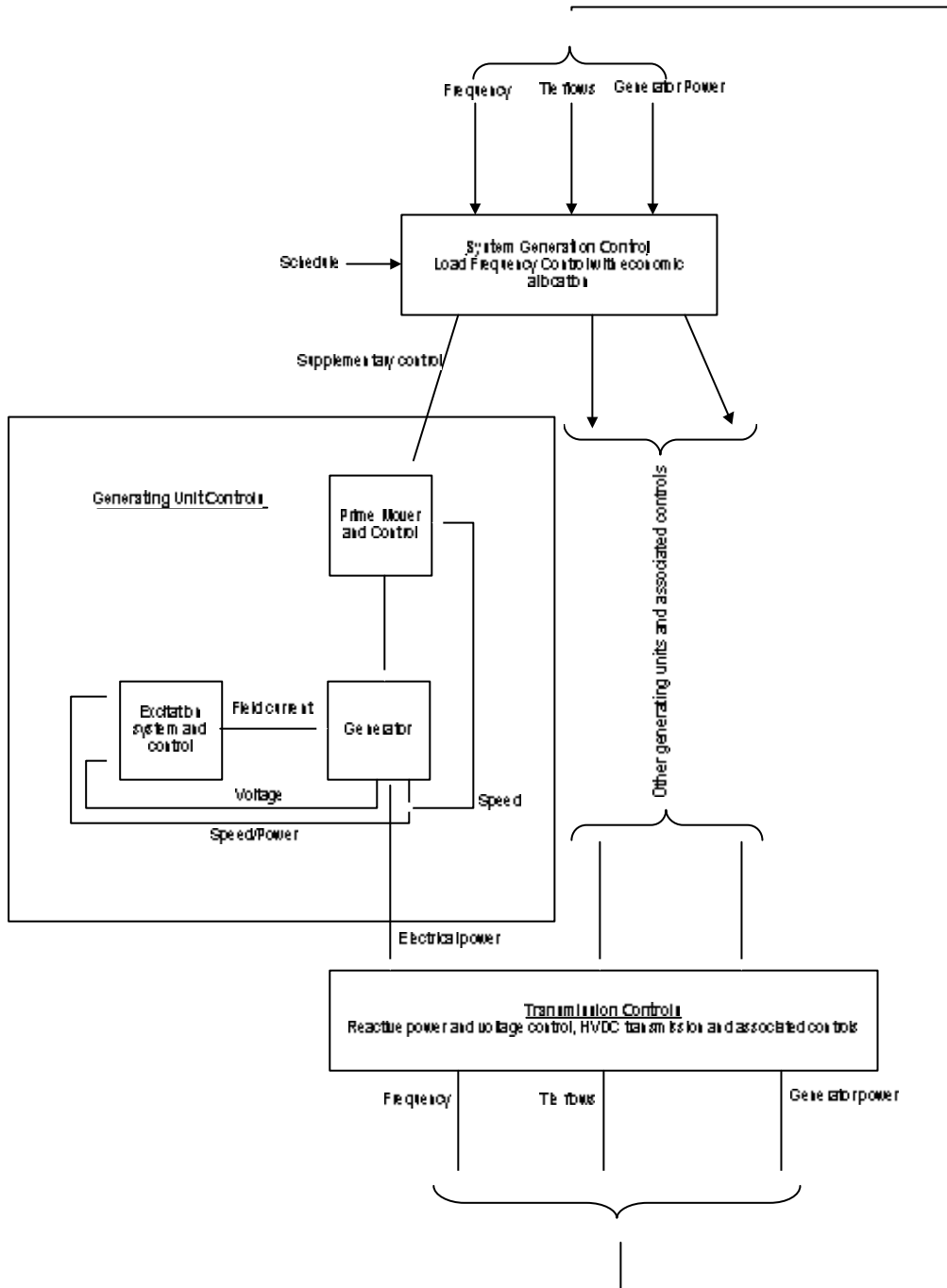


Figure 1-1: Power System Control elements: Overview. Shaded parts indicate parts considered in this study

In this thesis, two important power system problems are studied. The first one is the Load Frequency Control (LFC). The second problem is the power stability problem where the supplementary excitation control is used in damping oscillations of synchronous machine. This thesis will study the application of Variable structure controllers (VSC) to these problems. In literature, many authors investigated the application of VSC to both the LFC problem ([13]-[21]) and the design of power system stabilizers in ([38], [39], [53]-[58]). However, these methods emphasized more on using the linear model of the system excluding nonlinearities. Furthermore, these methods lack a systematic way in arriving at the switching feedback gains of the VSC. In this thesis, optimally designed VSC using iterative heuristic optimization algorithms is suggested and applied to power system dynamic problems. The models studied included the effect of nonlinearities.

The merits of VSC are improved transient behavior and robustness. In addition, this thesis introduces a simple and systematic way of arriving at the optimal settings of the controller. Conventionally, the design procedure of VSC involves two main steps:

- 1- The design of a suitable switching surface that will guarantee a stable behavior of the system once the states are sliding along it.
- 2- Designing a suitable control law that will guarantee the reaching condition and will maintain the states on the designed sliding surface. In this thesis, discontinuous type control law is adopted. However, unlike conventional methods of design where trial

and error is used to arrive at the optimal gains, the feedback gains are optimized by iterative heuristics algorithms.

VSC controllers suffer from the problem of chattering. The problem of reducing the chattering in the control signal of the VSC is also addressed in this thesis. This was done by two ways:

- 1- Including a scaled factor of the control effort or scaled factor of the deviation in the control effort into the objective function of the design.

- 2- Scaling the feedback gains of the VSC when the integral of square error converges.

Both methods were found to dramatically reduce the chattering.

The first problem tackled by this thesis is that of Load frequency control (LFC). In LFC, a sudden change in the loads causes a proportional change in frequency of the generating units. This change in frequency is feedback through the regulator and integral controller to the governor. A supplementary control signal, in our case from the VSC, is added with these signals and fed to the governor. The governor will then open or close the steam valve of the turbine to supply the required power. The VSC switching feedback gains and switching vectors are designed optimally using GA, PSO, and TS. The other problem studied in this thesis is that of electrical machines dynamics and damping of oscillations through supplementary excitation control. Conventionally, Power system stabilizers (PSS) are used for this purpose. However, this thesis will study the application of the VSC type stabilizer. Again, the VSC will

be tuned using iterative heuristic optimization algorithms to arrive at its optimal settings. For these two problems, various techniques were suggested in the literature. A summary of these methods is given in the following sections. First, an overview of the reported techniques applied to LFC problem will be discussed. Then, a literature survey of the methods used for damping oscillations in synchronous machine through supplementary excitation control is presented.

1.1 Load Frequency control

In the past years, many techniques were proposed for the supplementary control of LFC systems ([2]-[21], [23], [24]). Conventionally, PI and PID controllers are used for LFC ([2]-[4]). However, PI has many drawbacks, some of which are long settling time and relatively large overshoots in the transient frequency deviations. Furthermore, utilization of optimal control theory was examined in ([5], [6]). The controller design is normally based on the parameters of the linear incremental model of the power system which, in turn, depend on the condition of the power system. Therefore, the linear optimal controller is sensitive to variations in the plant parameters or operating conditions of the power system. Moreover, the linear optimal controller yields unsatisfactory dynamic response in the presence of Generation Rate Constraint (GRC) [7]. Furthermore, application of adaptive control theory to the LFC problem was found to eliminate some of the problems associated with optimal and

classical control methods. In [8], a model reference adaptive control was applied for the LFC problem based on the hyper stability method. However, the controller had problems when GRC is introduced. Other techniques of designing the secondary control loop for the LFC includes Neural Network methods ([9], [10]), Superconducting Magnetic Energy Storage (SMES) units applications [11], and spline techniques [12]. Furthermore, the application of VSC to the LFC problem was considered in ([13]-[21]). VSC possess some attractive features; mainly robustness and good transient response. In [13], a VSC controller was compared with conventional and optimal control methods for two equal-area nonreheat and reheat thermal systems. In that work, no systematic method for obtaining the switching vectors and optimum feedback gain of the VSC was discussed. Pole placement was utilized in designing the VSC for a single nonreheat LFC system in [14]. The gain settings were selected by trial and error. In [15] and [16], two area nonreheat and reheat thermal systems were studied. The former utilized simple control logic to switch between proportional and integral controllers excluding sliding modes. In [16], the same control logic was used to switch between VSC and Integral controllers to improve the dynamic response of the LFC system in comparison with conventional Integral controller. Furthermore, an approximating control law and a new switching function with integral action were proposed for a robust load frequency controller design [18] with a claimed reduction of chattering. However, the behaviour of the

control effort was not shown. In addition, the frequency response of the designed controller showed questionable response with GRC. Applying a stricter GRC was shown to give a better dynamic response, although it is known that a harsher GRC on the rate of generation will cause more degradation in the performance of the load frequency controller. Furthermore, fuzzy control was combined with equivalent and switching control in [19] to design a robust sliding mode LFC. Simulations of the system showed both improved dynamical performance and reduced chattering. Recently, researchers utilized the iterative heuristic optimization algorithms in tuning the controllers to obtain their optimum settings. Some of the recent attempts applied to the variable structure LFC problem can be found in ([20], [21]). In [20], Genetic Algorithms (GA) was used to optimize the feedback gains of the VSC applied to a single area non-reheat LFC. In [21], particle swarm optimization (PSO) was used for the same purpose. In both of [20] and [21], only the feedback gains were selected optimally. On the other hand, the switching vector was obtained from other design method reported in literature.

1.2 Supplementary excitation control of Synchronous machines

The need for power system dynamic and stability analysis has grown significantly in recent years. This is mainly due to the desire to utilize transmission networks for more flexible interchange transactions required for the current competitive environment [25].

Therefore, the application of advanced control technology to enhance the stability of power systems has attracted wide attention. An important problem in stability of power systems is the excitation control of synchronous machines. It is one of the most effective and economic techniques for enhancing the dynamic performance and transient stability of power systems. The significance of excitation control induced researchers to study and design new control methods for the problem such as Proportional-Integral-Derivative (PID) excitation control, Power System Stabilizers (PSS), Linear Optimal/Sub-Optimal Excitation Control (LOEC), Nonlinear Optimal Excitation Control (NOEC), Adaptive and Intelligent Control ([26]-[30]).

In recent years, Power System Stabilizers (PSS) were usually used to enhance the damping of power oscillations caused by several types of small disturbances in a power system. The conventional lead-lag compensation is adopted by most designers due to its simple structure and easy implementation [31]. Linear optimal excitation controller based on LQR theory has been developed to enhance power system stability [32]. They proved to be efficient for the improvement of power system stability under small disturbance compared with conventional excitation control and PSS. Intelligent control was also applied to power system control/stabilization ([33]-[35]) that included the use of neural networks in tuning existing PSS [33] or to replace the conventional PSS [34]. Fuzzy logic approach was also studied and applied to design PSS ([36], [37]).

Moreover, in reality power systems are subject to uncertainties in operation and external disturbances. The drawback of conventional approaches that relies on linearized models is that the designed controller will only be valid when the system dynamics exhibit small variations around the operating. Thus, robust decentralized model for excitation control was investigated by some authors ([31], [40]). Furthermore, nonlinear control designs for power systems have been introduced that utilize differential geometric tools to control system design. These designs are primarily based on the concept of external feedback linearization (EFL) ([41], [42]). A major problem of the EFL technique, however, is that it relies on the exact cancellation of the nonlinear terms to realize a linear input-output behavior. Therefore, with parametric disturbances in the interconnection models, the cancellation is no longer exact and the performance of the EFL could degrade with varying system conditions. To solve this problem, robust controllers with feedback linearizing control have been proposed in ([43], [44]). Furthermore, authors in ([45], [46]) introduced an adaptive extension of the feedback linearization scheme to achieve an asymptotically exact cancellation of terms. Moreover, stochastic model based feedback linearising control [47] and variable structure control [48] applied to nonlinear EFL were investigated by authors. However, most of these nonlinear controllers require full accessibility to all system states when feedback linearization is considered because they are based on state feedback. In practice, it is not always

possible and economical to measure all system's states. To solve this problem, authors in [49] applied state observer to the nonlinear field voltage control of generators. Recently, control of uncertain nonlinear dynamical systems using estimated perturbation for compensation has been a topic of interest [50]. The combination of sliding-mode state and perturbation observer (SPO) with the sliding-mode control (SMC) led to a high performance algorithm SMCSPO which utilizes partial state feedback [50] and provides robust performance. In [51], the perturbation estimation method and sliding-mode state observer design were studied and a robust observer-based nonlinear controller (RONC) was developed. The RONC was applied for the excitation control of synchronous generators interconnected in a multimachine power system to improve system stability. The RONC showed better performance and robustness in comparison with a conventional nonlinear state feedback linearizing controller (NFLC).

Furthermore, the use of adaptive feedback linearizing control scheme with Neural Networks is proposed in [52]. The controller is synthesized to adaptively compute an appropriate feedback linearizing control law at each sampling instant using estimates provided by the neural system model. In this way, the necessity for exact knowledge of the system dynamics, full state measurement, as well as other difficulties associated with feedback linearizing control for power systems are avoided in this approach.

Furthermore, a PSS design based on Variable Structure law is reported in ([38], [39], [53]-[58]). However, the switching feedback gains of the VSC were not chosen by a systematic way. In [57], a diagonalization method was proposed to choose the switching feedback gains of the VSC. The switching surface was determined optimally by minimizing a quadratic system performance index in the sliding mode operation. Furthermore, a VSC that operates satisfactory over a wide range of operating point was proposed in [38]. However, the feedback gains were again chosen by empirical experiments. In [39], a VSC PSS was proposed that operates over wide range of operating points by using a neural network to adapt the feedback gains of the controller. For each operating point, the feedback gains were chosen by Genetic Algorithms.

1.3 Thesis Contribution

The first step in conventional design of VSC for power system control problems is to linearize the model studied or use nonlinear transformations to formulate the system equations in suitable form. In this way, control theory methods, such as pole placement or optimal control, can be applied in the design of the controller. Furthermore, there is no clear way of choosing the switching feedback gains of VSC. For these reasons, this thesis proposes to formulate the design of VSC as an optimization problem where iterative heuristic optimization algorithms are used. In this way, the optimum settings of the VSC applied to power system control problems

can be found even with the presence of nonlinearities in the model. The present work is considered new since the proposed approach has not been used before in the design of VSC. In the optimization process, various objective functions were considered and investigated to reflect both improved dynamics of the power system and reduced chattering in the control signal of the controller. This method provides a systematic way of arriving at the optimal values for both the switching vector and the switching feedback gains of the VSC. Finally, the proposed design method was compared to other designs reported in literature. Promising results of comparison validate the significance of the proposed design procedure.

1.4 Thesis Structure

The chapters of the thesis are organized as follows:

Chapter 2 : gives a brief theoretical background of VSC and the iterative heuristic optimization algorithms used in the design procedure. Furthermore, the proposed design of VSC is then explained.

Chapter 3 : includes the first application of the proposed VSC design to the LFC problem. This includes single, two, and three areas LFC systems. The systems were studied with and without nonlinearities in the models.

Chapter 4 : studies the application of the proposed design of VSC to single machine system. This includes both synchronous machine connected to an infinite bus system. Linear and nonlinear models of synchronous machine were investigated.

Chapter 5 : Includes conclusion and discussion of the material presented in the thesis.

Moreover, direction for future research in this subject is also suggested.

CHAPTER 2

PROPOSED COMBINED VSC/ITERATIVE HEURISTIC ALGORITHMS OPTIMAL DESIGN

This chapter starts by reviewing some of the basic concepts of Variable Structure Control. Merits and demerits of VSC are also mentioned. Furthermore, a brief explanation of some reported methods of reducing chattering is included. In addition, an overview of the utilized iterative heuristic optimization algorithms is included. Finally, the proposed design procedure for VSC using iterative heuristic optimization algorithms is discussed.

2.1 Basic Concepts of VSC

The early work on Variable Structure Control was conducted by Russian authors before four decades. Interest in this method evolved after the comprehensive work and translation made by Itkis [70] and Utkin [72]. Variable Structure systems concepts have subsequently been utilized in many applications and engineering

problems including power systems ([58]-[64]), aerospace ([65]-[67]), and robotics ([68], [69]).

The fundamental requirement of this theory, as proposed by most authors, is to find the necessary and sufficient conditions for the existence of a sliding mode or regime on a designed sliding hyper-plane. Other requirements include the conditions that guarantee hitting the sliding hyper-plane from any location in the state space, the conditions for the stability of the sliding mode, and the conditions for invariance in sliding regime. Furthermore, sliding mode condition or the reaching condition is the condition under which states of the system are guaranteed to move towards and reach a sliding surface. There are various methods of defining this condition. The Lyapunov-function-like reaching condition is defined as follows:

$$\dot{V} = \mathbf{s}^T \dot{\mathbf{s}} < 0, \text{ where } V = \frac{1}{2} \mathbf{s}^T \mathbf{s}$$

The reaching law approach and the direct switching function approaches are respectively defined by

$$\dot{\mathbf{s}} = -k\mathbf{s} - q \operatorname{sgn}(\mathbf{s})$$

$$\lim_{\mathbf{s} \rightarrow +0} \dot{\mathbf{s}} < 0 \text{ and } \lim_{\mathbf{s} \rightarrow -0} \dot{\mathbf{s}} > 0$$

These conditions for achieving a sliding regime are discussed in details in ([70]-[72]).

The basic concept of VSC can be illustrated by the following example [85]:

Consider a second-order system described by the following equations,

$$\begin{aligned} \dot{x} &= y \\ \dot{y} &= 2y - x + u \\ u &= -\mathbf{y}x \end{aligned} \tag{2-1}$$

where

$$\mathbf{y} = \begin{cases} 4, & s(x,y) > 0 \\ -4, & s(x,y) < 0 \end{cases}$$

and

$$s(x, y) = x\mathbf{s}, \quad \mathbf{s} = 0.5x + y$$

Figure 2-1(a) shows a block diagram of the system $s(x, y)$ is called the switching surface. It consists of the product of two functions $x = 0$ and $\mathbf{s} = 0.5x + y = 0$. These functions represent switching lines that divide the phase plane into regions according to the sign $s(x, y)$ as shown in Figure 2-1(b). The main regions are defined as follows,

Region I: $s(x, y) = x\mathbf{s} > 0, \mathbf{y} = 4$, and the model is described as

$$\begin{aligned} \dot{x} &= y \\ \dot{y} &= 2y - x - 4x = 2y - 5x \end{aligned} \tag{2-2}$$

Region II: $s(x, y) = x\mathbf{s} < 0, \mathbf{y} = -4$, with state equations

$$\dot{x} = y$$

$$\dot{y} = 2y - x + 4x = 2y + 3x \quad (2-3)$$

The phase plane of these models is shown in Figure 2-2(a) and (b). Clearly, both models show unstable trajectories.

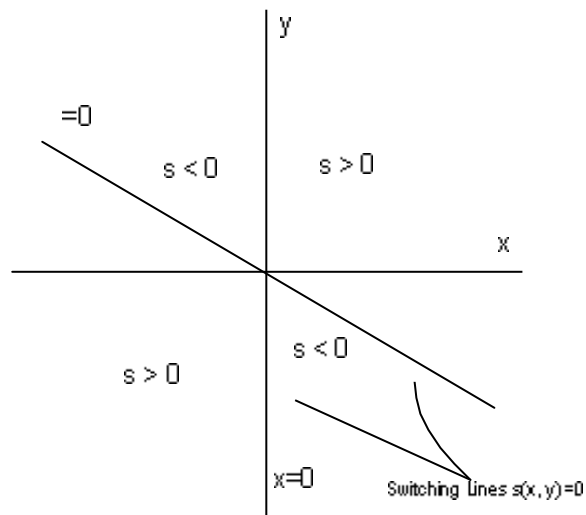
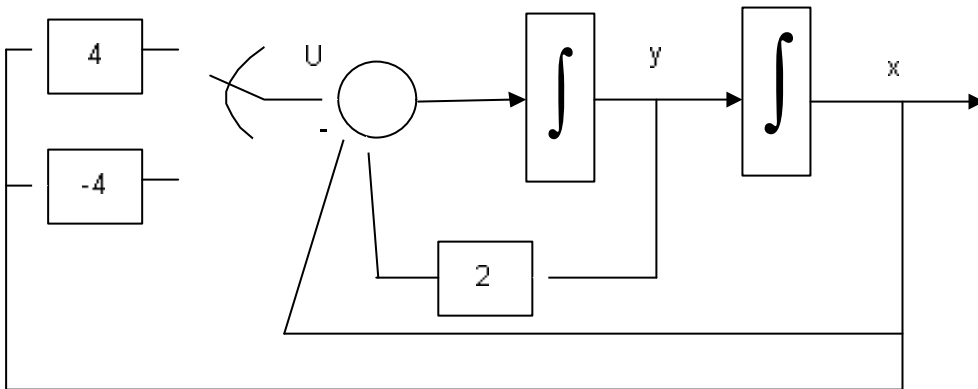


Figure 2-1: (a) Block diagram of VSC (b) Regions divided by the switching lines

The trajectory of the whole system is formed by combining the trajectories of the two subsystems depending on the location of the representative point in the phase plane with respect to the two regions. The trajectory of the whole system, as illustrated in Figure 2-2 (c), is stable.

The phase trajectory can be divided into two phases:

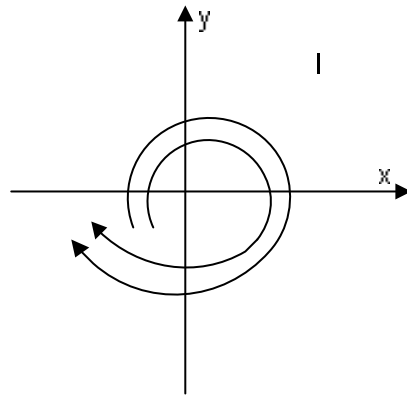
1) Reaching mode: where the trajectory moves toward the sliding surface from any point in the phase plane.

2) Sliding mode: where the trajectory is maintained on the sliding surface and moves towards the origin of the phase plane. During this mode the dynamics of the system can be described as follows:

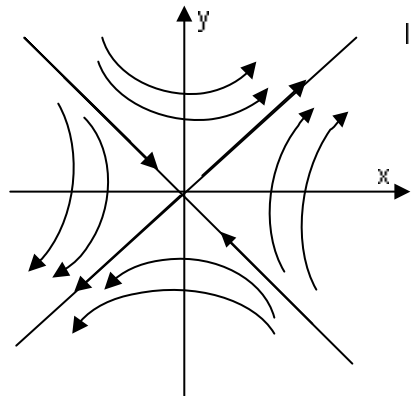
$$\mathbf{s} = 0.5x + y = 0.5x + \dot{x} \quad (2-4)$$

The dynamics of the system are therefore of lower order during the sliding mode.

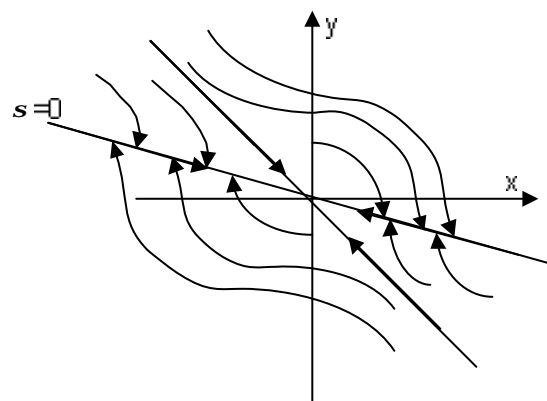
This type of control is called Variable structure system because the controller changes structure from that of equation (2-2) to equation (2-3) model depending on the location of the representative point in the phase plane.



(a)



(b)



(c)

Figure 2-2: Phase trajectories (a) System equation (2-2) (b) System equation (2-3) (c) Overall system

2.2 Merits and Demerits of VSC

The advantages of obtaining a sliding motion are: reduction in order and insensitivity to parameter variations implicit in the input channels. This allows the design of a robust controller against uncertainties in the parameters of the system. Furthermore, VSC allows the determination of the closed-loop dynamics of nonlinear system in a desired manner. This can be done by formulating the problem as a pole placement design and varying the coefficients of the sliding surface.

However, some of the problems of VSC are that the control effort usually has a chattering characteristic that makes its implementation impractical. The VSC ideally requires infinitely fast switching mechanism. Practically, it is impossible to realize this infinite rate of switching. This is due to the physical limits of actuators and time delays in control systems. The non-ideal fast switching causes the chattering. The high frequency components of the chattering are undesirable and can excite unmodelled high frequency plant dynamics which can lead to unforeseen instabilities [77].

Another underlying problem associated with VSC design is the selection of the feedback gains. Generally, the gains are chosen by trial and error such that they will satisfy certain system performance requirements. Recently, the problem of VSC feedback gains selection has been considered by [58]. Their approach essentially was to try all allowable values of the feedback gains and evaluate a performance index for

each possible set of feedback gains. The optimal feedback gains selected are those which minimize the performance index. This approach is numerically intensive especially for large numbers of feedback gains.

Furthermore, in conventional design methods of the switching surface for the variable structure controller for a nonlinear system, various transformations of the differential equations to a suitable canonical form is required [77]. An example of this design can be found in [84]. These transformations are complicated and are not always possible.

2.3 Reported Methods for Reducing Chattering

In literature, several authors used the concept of boundary layer control to reduce the chattering problem ([77]-[79]). In [78], a thin boundary layer in a neighborhood around the switching surface is suggested to smoothen the discontinuity in the control. The signum term in the control law u is replaced by $[\mathbf{s}(x)/(\mathbf{I}_{n-1})\mathbf{e}]$, where $\mathbf{s}(x)$ is the switching surface, \mathbf{I}_{n-1} is the $(n-1)^{\text{th}}$ coefficient of the switching surface and \mathbf{e} is the boundary layer. Furthermore, authors in [77] introduced a similar control law, where u is given by

$$u = u(t, x) = \begin{cases} -\frac{\mathbf{s}}{\|\mathbf{s}\|} \mathbf{r}, & \text{if } \|\mathbf{s}\| \geq \mathbf{e} \\ p(t, x), & \text{if } \|\mathbf{s}\| < \mathbf{e} \end{cases} \quad (2-5)$$

$p(t, x)$ is continuous function given by $p(t, x) = -[\mathbf{s}/\|\mathbf{s}\|]\mathbf{r}$ when $\|\mathbf{s}\| = \mathbf{e}$.

Authors in [77] state that these boundary layer controls do not guarantee asymptotic stability. This fact is proofed in [79]. Furthermore, using a saturation function instead of a switching degrades the steady state performance and robustness of the controller. Authors in [74] claim that the integral action can eliminate these disadvantages within tolerable range.

Another continuous control law of the form $[s(x)/(|s(x)+\mathbf{d}|)]$ was proposed by Ambrosino et. Al [81]. \mathbf{d} is a positive constant chosen arbitrary. Espana et al. [82] proposed a method that creates a switching region around the sliding hyperplane such the switching parameters are replaced inside the region by parameters that will satisfy $s(x) = 0$. This method is claimed to reduce the chattering effect and simultaneously allow a short reaching time.

Furthermore, another approach is tuning the reaching law [80]. In tuning the reaching law approach, chattering can be reduced by manipulating parameters q_i and k_i of the reaching law

$$\dot{S}_i = -q_i \operatorname{sgn}(S_i) - k_i S_i \quad i = 1, \dots, m \quad (2-6)$$

Decreasing q_i and increasing k_i results in both reduced chatter and reaching time respectively.

In [80], augmentation of linearizable systems with an integrator is used to reduce the chattering. Further reduction is also obtained by estimation of the uncertainty.

In [83], an auxiliary control input is used to replace the discontinuous control input during the steady state. The control input is given by

$$u = u_{eq} + u_d + u_x \quad (2-7)$$

u_{eq} is the continuous equivalent control, u_d is the discontinuous control, and u_x is an auxiliary continuous control. u_d is given by

$$u_d = k \operatorname{sgn}(S) \quad (2-8)$$

The discontinuous control is approximated by an average equivalent continuous control u_{ed}

$$u_{ed} = \mathbf{a}k - (1 - \mathbf{a})k \quad 0 \leq \mathbf{a} \leq 1 \quad (2-9)$$

The idea of this algorithm is to reduce k on approaching steady state response while maintaining u_d during transient response to preserve the robustness characteristics of the controller. The auxiliary control u_x will replace u_{eq} allowing the reduction of k and thus reducing the chattering. However, designing k and u_x involves choosing some parameters by trial and error.

2.4 Iterative heuristic optimization algorithms

This section gives an overview of the heuristic iterative algorithms used in this thesis. These algorithms include: Genetic algorithms, Particle swarm optimization, and Tabu search algorithm.

2.4.1 Genetic Algorithms (GA)

Genetic Algorithms (GA) are powerful domain independent search technique inspired by Darwinian theory of evolution [87]. It was invented by John Holland and his colleagues in 1970s [88] and was successfully applied to many engineering and optimization problems [88] and to various areas of power system such as economic dispatch ([89], [90]), unit commitment [91], reactive power planning ([92], [93]), power plant control ([94], [95]), and Generation expansion planning [96]. GA is an adaptive learning heuristic that imitate the natural process of evolution to progress toward the optimum by performing an efficient and systematic search of the solution space. A set of solutions, described as a population of individuals, are encoded as binary strings, termed as Chromosomes. This population represents points in the solution space. A new set of solutions, called Offsprings, are created in a new generation (iteration) by crossing some of the strings of the current generation. This process is called Crossover. Furthermore, the Crossover is repeated at every generation and new characteristics are introduced to add diversity. The process of altering some of the strings of the offsprings randomly is known as Mutation.

The basic steps of GA can be described as follows:

Step 1: Generation of Initial population of solutions represented by Chromosomes.

Step 2: Evaluation of the solutions generated using the fitness function which is usually the objective function of the problem under study.

Step 3: Selection of individual solutions that have higher fitness value. There are different selection methods such as Roulette wheel selection, Stochastic selection, and Ranking-based selection [88].

Step 4: Generation of new offsprings from the selected individual solutions. This is done for certain number of generations using two main operations:

- Crossover: There are various Crossover operators; the most common is the one-point crossover. In one-point Crossover, one bit in each solution, of two given binary coded solutions, is determined randomly and then swapped to generate two new solutions.
- Mutation: Incremental random changes applied in the selected offsprings by altering randomly some its bits. Mutation is usually probabilistically applied to only few members of the population and therefore has a small value.

Step 4: Steps 2 to 4 are repeated until a predefined number of generations have been produced.

Figure 2-3 shows the flow chart of the GA algorithm.

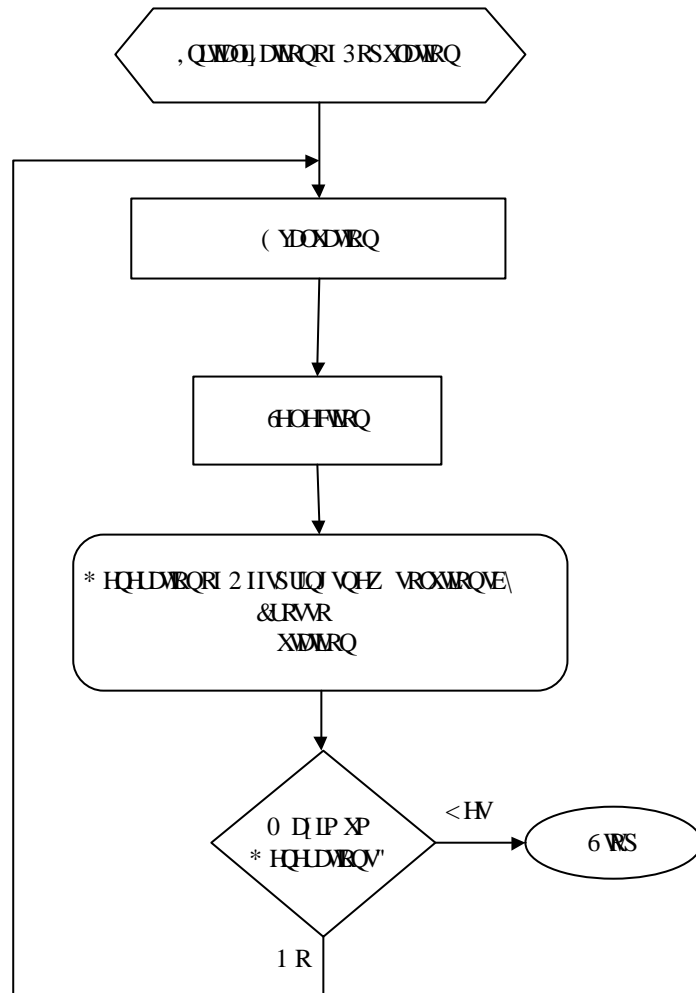


Figure 2-3: Flow chart of GA algorithm

2.4.2 Particle Swarm Optimization (PSO)

The Particle swarm optimization (PSO) is an evolutionary computation technique developed by Eberhart and Kennedy [97] inspired by social behaviour of bird flocking or fish schooling.

Similar to Genetic Algorithms (GA), PSO is a population based optimization tool. The system is initialized with a population of random solutions and searches for optima by updating generations. However, unlike GA, PSO has no evolution operators such as crossover and mutation. In PSO, the potential solutions, called particles x , are "flown" through the problem space by following the current optimum particles. Each Particle keeps track of its coordinates in the problem space which are associated with the best solution (fitness) it has achieved so far. The fitness value is also stored. This value is called particle best, $pbest$, and the particle(s) associated with it is denoted by x_{pbest} . Another "best" value that is tracked by the global version of the particle swarm optimizer is the overall best value, and its location, obtained so far by any particle in the population. This value is called global best, $gbest$, and the particle(s) is x_{gbest} .

The particle swarm optimization concept consists, at each time step t , updating the velocity and accelerating each particle towards $pbest$ and $gbest$ locations. Acceleration is weighted by a random term, with separate random numbers being generated for acceleration toward $pbest$ and $gbest$ locations.

The PSO algorithm applied in this study can be described briefly as follows:

Step 1: Initialize a population (array) of particles with random positions and velocities v on d dimension in the problem space. The particles are generated by randomly selecting a value with uniform probability over the d^{th} optimized search space $[x_d^{\min}, x_d^{\max}]$. Set the time counter $t = 0$.

Step 2: For each particle x , evaluate the desired optimization fitness function, J , in d variables.

Step 3: Compare particles fitness evaluation with x_{pbest} , which is the particle with best local fitness value. If the current value is better than that of x_{pbest} , then set x_{pbest} equal to the current value and x_{pbest} locations equal to the current locations in d -dimensional space.

Step 4: Compare fitness evaluation with population overall previous best. If current value is better than x_{gbest} , the global best fitness value then reset x_{gbest} to the current particle's array index and value.

Step 5: Update the time counter t , inertia weight w , velocity v , and position of x according to the following equations

Time counter update: $t = t + 1$

Inertia weight update: $w(t) = w_{\min} + (w_{\max} - w_{\min}) \left(\frac{m-t}{m-1} \right)$

Velocity update:

$$v_{id}(t) = w(t)v_{id}(t-1) + 2a(x_{idpbest}(t-1) - x_{id}(t-1)) + 2a(x_{idgbest}(t-1) - x_{id}(t-1))$$

Position of x update: $x_{id}(t) = v_{id}(t) + x_{id}(t-1)$

where w_{\min} and w_{\max} are the maximum and minimum values of the inertia weight w , m is the maximum number of iterations, i is the number of the particles that goes from 1 to n , d is the dimension of the variables, and a is a uniformly distributed random number in $(0, 1)$. The particle velocity in the d^{th} dimension is limited by some maximum value v_d^{\max} . This limit improves the exploration of the problem space. In this study, v_d^{\max} is proposed as

$$v_d^{\max} = kx_d^{\max}$$

where k is a small constant value chosen by the user, usually between 0.1-0.2 of x_d^{\max} [98].

Step 6: Loop to 2, until a criterion is met, usually a good fitness value or a maximum number of iterations (generations) m is reached. Another criteria used is to terminate the search process if there is no more improvement in fitness value for the last n iterations. In this case $n < m$

More details about PSO can be found in ([97], [98]).

2.4.3 Tabu Search Algorithm (TS)

Tabu Search Algorithm was proposed a few years ago by Fred Glover ([100], [101]) as a general iterative heuristic method for solving combinatorial optimization problems. Tabu Search is conceptually simple and stylish heuristic method. It has now become an established optimization methodology that is rapidly spreading in various fields. Planning and Scheduling, Transportation, Routing and Network Design, Continuous and Stochastic Optimization, Manufacturing and Financial Analysis are some of these applications[101]. The search method for the optimum solution is partially based on the hill climbing method that finds out a solution through creating a neighborhood around a solution and moving towards the best solution within the neighborhood. Tabu search succeeds in escaping local minimas by using a Tabu list that records the forbidden moves. Moves are classified as forbidden if certain conditions imposed on the moves are satisfied. The purpose of maintaining a Tabu list is to force the search process to avoid cycling and thus impose diversification.

At initialization the objective is make a broad examination of the solution space, diversification, but as candidate locations are recognized the search is narrowed to give local optimal solutions in a process of intensification.

The basic elements of Tabu Search are defined as follows:

- **Current Solution:** $x_{current}$: It is a set of solutions from which new trial values are generated.
- **Moves:** the process of generating trial solutions from $x_{current}$.
- **Candidate Moves:** It is a set of trial solutions, x_{trial} , generated from neighborhood of $x_{current}$.
- **Tabu list:** A list of forbidden moves that exceeded conditions imposed on moves in general.
- **Aspiration Criterion:** a device that override the tabu status of a move. There are different types of aspiration criteria used in literature ([99]-[101]). The criteria used here is to override the tabu status of a move if it produces a better solution than the best solution, x_{best} , seen so far.
- **Stopping Criteria:** these are the conditions that terminate the search process. In this study, the search process will stop when number of iterations reaches the maximum limit.

The Tabu Search algorithm can be described as follows:

Step 1: Generate Random initial solution, $x_{initial}$. Set $x_{best} = x_{initial} = x_{current}$.

Step 2: Trial solutions are generated randomly in the neighbourhood of the current solution.

Step 3: The objective function for trial solutions is computed and compared to best solution objective function value. If better solution is obtained then $x_{best} = x_{trial}$.

Step 4: Tabu Status of x_{trial} is tested. If it is not in the Tabu list, then add it to the list and set $x_{current} = x_{trial}$ and go to Step 7. If x_{trial} is in the Tabu list, go to Step 5.

Step 5: The Aspiration criterion is checked. If the criterion is satisfied, then the tabu status is overridden, Aspiration is updated, $x_{current} = x_{trial}$ and Step 7 follows. Otherwise, Step 6 follows.

Step 6: Check all the trial solutions by going back to Step 4. If all trial solutions are assessed, go to Step 7.

Step 7: Check the Stopping criterion. If satisfied, then stop. Otherwise, go to Step 2 for the next iteration.

These steps are illustrated in Figure 2-4.

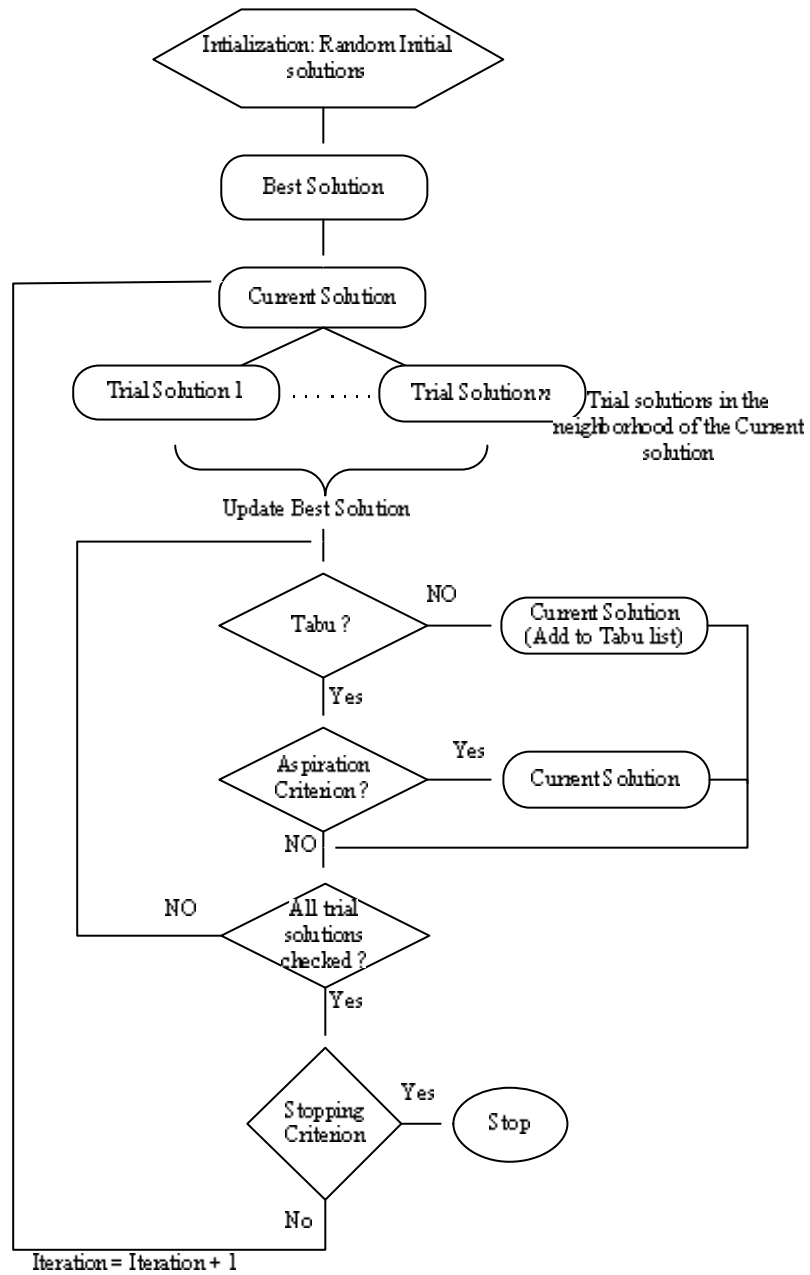


Figure 2-4: Flow chart of TS algorithm

2.5 Proposed design method of VSC

This thesis proposes to tune the parameters of the VSC using iterative heuristic optimization algorithms. The parameters of the VSC include both the switching vector values and the switching feedback gains. They are designed to give optimal performance of the controller. A performance index is chosen such that the objective of the controlled system is satisfied. Conventionally, the following objective function is used:

$$J = \int_0^{\infty} X^T Q X + U^T R U dt$$

Where Q and R are the weighting matrices of the state variable deviations and control effort respectively. Usually, both Q and R are chosen as diagonal matrices. To reduce the effect of chattering either the control effort or the deviation of the control signal is included in the performance index. The conventional VSC control laws are used for the designed system. A block diagram of the VSC is shown in Figure 2-5, where the control law is a linear state feedback whose coefficients are piecewise constant functions. Consider the linear time-invariant controllable system given by

$$\dot{X} = AX + BU \tag{2-10}$$

Where

X n -dimensional state vector

U m -dimensional control force vector

A $n \times n$ system matrix

B $n \times m$ input matrix

The VSC control laws for the system of Equation (2-10) are given by

$$u_i = -\mathbf{y}_i^T X = -\sum_{j=1}^n \mathbf{y}_{ij} x_j; \quad i = 1, 2, \dots, m \quad (2-11)$$

where the feedback gains are given as

$$\mathbf{y}_{ij} = \begin{cases} \mathbf{a}_{ij}, & \text{if } x_j \mathbf{s}_i > 0; i = 1, \dots, m \\ -\mathbf{a}_{ij}, & \text{if } x_j \mathbf{s}_i < 0; j = 1, \dots, n \end{cases} \quad (2-12)$$

and

$$\mathbf{s}_i(X) = C_i^T X = 0, \quad i = 1, \dots, m$$

where C_i are the switching vectors which are conventionally determined via a pole placement technique.

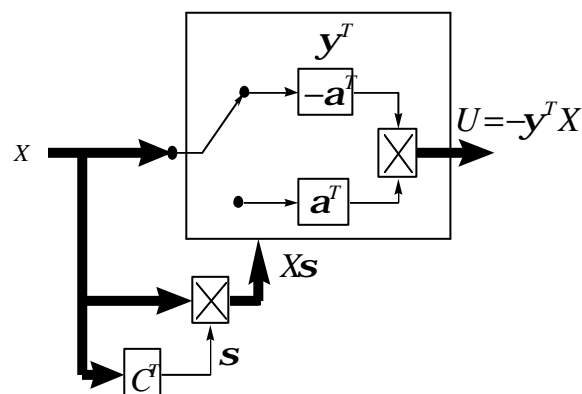


Figure 2-5: Block diagram of variable structure controller

The design procedure for selecting the constant switching vectors C_i can be found in [14]. It involves coordinate transformation to arrive at an expression suitable for use with pole placement technique.

In this thesis, we propose to find the optimal values of the switching vector and the switching feedback gains using iterative heuristic optimization algorithms. Some of the benefits of using iterative heuristic optimization algorithms in designing the VSC are:

1-The use of iterative methods in arriving at the optimal values of VSC provides a simple systematic way of designing the controller. This is especially valid when nonlinearities are included into the studied system. The proposed design requires no nonlinear transformations to formulate the system in canonical form. Conventionally, the system is transformed into suitable controllable form and then feedback control design techniques, such as linear optimal control theory or pole placement method, are used to find suitable switching surface. The proposed method cuts down this complexity of design.

2- The switching feedback gains are chosen in an optimal systematic way and not on trial and error basis.

The design procedure proposed in this thesis is shown in a flow chart form in Figure 2-6.

Furthermore, this thesis proposes to reduce the chattering in the control signal by:

1- Including a scaled value of the deviation in the control signal into the objective function being minimized. The chattering is characterized by sharp changes in the control value. Reducing these deviations will smoothen the control signal. The objective function can be written as follows (considering a discrete implementation):

$$J = \sum_{n=1}^m X(n)^T QX(n) + U_{dev}^T R U_{dev} \quad (2-13)$$

where

m = Number of samples

$$U_{dev} = U(n) - U(n-1)$$

2- Scaling the *optimum* feedback gains of the VSC on the convergence of the objective function. This is done as follows:

if $\Delta J < \varepsilon$
then $\mathbf{a}_{new} = m \cdot \mathbf{a}$
where $0 < m < 1$

J = Objective function being minimized.

ε = very small constant

\mathbf{a} = Optimum switching feedback gains

The benefits of this method are:

a) Usually when including a scaled value of the deviation of the control signal into the objective function, a compromise results between improved dynamic behavior and reduced chattering. Satisfying one will degrade the other. On the other hand, by

scaling the feedback gains on convergence of the objective function, the gains are maintained for the transient period to improve its dynamics and reduced when the system settles down. In this way, large control effort is maintained only for the transient period.

b) The controller is still a VSC controller, and therefore the beneficial features of the controller (such as robustness and good transient behavior) are preserved.

c) Simple: only alphas (switching feedback gains) are scaled

d) This idea comes from the fact that larger feedback gains reduce the reaching time on the expense of more chattering. Therefore, this large feedback gains can be maintained until the switching surface is reached and thereafter they can be reduced to minimize the chattering in the control signal.

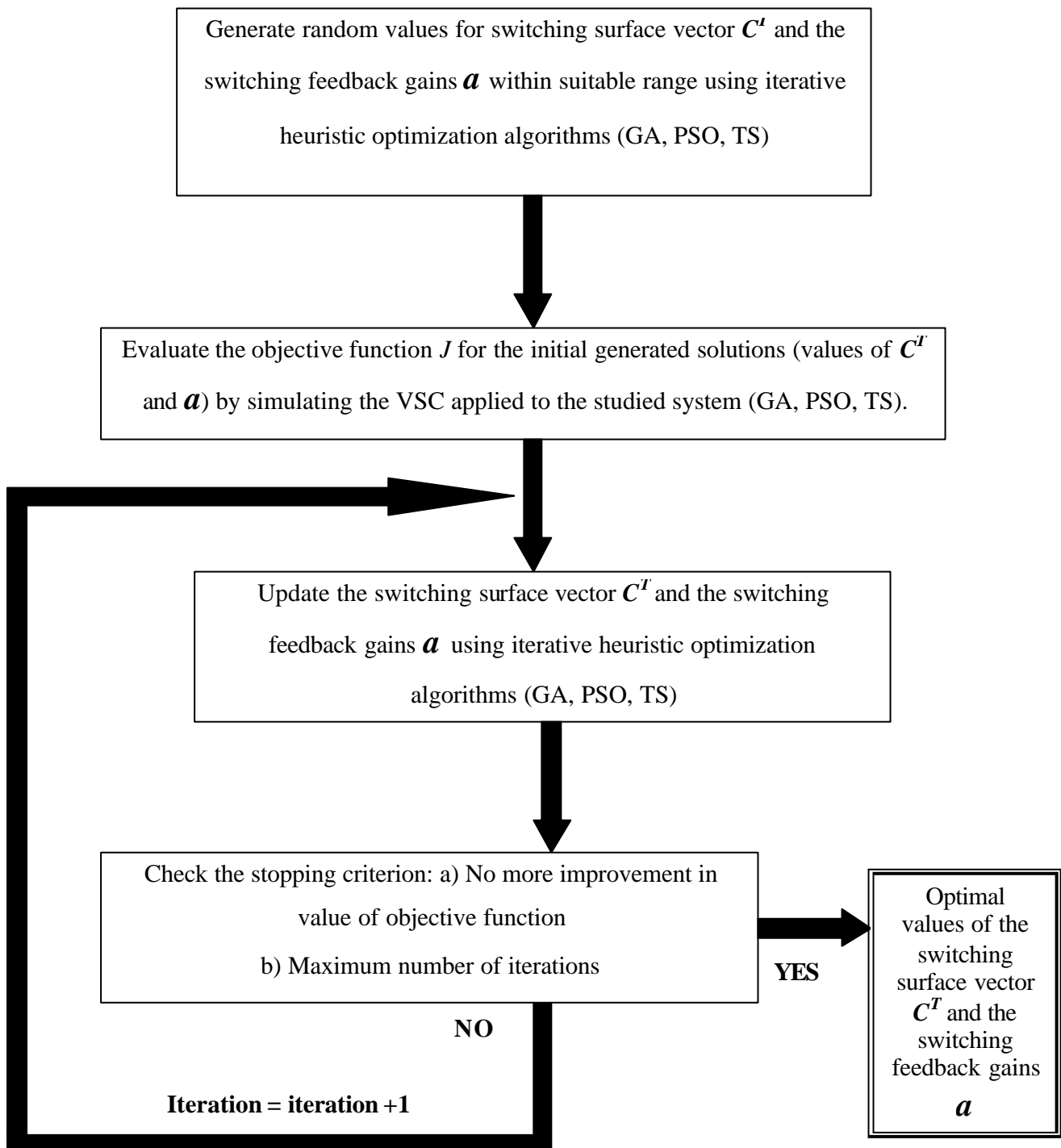


Figure 2-6: Flow chart of the proposed optimal design of VSC using iterative heuristic optimization algorithms

In this thesis, two important power system control problems will be studied with the proposed VSC design method applied. Figure 2-7 shows the division of the problems studied in this thesis. Load frequency control applications will be studied in chapter 3. This will include single area and multiareas with and without nonlinearities. Chapter 4 will investigate the application of the proposed design of VSC to the stability of a single synchronous machine connected to infinite bus. Chapter 5 will include discussion and conclusion of the results of application of the proposed VSC controller to the studied power system problems.

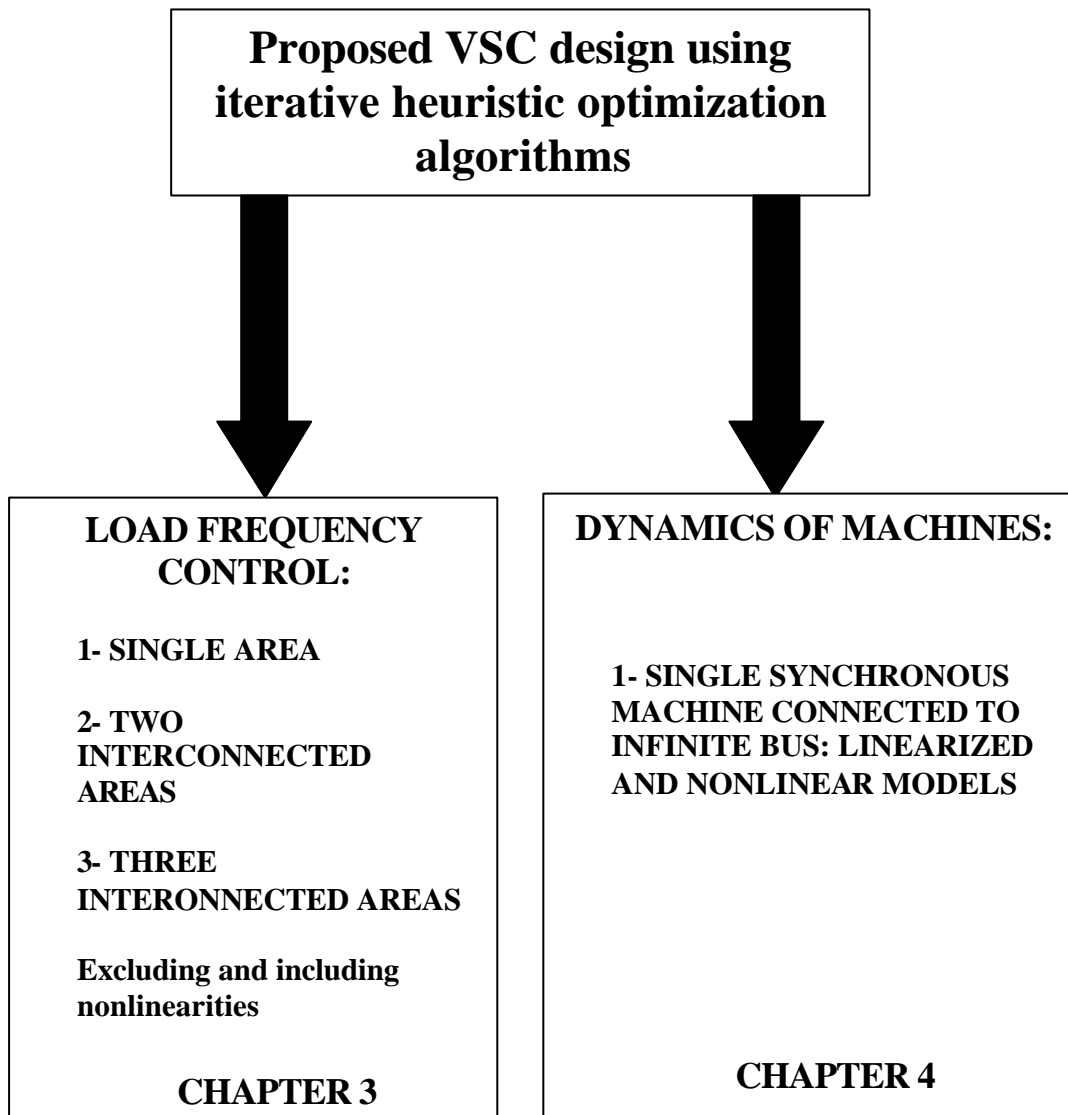


Figure 2-7: Power system dynamic problems tackled in this thesis using the proposed VSC optimal design

CHAPTER 3

APPLICATION OF THE PROPOSED VSC DESIGN TO THE LOAD FREQUENCY CONTROL PROBLEM

3.1 Introduction

The Load Frequency control (LFC) or Automatic Generation Control (AGC) has been one of the most important subjects concerning power system engineers in the last decades. In a single area, mechanical power is produced by a turbine connected to a synchronous generator. The turbine steam flow determines the frequency of the current and voltage waveforms at the output of the generator. An exact forecast of real power demand is impossible due to random changes in the load and therefore an imbalance occurs between the real power generation and the load demand (plus losses) [102]. This causes kinetic energy of rotation to be either added to or taken from the generating units (generator shaft either speed up or slow down) and the frequency of system varies as a result. Therefore, a control system is required to detect the load changes and command the steam valve to open or close more so that the turbine increase or decrease its mechanical power production and stabilize the

shaft speed and hence the system frequency. Modern real power systems constitute interconnected neighboring areas. The study of interconnected systems is essential to improve the dynamic behavior of power systems. This chapter addresses the application of the proposed VSC to the Load Frequency problem for both single and interconnected power systems areas. Studies conducted in the past have shown that area-frequencies and tie-line power can undergo prolonged fluctuations following a sudden change in power in an interconnected power system [7]. The main cause of these fluctuations is the nonlinearities present in the system. The most important nonlinearities are: governor dead band backlash and generation rate constraint. A multi-area LFC system constitutes a number of single areas connected by a tie line. This tie line allows the flow of power between the areas. Consequently, a disturbance in one area influences the frequency output of other areas as well as the tie line power. The objective of the LFC system is to minimize deviations of both frequency of all areas and tie line power interchanges. Various techniques were proposed for the design of single and multi-area LFC. However, these techniques are of two types: Primary and Supplementary. The former type of design includes tuning the parameters of the primary control of LFC. A good example of this technique is found in [149], where the optimum value of the speed regulation for an interconnected system is investigated. Supplementary type LFC techniques were discussed in Chapter 1. This chapter studies the application of the proposed design of VSC to

single, two, and three area power systems. The effect of including the nonlinearities into the models is also considered.

3.2 Proposed VSC Design for a Single area Power system

3.2.1 Linear and Nonlinear Models of a single area LFC system

The model for LFC of a nonreheat turbine for single area power system excluding nonlinearities is shown in Figure 3-1 (a) [14]. The model shows the feedback of the change in frequency to turbine through speed regulator and an integral controller. The dynamic model in state variable form can be obtained from the transfer function model and is given as:

$$\dot{X} = AX(t) + Bu(t) + Fd(t) \quad (3-1)$$

Where X is a 4-dimensional state vector, u is 1-dimensional control force vector, d is 1-dimensional disturbance vector, A is 4×4 system matrix, B is a 4×1 input vector, and F is 4×1 disturbance vector.

$$A = \begin{bmatrix} -1/T_p & K_p/T_p & 0 & 0 \\ 0 & -1/T_i & 1/T_i & 0 \\ -1/RT_g & 0 & -1/T_g & -1/T_g \\ K & 0 & 0 & 0 \end{bmatrix}$$

$$B^T = \begin{bmatrix} 0 & 0 & \frac{1}{T_g} & 0 \end{bmatrix}$$

$$F^T = \begin{bmatrix} \frac{K_p}{T_p} & 0 & 0 & 0 \end{bmatrix}$$

T_p : the plant model time constant,

T_t : the turbine time constant,

T_g : the governor time constant

K_p : the plant gain,

K : the integral control gain

R : the speed regulation due to governor action.

x_2 , x_3 , and x_4 are respectively the incremental changes in generator output (p.u. MW), governor valve position (p.u. MW) and integral control. The control objective in the LFC problem is to keep the change in frequency (Hz) $\Delta w = x_1$ as close to zero as possible when the system is subjected to a load disturbance d by manipulating the input.

The model in Figure 3-1(a) excludes system nonlinearities. Figure 3-1(b) and (c) show other models considered in this study that include two types of nonlinearities: Generation rate constraint (GRC) and governor dead band nonlinearity. Figure 3-1 (b) considers the effect of GRC. The GRC is caused by the mechanical and

thermodynamic constraints in practical steam turbines systems. It imposes limits on the rate of change of generated power. A typical value of 0.1 p.u./min [7] has been chosen in this study. The model of Figure 3-1(b) also has a limiter on the integral control values to prevent excessive control. The second model, Figure 3-1 (c), applies limits to the position of the governor valve and the rate of its change [19]. It also includes the governor dead band backlash. The dead band of the speed governor is defined as “the magnitude of the change in steady-state speed within which there is no resulting change in the position of the governor-controlled valves or gates” [103]. A good reference that discusses the effect of dead band on LFC systems is found in [106]. The effect of dead band on a given sinusoidal input is illustrated in Figure 3-2.

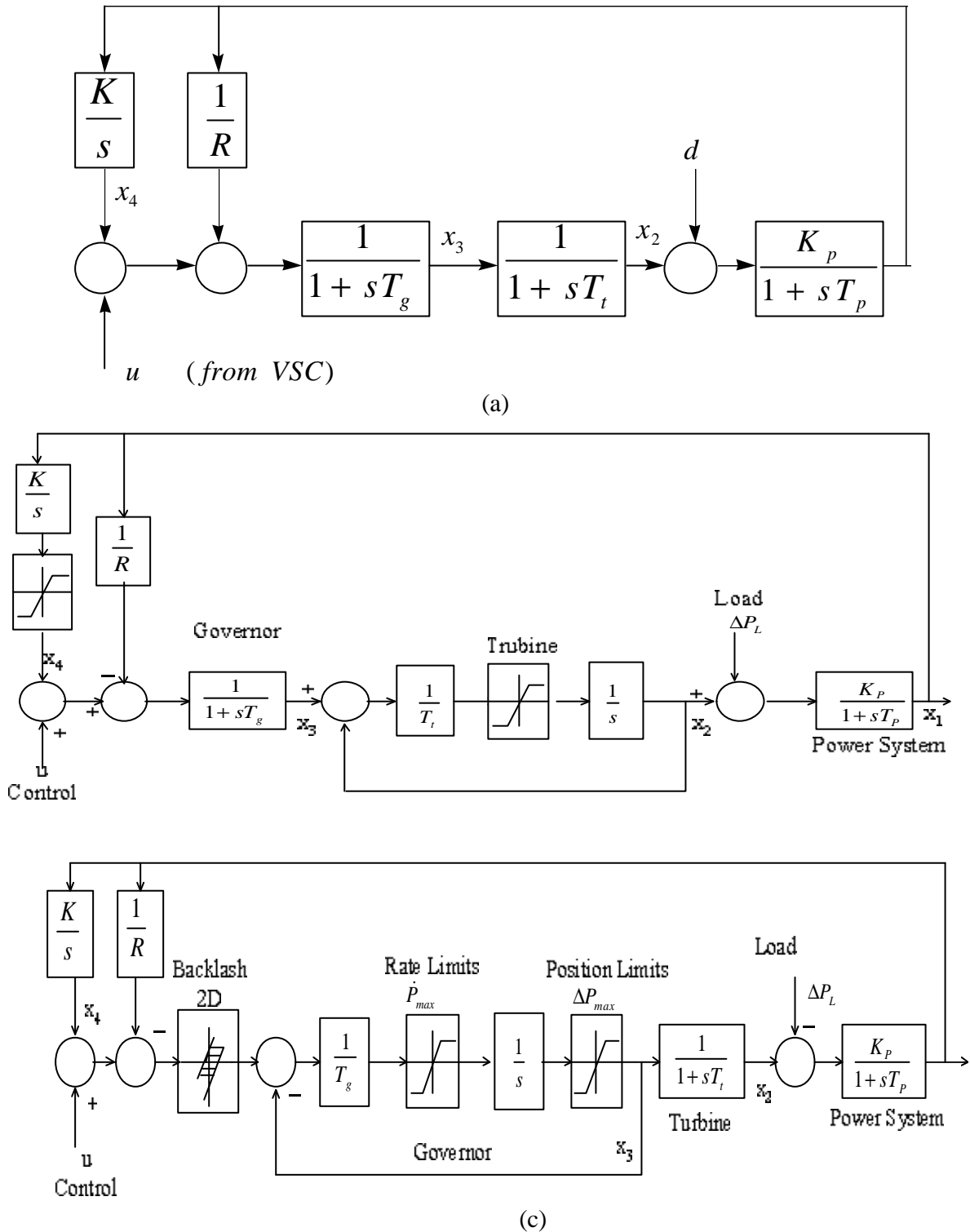
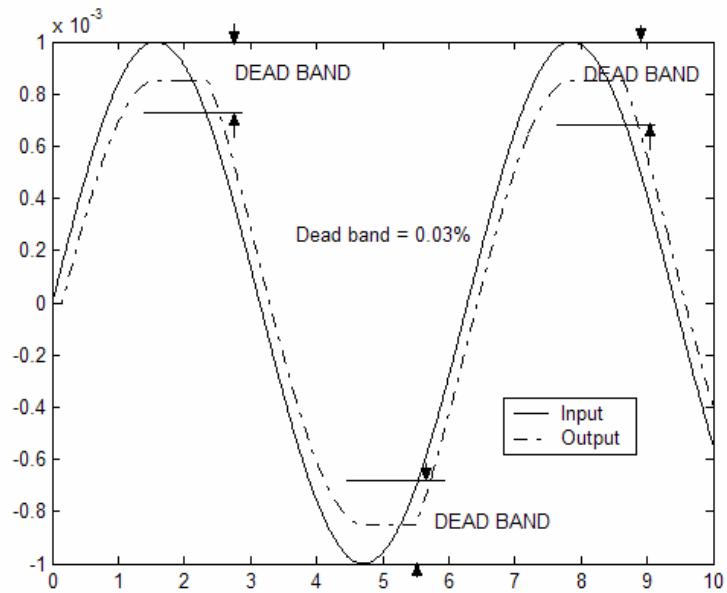
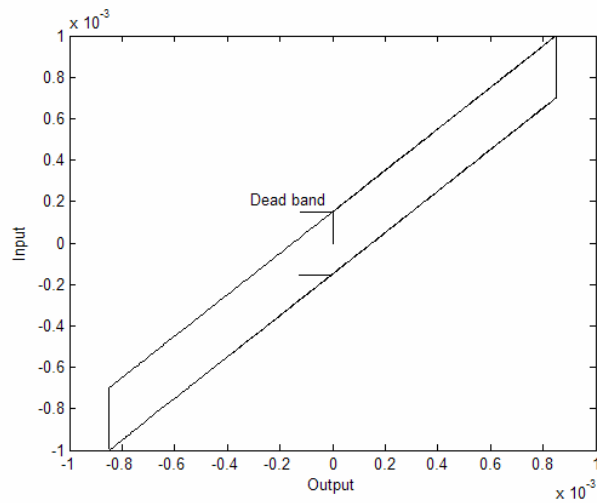


Figure 3-1: Single area LFC system (a) Excluding nonlinearities (b) with Generation rate constraint (GRC) (c) with GRC and governor dead band backlash



(a)



(b)

Figure 3-2: Effect of Dead band on a given input

3.2.2. Proposed VSC design for a single area LFC system excluding nonlinearities

The design procedure explained in Chapter 2 is applied to design a VSC for a single area LFC excluding nonlinearities. Different objective functions were used for optimization procedure. They are given below:

$$J_1 = \int_0^{\infty} \mathbf{D}\mathbf{w}^2 dt \quad (3-2)$$

$$J_2 = \int_0^{\infty} q_1 \mathbf{D}\mathbf{w}^2 + q_2 u^2 dt \quad (3-3)$$

$$J_3 = \int_0^{\infty} q_1 \mathbf{D}\mathbf{w}^2 + q_2 \mathbf{D}u^2 dt \quad (3-4)$$

where

J_1 : reflects the objective of the LFC where the deviation in frequency $\Delta\mathbf{w}$ is minimized.

J_2 : includes the control effort. In this way, the control effort will be minimized and therefore the chattering effect will be reduced.

J_3 : deviation of the chattering is included here. Since chattering is characterized by a dramatic change in the control signal, inclusion of deviation of the control effort in the performance index will allow smoothening of the control signal and thus further reduce chattering.

The parameters of the system under study [14], Figure 3-1, are given below:

$$\begin{array}{ll}
 T_p = 20 \text{ s} & K_p = 120 \text{ Hz p.u. MW}^{-1} \\
 T_t = 0.3 \text{ s} & K = 0.6 \text{ p.u. MW rad}^{-1} \\
 T_g = 0.08 \text{ s} & R = 2.4 \text{ Hz p.u. MW}^{-1}
 \end{array}$$

The proposed VSC design using PSO algorithm described in Chapter 2 has been applied to minimize the performance indices for optimal selection of the switching vector and feedback gains. The PSO parameters used are the number of particles $n = 15$, maximum number of iterations $m = 500$, dimension $d = 4$, $w_{max} = 0.9$, $w_{min} = 0.4$, and the maximum velocity constant factor $k = 0.1$. The algorithm is terminated when there is no significant improvement in the value of the performance index. The system is subjected to a step load change of 0.03 p.u. (3%). Table 3-1 (a) shows the performance indices and weighting coefficients used in different designs. The optimal switching vectors and feedback gains are given in Table 3-1(b). The values of Design No.1 in Table 3-1(b) were taken from [14], where pole placement is used to obtain the switching vector. The feedback gains were obtained by trial and error. In designs No. 2 and 3 [20], the authors used GA to arrive at the optimal feedback gains. The switching vector was obtained from [14].

Table 3-1: (a) Performance indices and weighting coefficients for different designs
 (b) Switching vectors, C^T , and feedback gains, a of VSC designs. Design number 1
 was obtained from [14]. Designs number 2 and 3 were obtained from [20]

(a)

No.	Performance Index, J	q_1	q_2
1	-	-	-
2	J_1	-	-
3	J_2	1	1
4	J_1	-	-
5	J_2	1	1
6	J_2	1	0.5
7	J_3	1	1
8	J_3	1	0.5

(b)

No.	C^T	a
1	[5.16 4.39 1 16]	[6 6 2 0]
2	[5.16 4.39 1 16]	[2.08 0.025 1.40 0]
3	[5.16 4.39 1 16]	[0.76 0.002 1.40 0]
4	[4.62 1.39 0.085 30]	[3 3 3 3]
5	[1.97 1.65 0.28 2.44]	[0.76 0 0 0]
6	[3.25 0 2.32 2.34]	[1.11 0 0 0]
7	[2.77 0.75 0.84 4.95]	[2 0.005 0.797 1.06]
8	[5 0.7423 1.7130 5]	[2 0 0 2]

The dynamic performance of the system for the present optimum switching vectors and feedback gains is shown in Figure 3-3. Figure 3-3 (a) shows the convergence of the performance index for the different designs of Table 3-1

The following can be concluded from the results of this simulation

- 1) The new design method gives a tradeoff between improved frequency response and chattering reduction. Designs number 5-8 gave a significant reduction in chattering, Figure 3-3 (f), with some degradation in frequency response, Figure 3-3 (c).
- 2) Therefore, the designer can control the compromise between frequency and chattering reduction by altering the values of q_1 and q_2 of the performance indices.
- 3) In design number 4, a significant improvement in the frequency deviation was achieved, Figure 3-3(b). However, there was an increased chattering in the control effort as shown in Figure 3-3(e).
- 4) The LFC is robust for change in the type of load disturbance applied to the system. This is depicted in Figure 3-4(a).

The last point brings an idea of obtaining a VSC design that will both improve the dynamic behavior of the system and reduce chattering. It is noticed that those designs with reduced chattering have a relatively small feedback gains. Furthermore, it is known that a larger feedback gain in VSC will guarantee a faster reaching time and hence improved dynamics. Therefore, the following is proposed:

For the optimum values of feedback gains and switching vector (in this case design no. 4 values are tested) values:

if $\Delta J < \varepsilon$
then $\mathbf{a}_{new} = m.\mathbf{a}$
where $0 < m < 1$

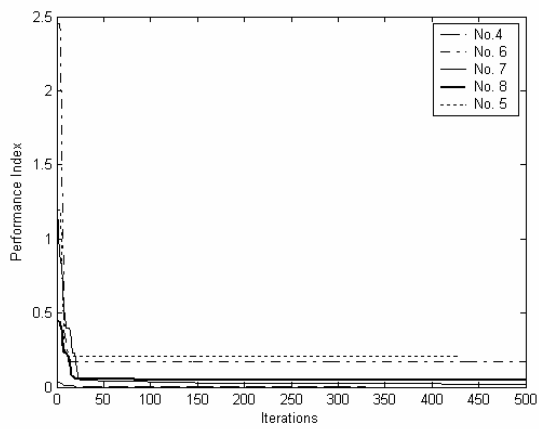
J = Objective function being minimized. In this case it is $\int D\mathbf{w}^2 dt$

ε = very small constant

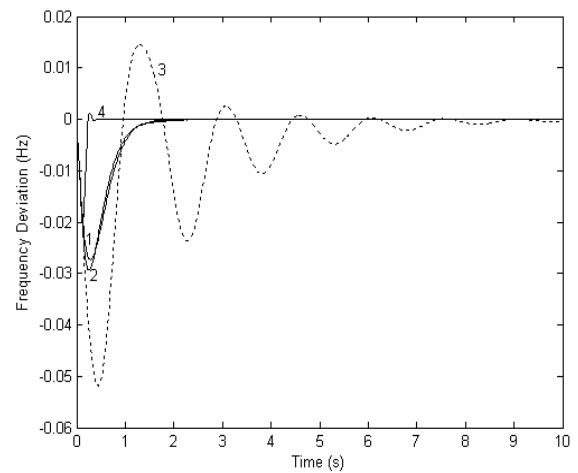
\mathbf{a} = Optimum switching feedback gains

This method was applied on design no. 4 of Table 3-1. The threshold $\varepsilon = 1 \times 10^{-5}$ and the scaling factor m was chosen = 0.3. Figure 3-4(b)-(d) shows the application of this method.

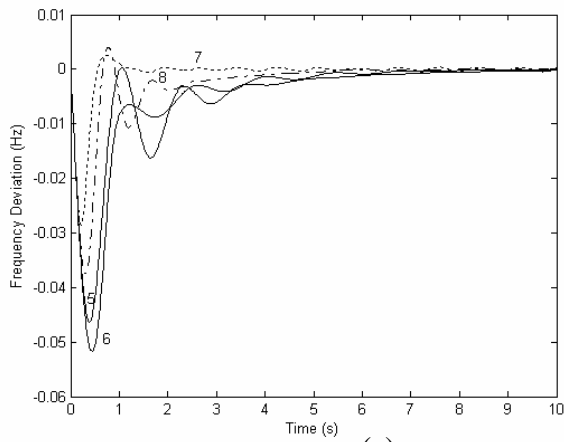
It is shown that the chattering is dramatically reduced with out a noticeable degradation in the performance of the system.



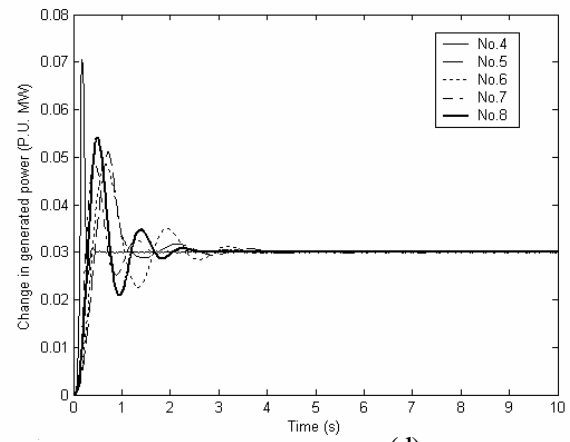
(a)



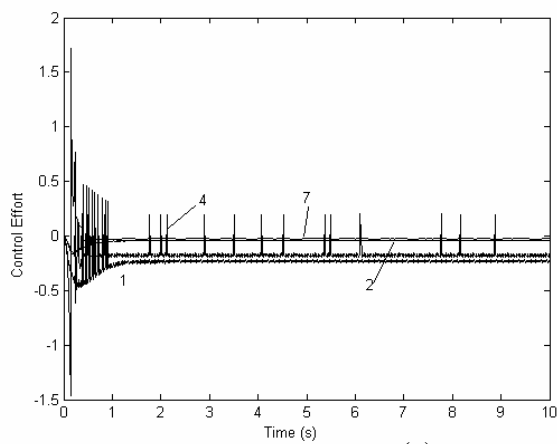
(b)



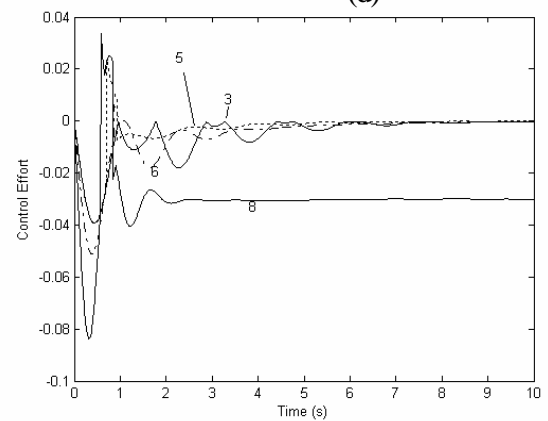
(c)



(d)



(e)



(f)

Figure 3-3: (a) Convergence of objective function (b) Frequency deviation for designs no. 1-4 (c) Frequency deviation for designs 5-8 (d) Change in generated power for designs 4-8 (e) Control effort for designs 3, 5, 6, and 8

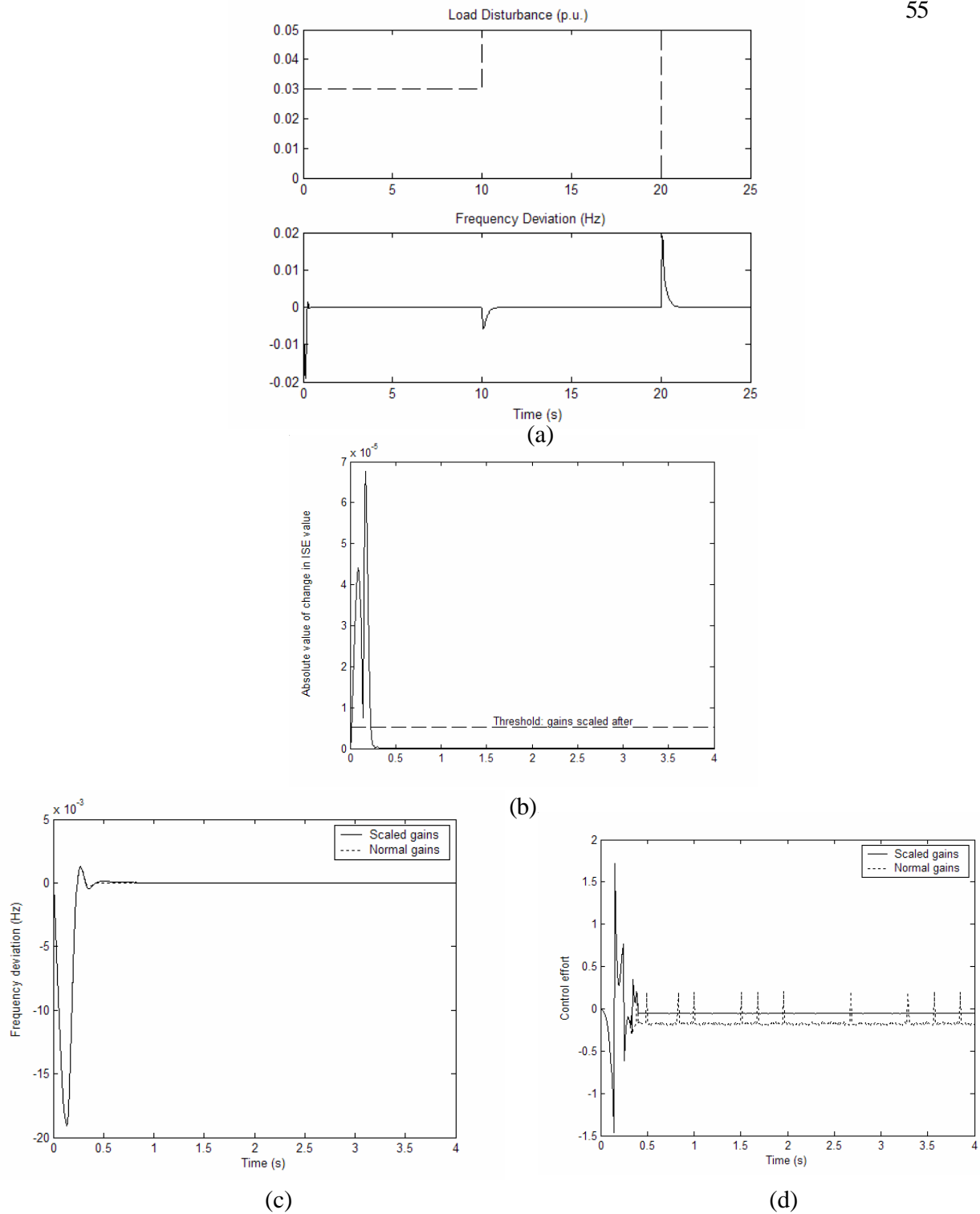


Figure 3-4: (a) Robustness against change in load disturbance (Design no. 4) (b-d) Scaling of switching feedback gains (b) Convergence of deviation of the performance index (b) Frequency deviation (c) Control effort

3.2.3 Proposed VSC design for a single area LFC with nonlinearities included in the model

In this section the two nonlinear models of single area LFC system of Figure 3-1 (b) and (c) are studied. The Tabu search algorithm is used as the search engine for the optimal settings of the controller. Two cases are investigated:

CASE I: In this case comparison with a robust controller design of Wang method [118] was investigated. The LFC model with GRC, Figure 3-1 (b), was used. The following are the parameters of the system [118]:

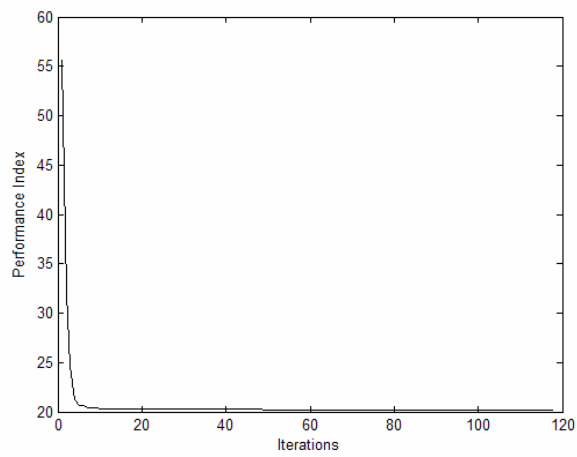
$$\begin{aligned} 1/T_p &= 0.0665 & 1/RT_g &= 6.86 \\ 1/T_t &= 3.663 & K_p/T_p &= 8 \\ 1/T_g &= 13.736 & K &= 0.6 \end{aligned}$$

A GRC of 0.1 p.u. MW per minute = 0.0017 p.u. MW/sec was included in the model. The response of the system for 0.01 p.u. disturbance is tested. The design procedure described in Chapter 2 for TS algorithm is used with J_3 of section 3.2.2 as the objective function. The weighting coefficients were both unity. A Tabu list of size =7 is used in this case. The following optimal settings of the VSC were obtained:

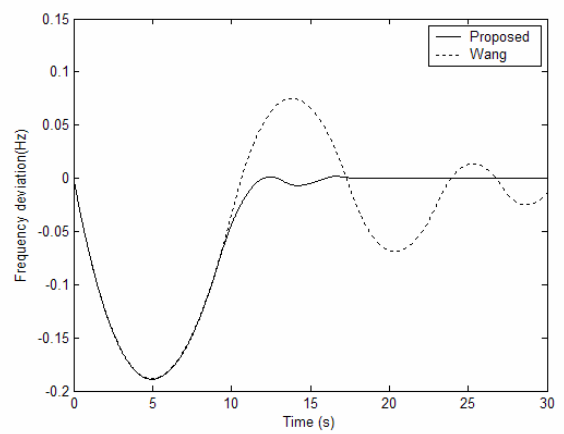
$$\begin{aligned} C^T &= [1.6384 \quad 28.9077 \quad 9.3736 \quad 6.8697] \\ a &= [0.2616 \quad 0.3022 \quad 0.8951 \quad 0.0335] \end{aligned}$$

Figure 3-5 shows the convergence of the performance index and dynamical response of the system to the load disturbance. Figure 3-6 shows the robustness of LFC system

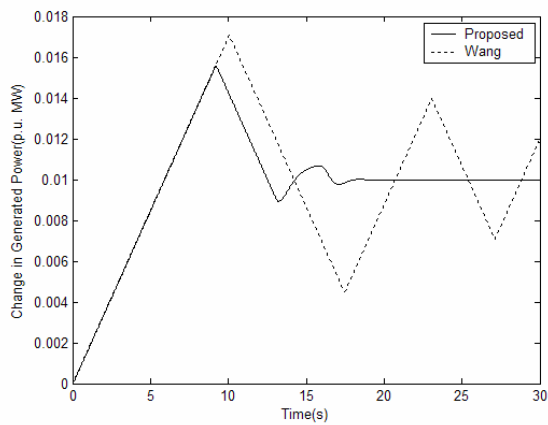
with the proposed VSC design against varying the system parameters, such as $1/T_p$, $1/T_g$, $1/RT_g$, $1/T_i$, and K_p/T_p , by 25%.



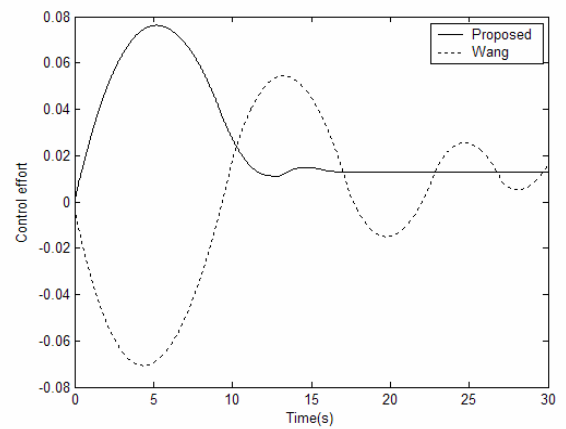
(a)



(b)

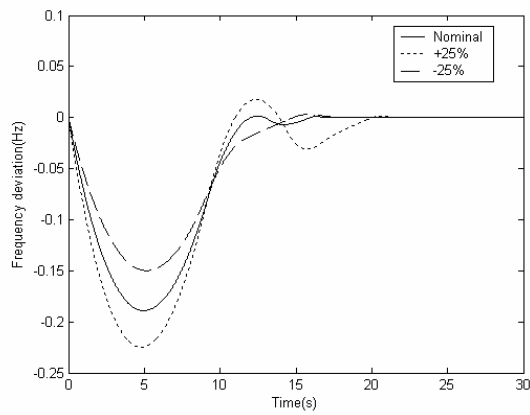


(c)

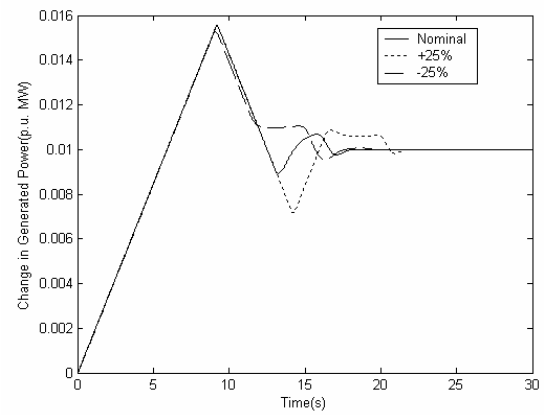


(d)

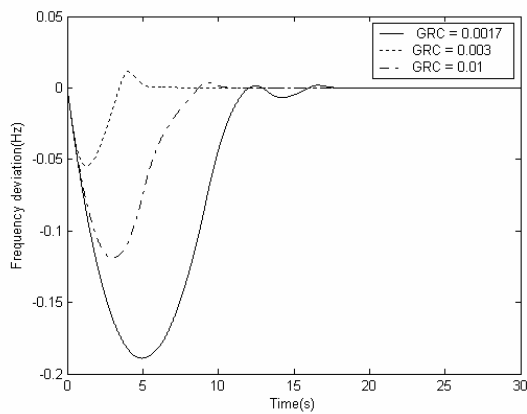
Figure 3-5: (a) Convergence of performance index (b) Frequency deviation (c) Change in generated power (d) Control effort



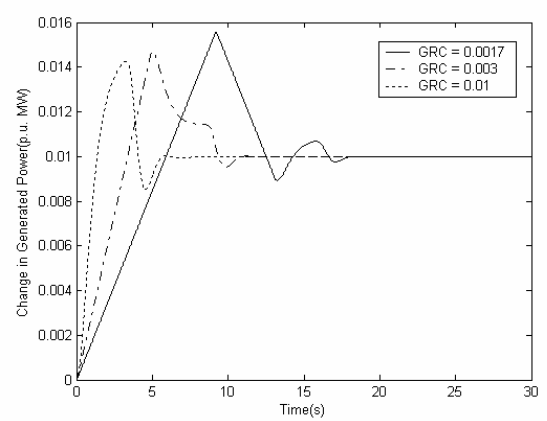
(a)



(b)



(c)



(d)

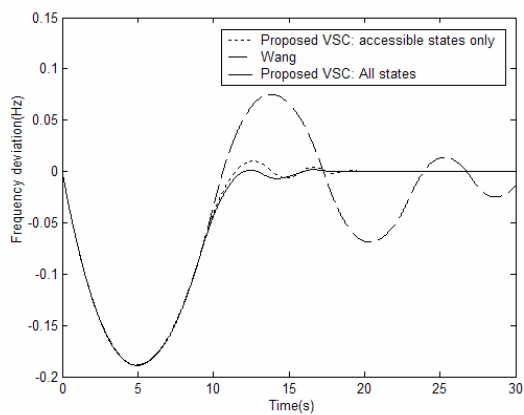
Figure 3-6: (a)-(b) Robustness of the system with the proposed VSC design for 25% change in $1/T_p$, $1/T_g$, $1/RT_g$, $1/T_b$, and K_p/T_p (c)-(d) Effect of varying the GRC on the controller robustness

Furthermore, the complexity of the VSC can be reduced if only the accessible states are feedback. This was done for the same above system with the same parameter values. The states fed back are Dw (frequency deviation) and DP_g (change in generated power). Again, J_3 was used in the optimization process using Tabu search algorithm. The following are the optimal settings of the controller:

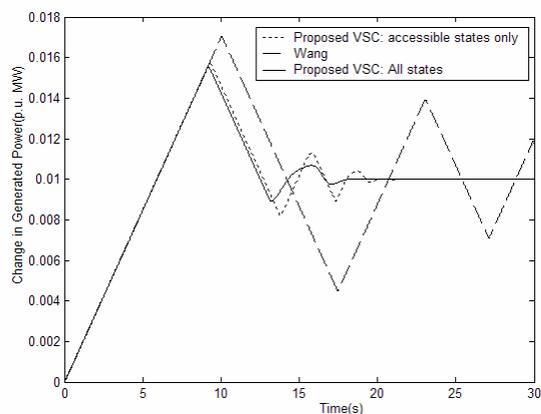
$$C^T = [0.2225 \quad 26.697]$$

$$a = [0.3689 \quad 0.6368]$$

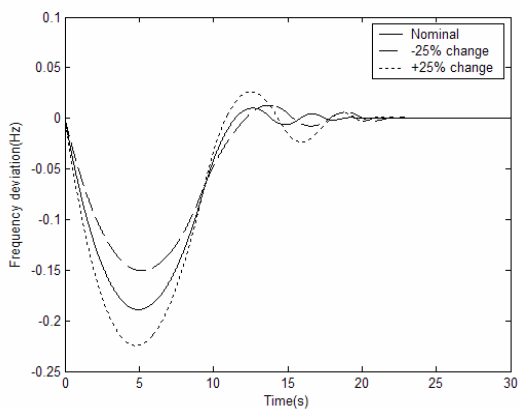
Figure 3-7 shows the results of the application of the proposed VSC. As shown in Figure 3-7 (a) and (b), the proposed VSC design improves the dynamical response of the system even if only the accessible states are feedback. In addition, the system maintains its robustness as shown in Figure 3-7(c) and (d) with only the two accessible states used in the design.



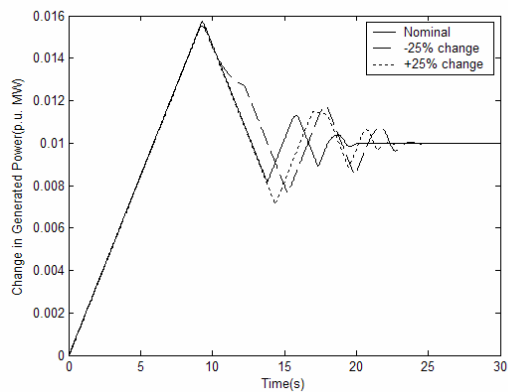
(a)



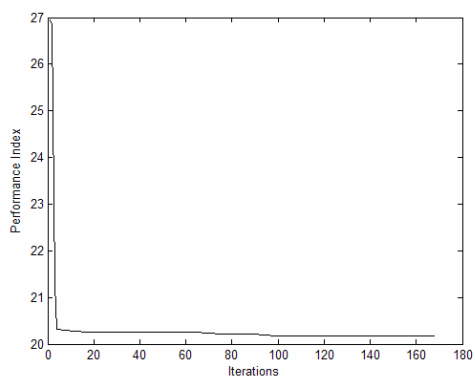
(b)



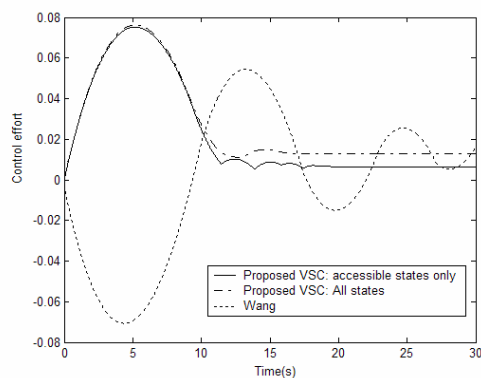
(c)



(d)



(e)



(f)

Figure 3-7: Proposed VSC design with accessible states only: (a) Frequency deviation (b) Change in generated power (c) Robustness of frequency deviation (d) Robustness of change in generated power (e) Convergence of performance index (f) Control effort

CASE II: In this case the LFC system model of Figure 3-1(c) was simulated with governor dead band included in the model. The following parameters were used ([14], [19]):

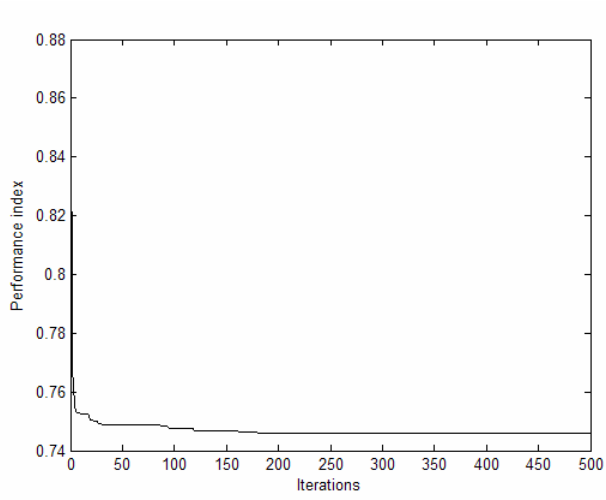
$$\begin{aligned} T_p &= 20 \text{ s} & K_p &= 120 \text{ Hz p.u.MW}^{-1} \\ T_t &= 0.3 \text{ s} & K &= 0.6 \text{ p.u. MW rad}^{-1} \\ T_g &= 0.08 \text{ s} & R &= 2.4 \text{ Hz p.u. MW}^{-1} \end{aligned}$$

Again, the proposed design procedure using TS was applied to the studied system. Tabu list size of 7 and maximum iterations of 500 were used. Performance index J_I of section 3.2.2 was used in the search process. The system is subjected to a step load change of 0.005 p.u.MW. A backlash of deadband $2D = 0.001$ and generation limits $\dot{P}_{max} = 0.1$ p.u.MW/min and $\Delta P_{max} = 0.03$ p.u.MW are applied. The convergence of the performance index is shown in Figure 3-8 (a). The optimal settings of VSC are:

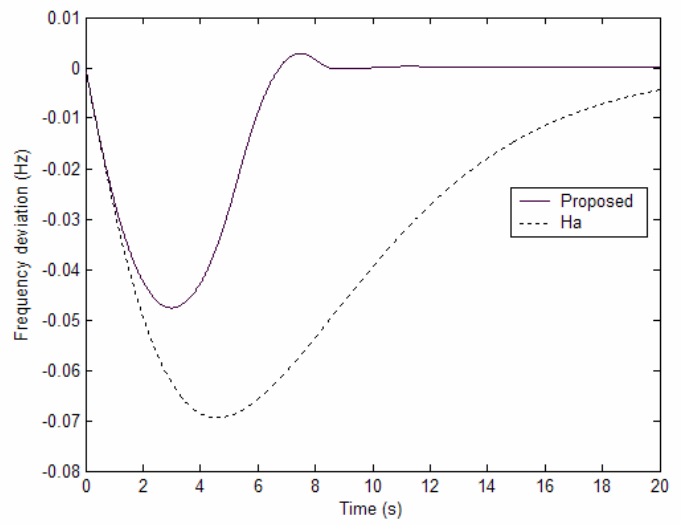
$$\mathbf{C}^T = [14.8804 \quad 37.3156 \quad 47.5501 \quad 2.9652]$$

$$\mathbf{a} = [3.3792 \quad 4.7826 \quad 4.4277 \quad 0.5580]$$

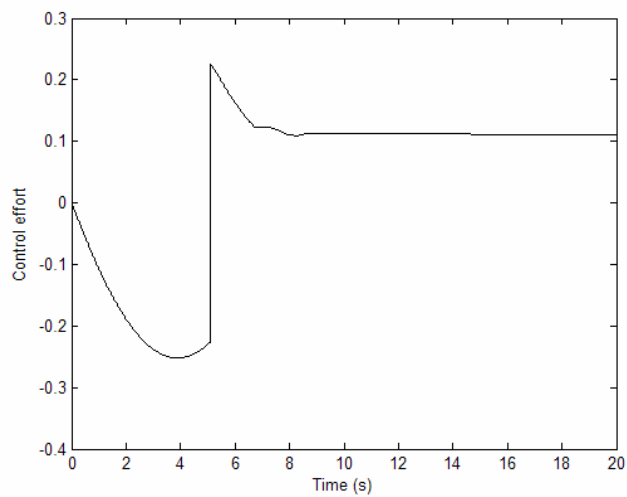
The convergence of the performance index and the dynamics of the system are shown in Figure 3-8. Figure 3-8 (d) shows the robustness of the system under parameter variations. It is very clear that the proposed design is very robust.



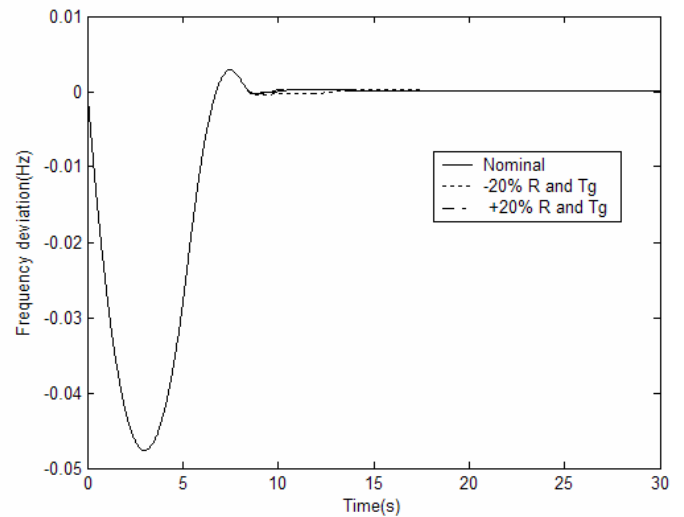
(a)



(b)



(c)



(d)

Figure 3-8: (a) Convergence of performance index (b) Frequency deviation (c) Control effort (d) Robustness of the proposed design

From the previous simulation results, the following can be concluded:

- a) The new optimal design method allows the design of VSC with improved dynamical behavior. Figures 3-5(b) and (c) of case I and Figure 3-8 (b) of case II shows this improvement.
- b) Smooth control effort was achieved. This is depicted in Figures 3-5 (d) and 3-8 (c).
- c) The system was robust for changes in its parameters. This is shown in Figures 3-6(c)-(d) and 3-8(d).
- d) A robust VSC with both improved dynamic behavior and smooth control effort was designed with only the accessible states, Figure 3-7.
- d) The new proposed design allows the inclusion of nonlinearities into the model of the studied system. Both models of the studied cases of this section included nonlinearities.

3.3 Two area Interconnected Power system areas

In this section, application of the proposed VSC design to two area interconnected power system is investigated. Figure 3-9 [105] shows the model of the system. The model shown includes nonlinearities in the form of Generation rate constraint and governor dead band backlash.

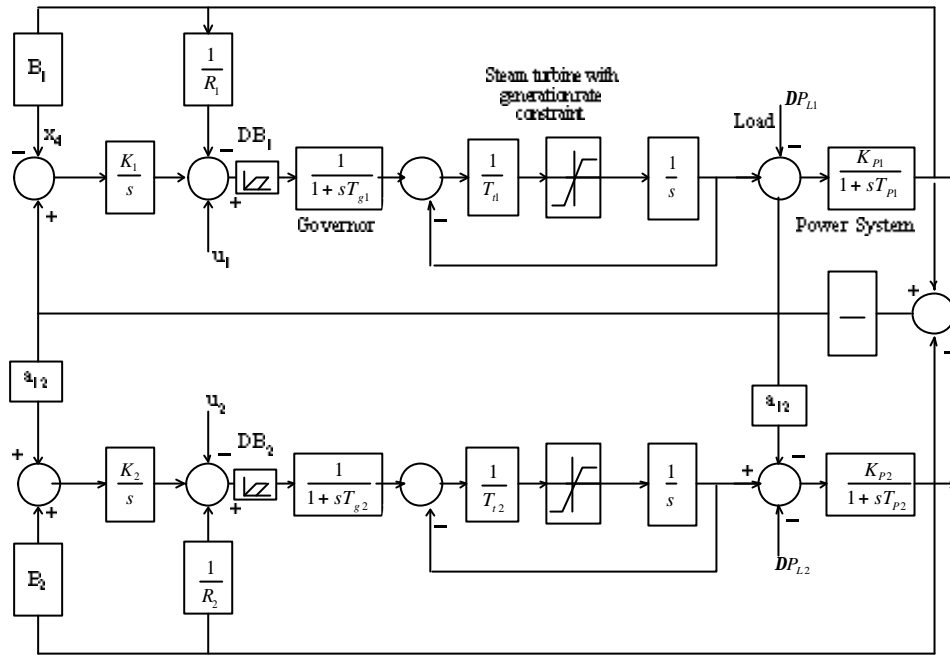


Figure 3-9: Two area interconnected LFC system with nonlinearities

3.3.1 The Proposed design of VSC applied to Two Interconnected LFC areas excluding nonlinearities

In this part, nonlinearities in the form of governor dead band (DB in Figure 3-9) and generation rate constraint are excluded from the model. The parameters of the system used for this part are:

$$\begin{aligned}
 T_{p1} &= T_{p2} = 20\text{s} & K_{p1} &= K_{p2} = 120 \text{ Hz p.u. MW}^{-1} \\
 T_{i1} &= T_{i2} = 0.3\text{s} & K_1 &= K_2 = 0.6 \text{ p.u. MW rad}^{-1} \\
 T_{g1} &= T_{g2} = 0.08\text{s} & R_1 &= R_2 = 2.4 \text{ Hz p.u. MW}^{-1} \\
 2pT_{i2} &= 0.545 \text{ p.u. MW} & B_1 &= B_2 = -a_{12} = 1
 \end{aligned}$$

The above system is simulated for a load disturbance in area 1. As mentioned before, a disturbance in one area affects the others due to the interconnection between them. Different designs of VSC will be investigated and applied for the above system.

3.3.1.1 Design of an optimal feedback gains with fixed switching surface controller

The design of an optimal VSC for interconnected system is compared with that in [17]. In [17], pole placement and optimal control techniques were used to arrive at the optimal switching surface C . The feedback gains were chosen arbitrary. In this thesis, the feedback gains were selected using iterative heuristic algorithms. In this example, Particle swarm optimization is used to arrive at the optimal feedback gains. The interconnected system is simulated for a 0.03 p.u. disturbance in area 1. The switching surface value is given by [17]:

$$C^T = \begin{bmatrix} 2.423 & 2.73 & 1 & 4.06 & -1.36 & -0.4355 & -0.311 & 0 & -0.945 \\ -0.750 & -0.449 & 0 & -2.36 & 0.9933 & 2.84 & 2.89 & 1 & 5.873 \end{bmatrix}$$

The feedback gains used in [17] are:

$$\begin{aligned} \mathbf{a}_{11} &= \mathbf{a}_{14} = -\mathbf{b}_{11} = -\mathbf{b}_{14} = 1 \\ \mathbf{a}_{26} &= \mathbf{a}_{29} = -\mathbf{b}_{26} = -\mathbf{b}_{29} = 1 \end{aligned}$$

and all other \mathbf{a}_{ij} and $\mathbf{b}_{ij} = 0$.

Particle Swarm optimization is applied with the following settings: $n = 15$, maximum number of iterations = 500, $w_{max} = 0.9$, $w_{min} = 0.4$, and the maximum velocity constant

factor $k = 0.1$. Different objective functions were tested for the optimal design. They are given below:

$$J_1 = \int_0^{\infty} \mathbf{D}\mathbf{w}_1^2 + \mathbf{D}\mathbf{w}_2^2 + \mathbf{D}P_{ie}^2 + \mathbf{D}P_{g1}^2 + \mathbf{D}P_{g2}^2 dt \quad (3-5)$$

$$J_2 = \int_0^{\infty} \mathbf{D}\mathbf{w}_1^2 + \mathbf{D}\mathbf{w}_2^2 + \mathbf{D}P_{ie}^2 + 0.3\mathbf{D}P_{g1}^2 + 0.3\mathbf{D}P_{g2}^2 + 0.5\mathbf{D}u_1^2 + 0.1u_2^2 dt \quad (3-6)$$

$$J_3 = \int_0^{\infty} |\mathbf{D}\mathbf{w}_1|t + |\mathbf{D}\mathbf{w}_2|t + |\mathbf{D}P_{ie}|t + 0.7\mathbf{D}P_{g1}^2 + \mathbf{D}P_{g2}^2 + 0.5\mathbf{D}u_1^2 + 0.1\mathbf{D}u_2^2 dt \quad (3-7)$$

J_1 : ensures internal stability of the interconnected systems. The various terms are equally scaled without including the control effort signal.

J_2 : includes scaled values of the deviation in the control signal. This will allow the design of VSC with reduced chattering in the control signal.

J_3 : investigates minimizing the integral absolute time of some of the parameters of the interconnected systems. The IAET ensures that internal parameters of the LFC area go to the desired steady state value. Again, scaled values of the deviation in the control signals are included.

The values of the optimum switching feedback gains for each objective function are given below.

a) Objective function J_1 :

$\mathbf{a}_1 =$

$$\begin{matrix} \hat{e} & \dot{e} & \ddot{e} & \hat{u} & \dot{u} & \ddot{u} \\ \begin{matrix} 1.0000 & 0.0064 & 1.0000 & 0 & 0.4155 & 0.2450 & 0.6826 & 0.9410 & 0.3737 \\ 1.0000 & 1.0000 & 0.5401 & 0.7377 & 0.5558 & 0.4905 & 0.7339 & 0.4242 & 1.0000 \end{matrix} \end{matrix}$$

b) Objective function J_2 :

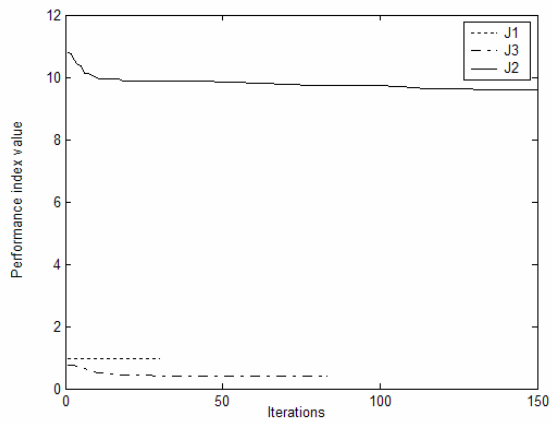
$$\mathbf{a}_2 = \begin{matrix} \hat{e} & \dot{e} & \ddot{e} & \hat{u} & \dot{u} & \ddot{u} \\ \begin{matrix} 0.8947 & 0 & 0 & 0 & 0 & 0 & 0 & 0 & 0 \\ 0 & 0 & 0 & 0.3135 & 0 & 0.1766 & 0 & 0.2188 & 0.3029 \end{matrix} \end{matrix}$$

c) Objective function J_3 :

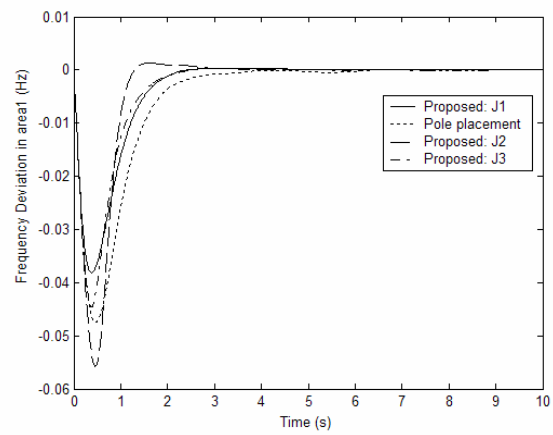
\mathbf{a}_3

$$\begin{matrix} \hat{e} & \dot{e} & \ddot{e} & \hat{u} & \dot{u} & \ddot{u} \\ \begin{matrix} 0.1110 & 0.5530 & 0 & 0.2217 & 0.5529 & 0.4248 & 0.7176 & 0 & 0.3639 \\ 0.0000 & 0.0028 & 0 & 0.2215 & 0.4568 & 0 & 0.2586 & 0.3392 & 0.552 \end{matrix} \end{matrix}$$

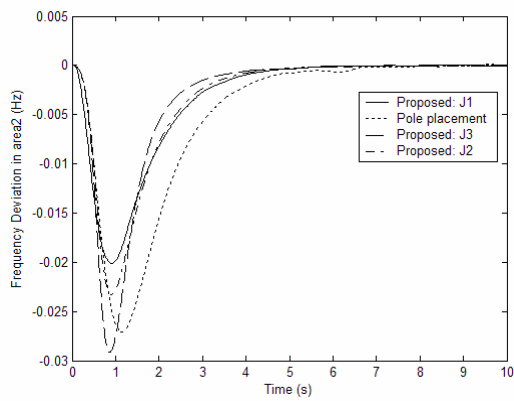
Figure 3-10(a) shows the convergence of the different objective functions. Figure 3-10(b)-(f) shows the dynamic response of the system for a 0.03 p.u. load disturbance in area 1. The results show that using objective function J_1 gives the best dynamics for the system; this includes both reduced overshoot and faster settling of the parameters. However, this is on the expense of more fluctuations in the control signal, Figure 3-11. Objective function J_2 provides the best compromise in terms of both improved dynamic behavior compared with the pole placement method and smooth control signal.



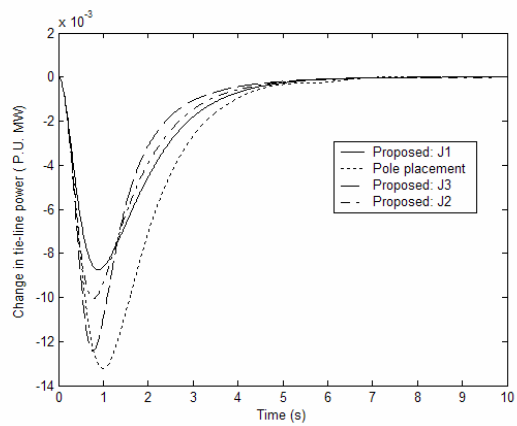
(a)



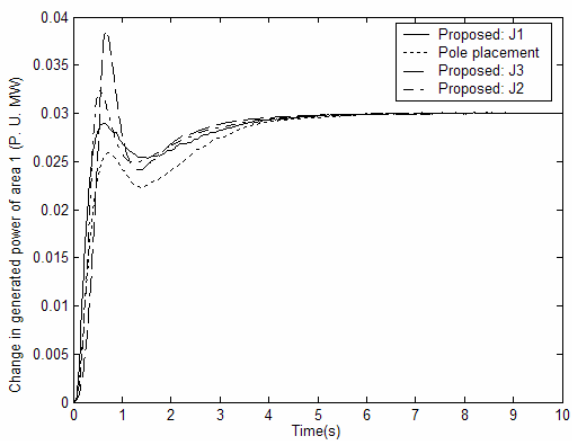
(b)



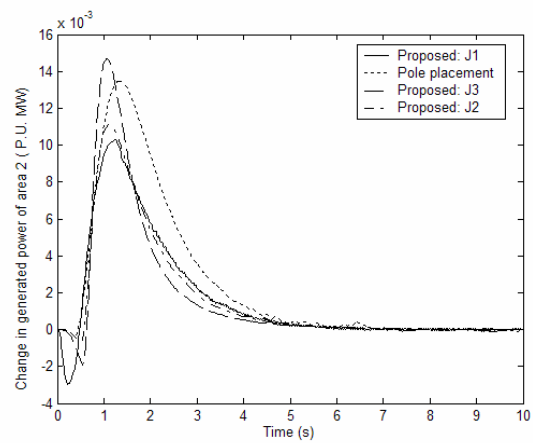
(c)



(d)



(e)



(f)

Figure 3-10: (a) Convergence of performance index (b)-(f) Dynamical behavior of the interconnected system for a 0.03 p.u. load disturbance in area 1 (... [17])

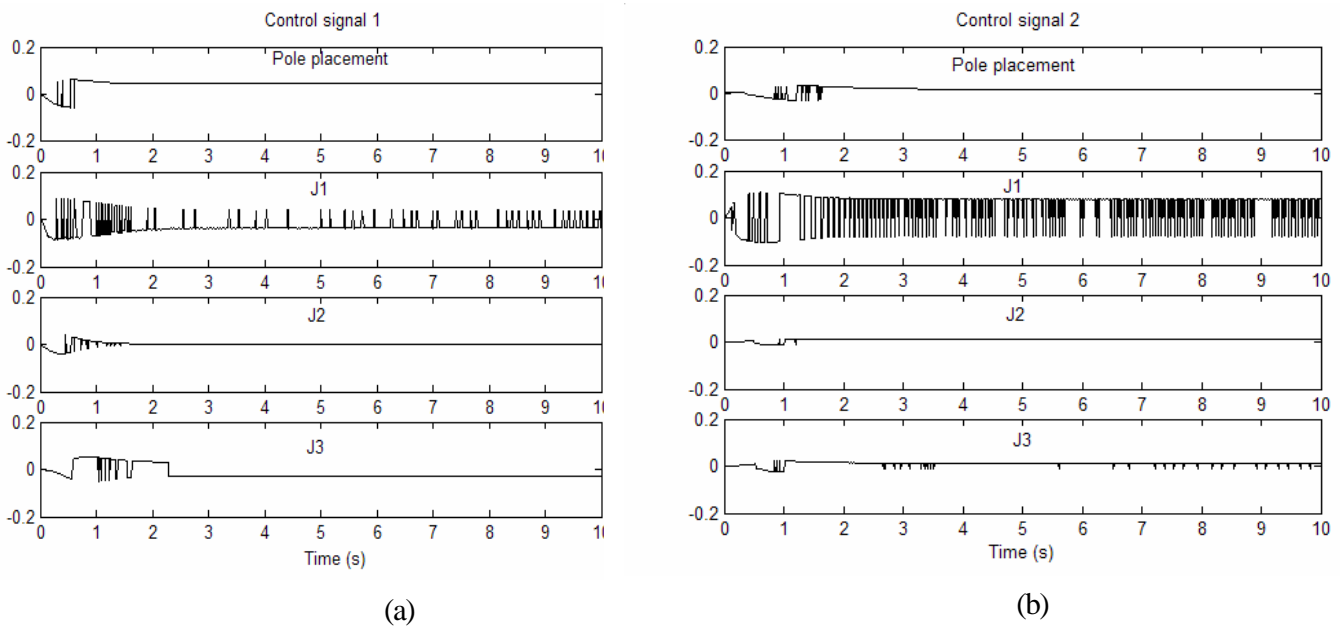


Figure 3-11: (a) Control effort in area 1 (b) Control effort 2

3.3.1.2 Design of an optimal switching vector values with fixed feedback gains controller

The same system considered in section 3.3.1.1 is designed with VSC of arbitrarily chosen feedback gains. The switching vector was optimized using Tabu search algorithm. A Tabu list of size 7 was used for the simulation. The search process was terminated when there is no more improvement in the objective function value. The objective function used for search process is:

$$J = \int_0^{\infty} \left(Dw_1^2 + Dw_2^2 + DP_{tie}^2 + 0.1Du_1^2 + 0.1Du_2^2 \right) dt \quad (3-8)$$

This objective function satisfies the goal of LFC in damping oscillations of frequency deviation for both areas and maintaining a pre-specified value for tie line power.

Also, it includes a scaled value of the deviation in the control signals to reduce chattering.

The feedback gains used are [14]:

$$\mathbf{a} = \begin{bmatrix} 1 & 0 & 0 & 1 & 0 & 0 & 0 & 0 & 0 \\ 0 & 0 & 0 & 0 & 0 & 1 & 0 & 0 & 1 \end{bmatrix}$$

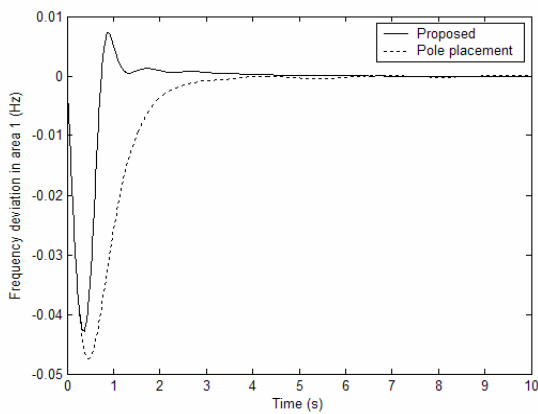
The optimum switching surface found by Tabu search is given below:

$$\mathbf{C}^T =$$

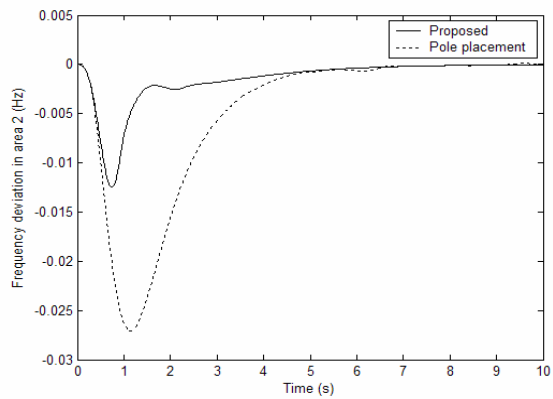
$$\begin{bmatrix} 8.7978 & 4.0011 & 1.9865 & 9.5682 & 4.3232 & -0.1244 & -1.8277 & 3.0933 & 2.2354 \\ 4.5359 & 0.0877 & 1.0134 & 2.1449 & 6.2365 & 7.2116 & 7.3875 & 2.6093 & 9.4279 \end{bmatrix}$$

The interconnected system was simulated for a 0.03 p.u. load disturbance in area 1.

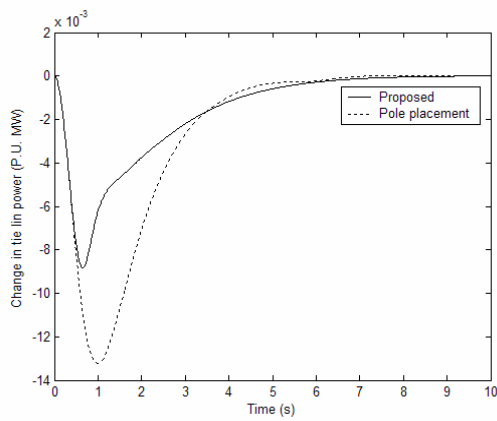
The convergence of the performance index and dynamic behavior of the system are shown in Figure 3-12. The results show an overall improved dynamic behavior in terms of settling time. However, the change in generated power of area 1 is of larger overshoot. The control signal of VSC with TS tuning exhibits less fluctuations in comparison with that of the pole placement designed VSC, Figure 3-13.



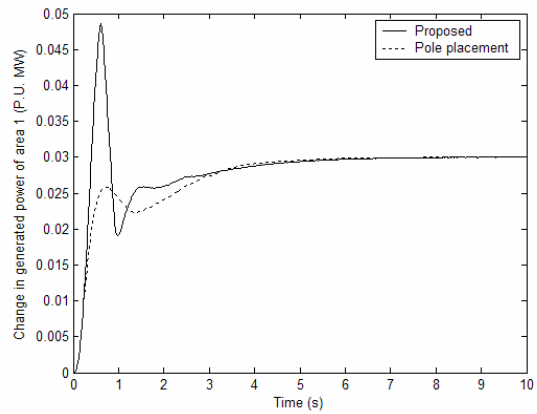
(a)



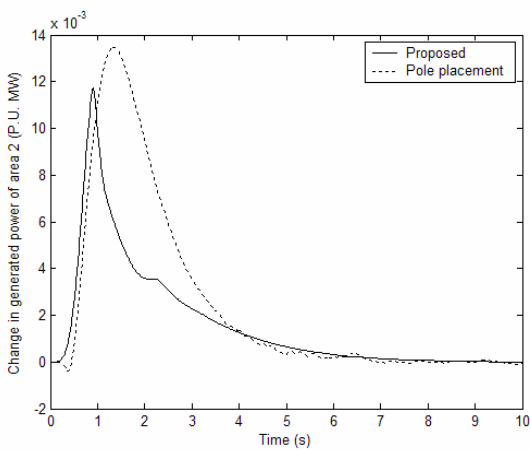
(b)



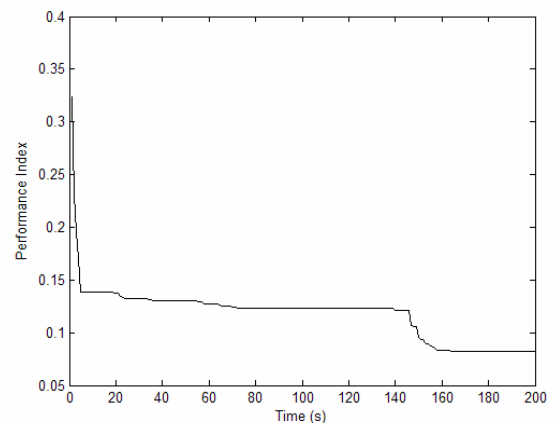
(c)



(d)



(e)



(f)

Figure 3-12: (a)-(e) Dynamic response of two area LFC system for 0.03 p.u. load disturbance in area 1 (f) Convergence of performance index value (... [17])

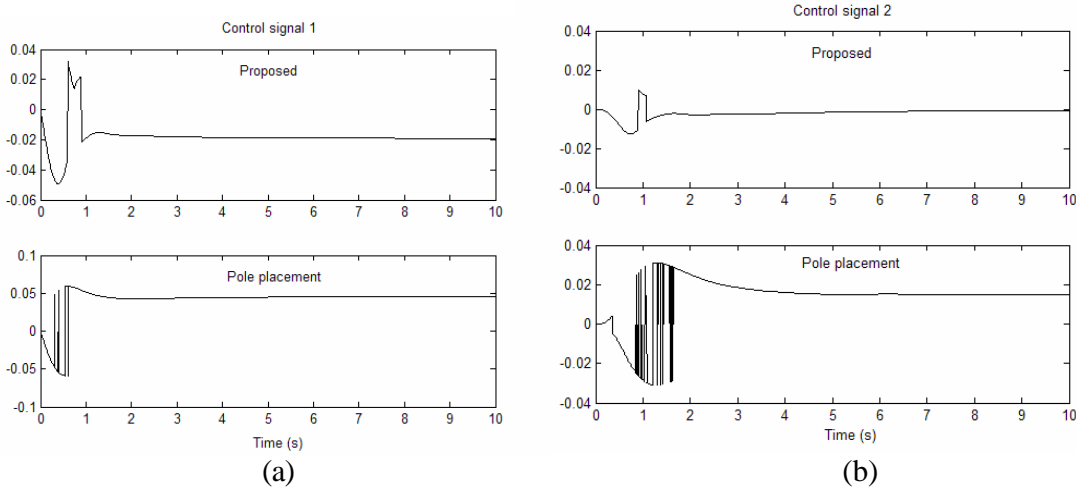


Figure 3-13: (a) Control signal to area 1 (b) Control signal to area 2

3.3.1.3 Design of a full switching surface and feedback gains controller

In this section, we propose to design the whole VSC controller by iterative heuristic search method. Both switching feedback gains and switching vector values are optimally chosen. Different iterative heuristic search methods were used to find the optimum settings of the controller. First, PSO is used for two different objective functions and compared with pole placement and optimal control methods of [17]. Secondly, the three heuristic iterative methods, GA, PSO, and TS, are compared with each other and with the optimal control and pole placement methods of [17].

PSO is used to optimize the settings of the VSC with the following objective functions:

$$J_1 = \int_0^{\infty} t |Dw_1| + t |Dw_2| + t |DP_{ie}| + 0.1.Du_1 + 0.1.Du_2 dt \quad (3-9)$$

$$J_2 = \int_0^{\infty} t |Dw_1| + t |Dw_2| + t |DP_{ie}| + Du_1 + Du_2 dt \quad (3-10)$$

The two objective functions include the absolute error of the parameters of the LFC areas multiplied by time. This product ensures that the oscillations in frequency and tie line power are damped out. However, the second objective function gives more importance for the deviation in the control signal. The settings of PSO are: $n = 15$, maximum number of iterations = 500, $w_{max} = 0.9$, $w_{min} = 0.4$, and the maximum velocity constant factor $k = 0.1$. The switching vectors and feedback gains of the VSC controller are respectively:

a) Objective function J_1 :

$$C_1^T =$$

$$\begin{bmatrix} 15.2533 & 0.0940 & 8.2141 & 25.0000 & 10.3070 & 1.4196 & 5.3505 & 6.8248 & 8.4027 \\ 3.5198 & 0 & 9.0405 & 16.4678 & 11.0167 & 15.2840 & 19.9216 & 9.9778 & 19.9487 \end{bmatrix}$$

$$a_1 =$$

$$\begin{bmatrix} 0.5266 & 0.2547 & 0.8632 & 0.1034 & 0.3701 & 0.0311 & 1.0000 & 0.6588 & 0.5286 \\ 0.6010 & 0.0655 & 0.8293 & 0.4734 & 0.0733 & 0.1616 & 0.5627 & 0.6725 & 1.0000 \end{bmatrix}$$

b) Objective function J_2 :

$$C_2^T =$$

$$\begin{bmatrix} 17.1663 & 2.2094 & 11.1571 & 25.0000 & 10.0757 & 7.5215 & 6.9700 & 12.0840 & 25.0000 \\ 0 & 0 & 9.5575 & 10.6394 & 6.7805 & 25.0000 & 25.0000 & 20.1510 & 25.0000 \end{bmatrix}$$

$$a_2 =$$

$$\begin{bmatrix} 1.0000 & 0 & 0.5273 & 0.6121 & 0.6924 & 0.8181 & 0.4264 & 0.6283 & 0.2042 \\ 0.5900 & 0.3273 & 0.0004 & 0.3805 & 0.4984 & 0 & 0.2279 & 1.0000 & 0.5463 \end{bmatrix}$$

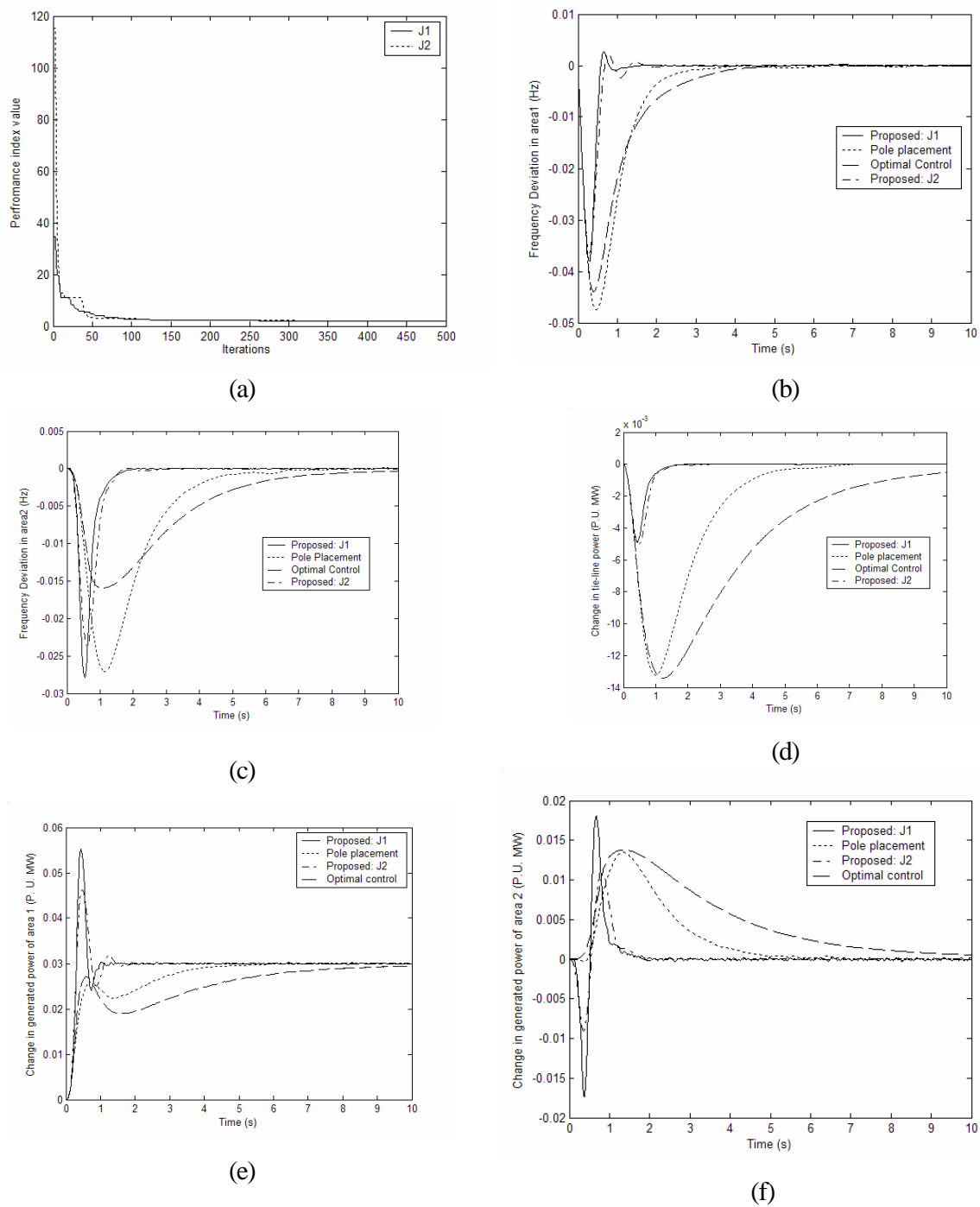


Figure 3-14: (a) Convergence of the objective functions (b)-(f) Dynamical behavior of the interconnected system following a disturbance of 0.03 p.u. in area 1 (... , --- [17])

The above design provides an improved overall dynamic behavior for the system in terms of under shoot for frequency deviation of area 1 and change in tie line power and in terms of reduced settling for the other parameters, Figure 3-14. Furthermore, by including a scaled value of the deviation of the control signal into the objective function, a smoother control signal can be obtained. This is shown in Figure 3-15.

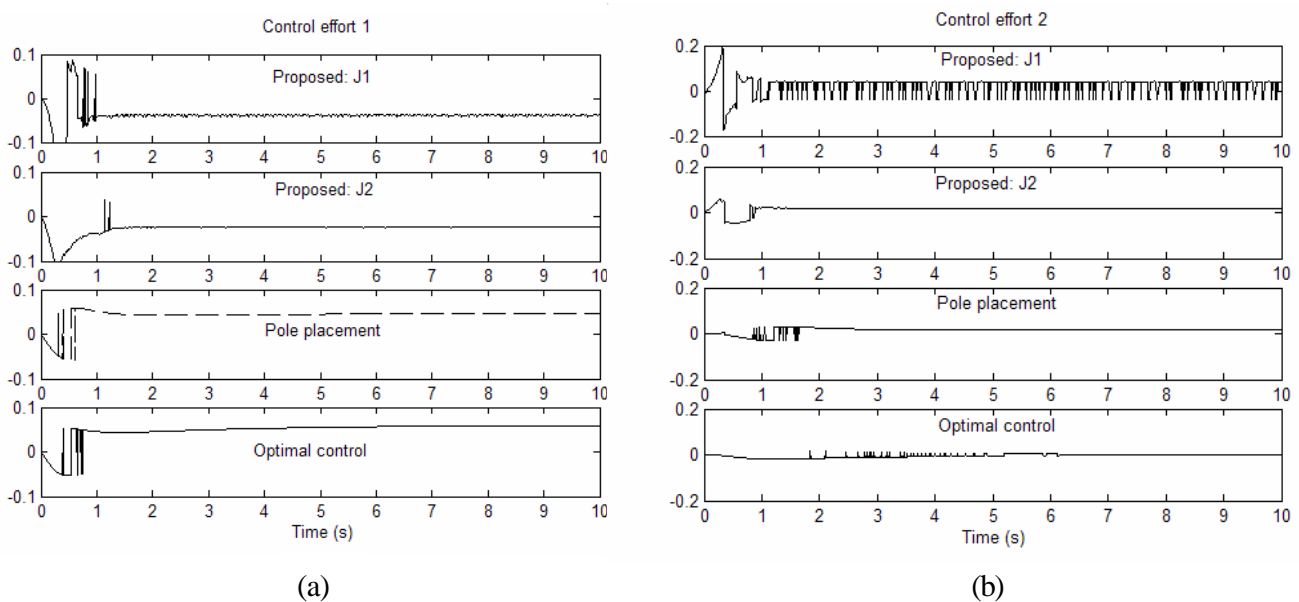


Figure 3-15: (a) Control signal 1 (b) Control signal 2

The next step is to use all the iterative heuristics algorithms to tune the VSC controller applied to the interconnected system. Objective function J_2 of this section is used for the design of VSC, since it shows the best performance.

For the PSO, $n = 15$, maximum number of iterations = 500, $w_{max} = 0.9$, $w_{min} = 0.4$, and the maximum velocity constant factor $k = 0.1$ is used. For the GA, a crossover

rate = 1 and mutation rate = 0.001 is used. A tabu list size of 7 and maximum of 300 iterations is set for the Tabu search. The optimum settings of the VSC for each algorithm are given below:

a) **PSO :**

For completion, the switching vectors and feedback gains of the PSO design found before are given below:

$$C^T =$$

$$\begin{bmatrix} 17.1663 & 2.2094 & 11.1571 & 25.0000 & 10.0757 & 7.5215 & 6.9700 & 12.0840 & 25.0000 \\ 0 & 0 & 9.5575 & 10.6394 & 6.7805 & 25.0000 & 25.0000 & 20.1510 & 25.0000 \end{bmatrix}$$

$$a =$$

$$\begin{bmatrix} 1.0000 & 0 & 0.5273 & 0.6121 & 0.6924 & 0.8181 & 0.4264 & 0.6283 & 0.2042 \\ 0.5900 & 0.3273 & 0.0004 & 0.3805 & 0.4984 & 0 & 0.2279 & 1.0000 & 0.5463 \end{bmatrix}$$

b) **TS :**

$$C^T =$$

$$\begin{bmatrix} 17.0078 & 11.6931 & 1.6450 & 23.0323 & 1.3789 & 7.9054 & 9.7575 & 2.1758 & 21.3989 \\ 0.3175 & 7.9823 & 3.3351 & 14.8617 & 3.9895 & 21.1115 & 23.8684 & 11.0481 & 23.8650 \end{bmatrix}$$

$$a =$$

$$\begin{bmatrix} 0.8782 & 0.8358 & 0.1408 & 0.1586 & 0.2947 & 0.6926 & 0.8353 & 0.6695 & 0.3149 \\ 0.7084 & 0.1129 & 0.0791 & 0.1544 & 0.5307 & 0.2709 & 0.0954 & 0.0592 & 0.0403 \end{bmatrix}$$

c) **GA :**

$C^T =$

$$\begin{bmatrix} 10.3512 & 6.2777 & 2.8331 & 24.1297 & 2.1240 & 2.7883 & 3.9862 & 2.4385 & 3.4977 \\ 2.1895 & 0.0786 & 7.9366 & 7.9277 & 12.9069 & 15.4481 & 15.8318 & 14.8816 & 23.3902 \end{bmatrix}$$
 $a =$

$$\begin{bmatrix} 0.9331 & 0.4830 & 0.1044 & 0.9087 & 0.8203 & 0.6982 & 0.0452 & 0.7398 & 0.1264 \\ 0.6112 & 0.3228 & 0.2328 & 0.2840 & 0.3225 & 0.1842 & 0.9548 & 0.8062 & 0.1903 \end{bmatrix}$$

Table 3-2 shows a comparison between the three algorithms in terms of time of execution and minimum value of objective value reached. For this problem, PSO was able to find the best minimum value in shortest time.

Table 3-2: Comparison between the three algorithms for VSC design applied to interconnected LFC areas excluding nonlinearities

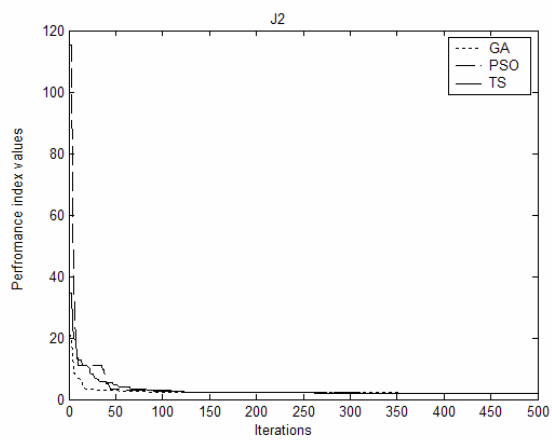
Algorithm	Computation time (Mins)	Minimum value (J_2)
PSO	41.8759	1.9581
TS	319.1559	2.0957
GA	768.1168	2.1027

Figure 3-16(a) shows the convergence of J_2 for each algorithm. Figure 3-16(b)-(f) shows the dynamic response of the system for a 0.03 p.u. disturbance in area 1. The response of the system with the designed VSC for different algorithms is almost similar. The proposed design of VSC compared to other designs provides smaller under shoot for frequency deviation of area 1 and deviation of tie line power. It also

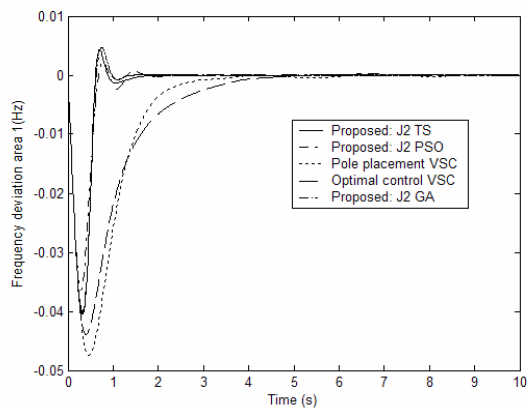
enhances the settling behavior of the change in generated power for both areas and settling time of the deviation of frequency for area 2. Figure 3-17 shows the control signal for both areas. The proposed VSC design provides a smooth control effort compared with optimal control and pole placement designs of VSC. The TS VSC design gave the smoothest control signal.

The following can be concluded from the shown results:

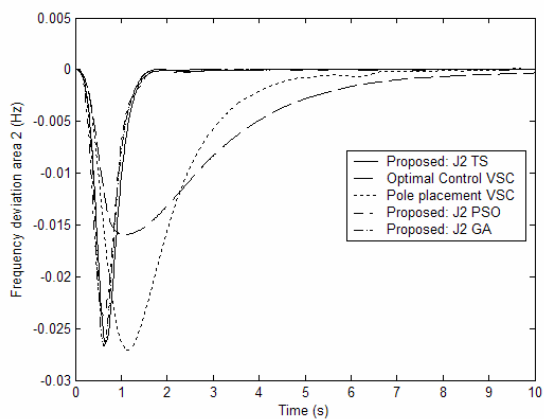
- a- Heuristic iterative search algorithms can provide an efficient tool in tuning the VSC controller applied to interconnected LFC areas. Optimal settings of the controller can be achieved by choosing a proper objective function that reflects the goal of the designer. This is depicted in Figures 3-10, 3-12, 3-14, and 3-16.
- b- A smooth control signal can be achieved by the new design method. This is done by including a scaled version the deviation in the control effort into the objective function. This is shown in Figures 3-11, 3-13, 3-15, and 3-17.



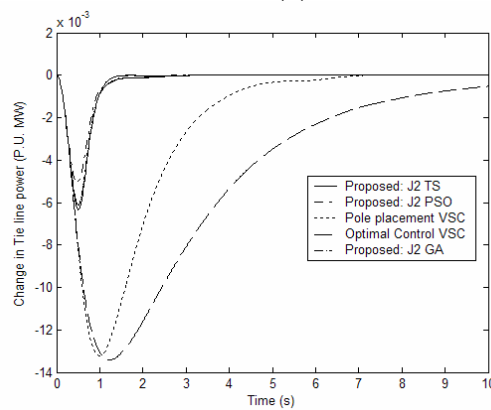
(a)



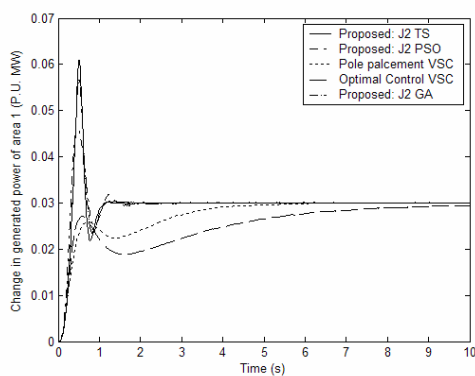
(b)



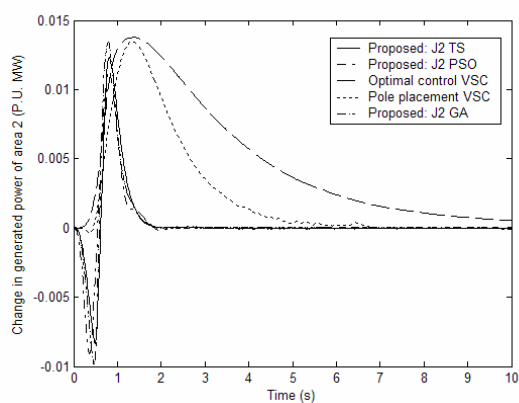
(c)



(d)



(e)



(f)

Figure 3-16: (a) Convergence of performance index (b)-(f) Dynamic behavior of the system following a 0.03 p.u. disturbance in area 1 (...;---[17])

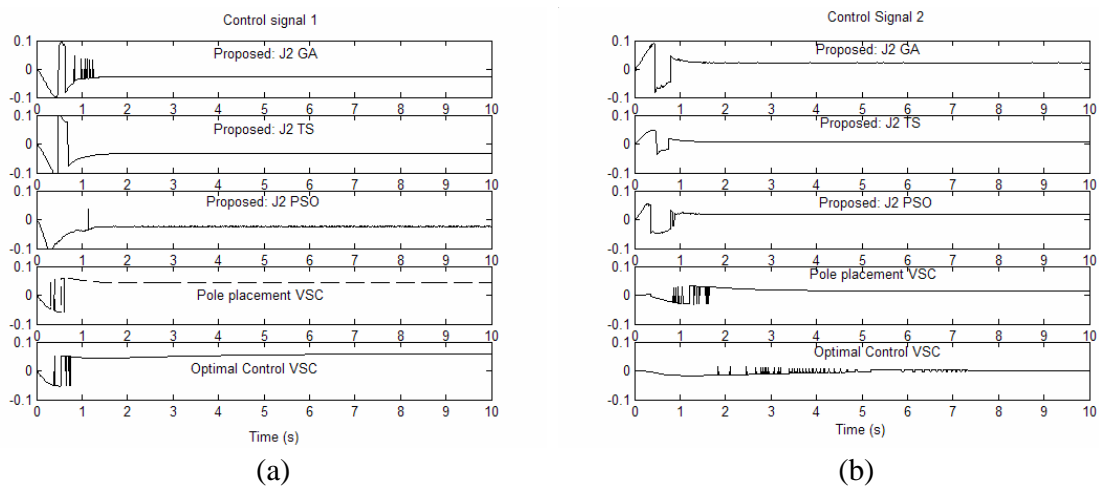


Figure 3-17: (a) Control effort 1 (b) Control effort 2

3.3.2 Interconnected LFC areas with nonlinearities

In this part, nonlinearities will be included into the LFC model. Our design method will be compared with the one proposed in [105]. In [105], a new Linear Quadratic Regulator (LQR) based on structured singular values (SSVs) was presented in designing a robust LFC for two area interconnected power systems. This method showed promising results compared with other design techniques reported in literature. Therefore, our proposed method is compared with it. The studied system is shown in Figure 3-9. First, for the purpose of comparison, the governor dead band (DB) will be excluded since it is not considered in [105]. Later on, the effect of governor dead band will be incorporated. The values of the parameters used for the interconnected system are as follows:

$$\begin{aligned}
T_{p1} &= T_{p2} = 20\text{s} & K_{p1} &= K_{p2} = 120 \text{ Hz p.u. MW}^{-1} \\
T_{i1} &= T_{i2} = 0.3\text{s} & K_I &= K_2 = 1 \text{ p.u. MW rad}^{-1} \\
T_{g1} &= T_{g2} = 0.08\text{s} & R_1 &= R_2 = 2.4 \text{ Hz p.u. MW}^{-1} \\
B_1 &= B_2 = 0.425 \text{ p.u. MW/Hz} & T_{12} &= 0.545 \text{ p.u. MW} \\
a_{12} &= -1 & \text{GRC (Generation rate constraint)} &= 0.015
\end{aligned}$$

Furthermore, the conventional integral controller will also be included in the comparison. The gains of the integral controller were of unity value in [105]. To have a fair comparison, the optimum gains of the integral controller should be used. These optimum gains were found using PSO.

The objective function used in the optimization process is:

$$J = \int_0^{\infty} 0.35 \cdot Dw_1^2 + 0.35 \cdot Dw_2^2 + 0.15 \cdot t |Dw_1| + 0.15 \cdot t |Dw_2| dt \quad (3-11)$$

The following are the optimum gains of the integral controller:

$$K_I = 0.5512$$

$$K_2 = 0.0100$$

3.3.2.1 Proposed Centralized VSC controller

The control laws of equations 2-11 and 2-12 are used in this part.

For the proposed design, the following objective functions are used:

$$J_1 = \int_0^{\infty} 0.75 \cdot t |Dw_1| + t |Dw_2| + 0.5 \cdot t |DP_{ie}| dt \quad (3-12)$$

$$J_2 = \int_0^{\infty} Dw_1^2 + Dw_2^2 + DP_{ie}^2 + Du_1^2 + Du_2^2 dt \quad (3-13)$$

The first objective function emphasizes on improving the dynamical behavior of the LFC system. This was done by including the absolute error time of the internal parameters of the LFC system into the objective function. On the other hand, the second objective function includes the deviation of the control effort to reduce the chattering in the signal. The three heuristic iterative methods, namely PSO, TS, and GA, are used. The results of each method are as follows.

a) **Particle swarm optimization:**

The settings used are: $n = 15$, maximum number of iterations = 500, $w_{max} = 0.9$, $w_{min} = 0.4$, and the maximum velocity constant factor $k = 0.1$. The optimum switching vector values and feedback gains are given below:

i) Objective function J_I :

$$C_I^T =$$

$$\begin{matrix} \hat{e} & \hat{u} \\ 30.0000 & 13.0638 & 4.8552 & 24.9203 & 17.8597 & -3.0000 & -3.0000 & 4.9979 & -3.0000 & \hat{u} \\ 12.0642 & 17.4207 & 3.4430 & 23.6198 & 13.0664 & 17.6442 & 30.0000 & 5.8677 & 18.7206 & \hat{u} \end{matrix}$$

$$a_I =$$

$$\begin{matrix} \hat{e} & \hat{u} \\ 3.3757 & 0.0010 & 4.5620 & 0.0010 & 7.4638 & 2.4800 & 0.0010 & 4.7885 & 1.2752 & \hat{u} \\ 0.0010 & 0.0010 & 0.0010 & 1.8695 & 5.4026 & 5.5483 & 8.6752 & 0.0010 & 5.8926 & \hat{u} \end{matrix}$$

ii) Objective function J_2 :

$$C_2^T =$$

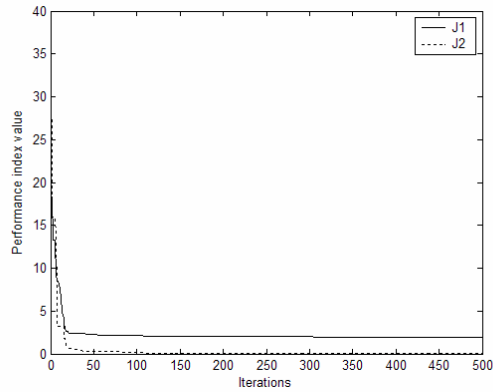
$$\begin{bmatrix} 17.5282 & 23.4810 & 1.6520 & 16.5393 & 24.5775 & 6.4494 & 13.9074 & 7.1777 & 30.0000 \\ 13.5409 & 3.1294 & 2.8040 & -2.8377 & 23.3587 & 2.0022 & 4.0492 & 12.0614 & 22.2385 \end{bmatrix}$$

$$a_2 =$$

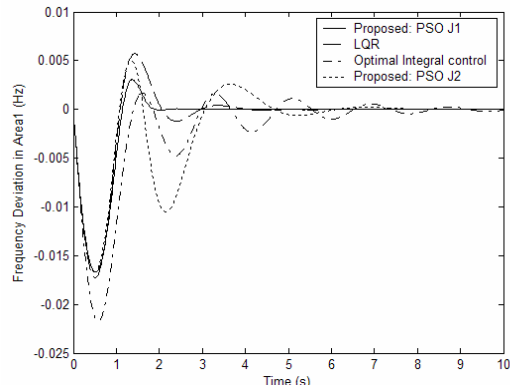
$$\begin{bmatrix} 5.3594 & 0.0697 & 0.0010 & 5.0151 & 1.3586 & 0.0010 & 5.8891 & 4.3556 & 2.8171 \\ 0.0010 & 9.0000 & 0.0010 & 8.9998 & 5.8002 & 0.1515 & 0.1642 & 9.0000 & 9.0000 \end{bmatrix}$$

The system is simulated for a 0.01 p.u. load disturbance in area 1. The convergence of the objective functions and dynamic response of the interconnected system are shown in Figure 3-18(a)-(d).

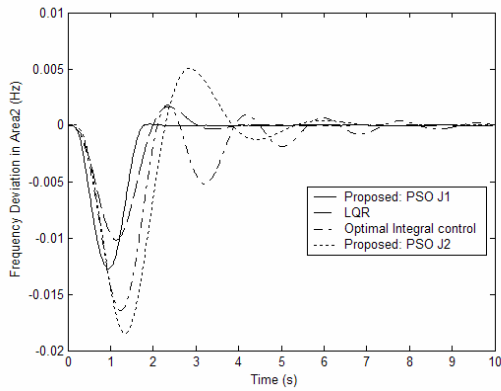
The first objective function, J_1 , allows the design of a VSC controller with improved dynamic behaviour, as seen in Figure 3-18 (b)-(d). This is on the expense of increased fluctuations in the control signal, Figure 3-18(e)-(f). Including the deviation of the control effort into the objective function, J_2 , reduced dramatically the chattering in the control signal, Figure 3-18(e) and (f). This reduction in the chattering was on the price of degradation in the dynamic behaviour of the controller.



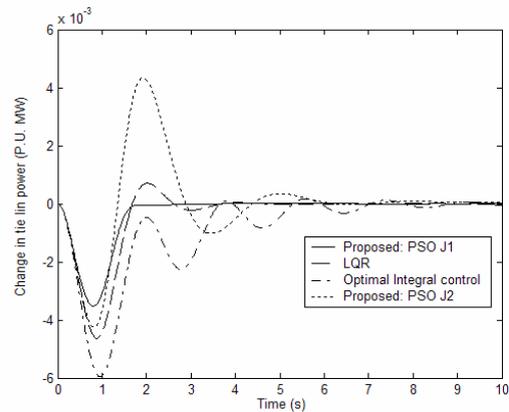
(a)



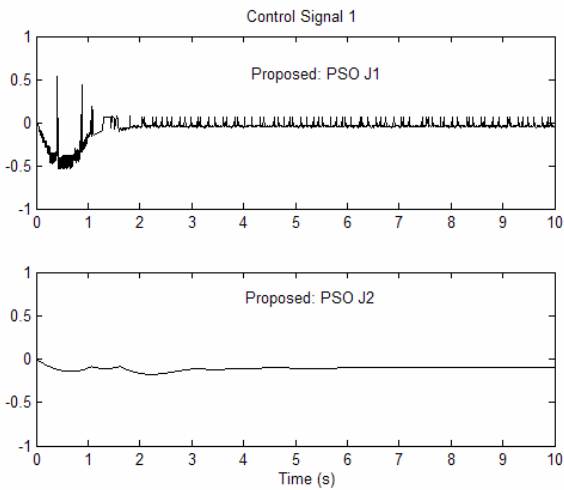
(b)



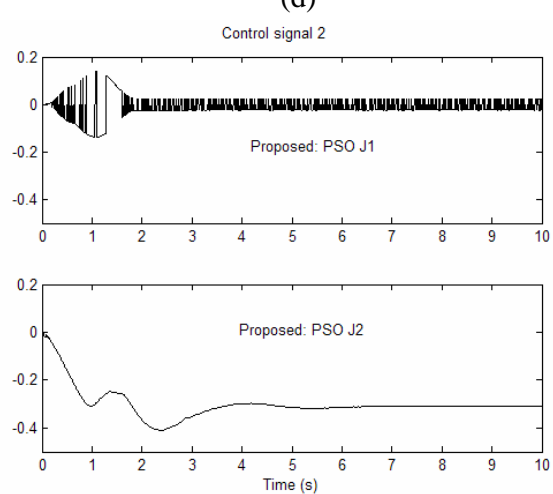
(c)



(d)



(e)



(f)

Figure 3-18: (a) Convergence of objective functions (b)-(d) Dynamic response of the system for a 0.01 p.u. load disturbance in area 1 (e) Control signal 1 (f) Control signal 2

b) Tabu Search algorithm:

Tabu search algorithm described in chapter 2 is applied in the design of a centralized VSC applied to two interconnected LFC areas. The optimal settings are given below:

i) Objective function J_I :

$$C_I^T =$$

$$\begin{matrix} \acute{e} & 4.3644 & 3.2357 & 1.5598 & 6.9635 & -2.1297 & 2.3790 & 1.8512 & -0.0423 & 6.2382 \\ \hat{e} & -3.8772 & 1.5404 & -1.7849 & -0.0903 & 4.0369 & 3.4296 & 9.2867 & 0.3621 & 3.6863 \end{matrix} \begin{matrix} \grave{u} \\ \grave{u} \end{matrix}$$

$$a_I =$$

$$\begin{matrix} \acute{e} & 3.0964 & 0.9762 & 0.3309 & 0.0470 & 4.6673 & 0.2890 & 0.1491 & 0.6938 & 4.8316 \\ \hat{e} & 6.9800 & 0.4475 & 0.5276 & 3.2127 & 4.2904 & 2.5445 & 2.5138 & 7.8025 & 4.7717 \end{matrix} \begin{matrix} \grave{u} \\ \grave{u} \end{matrix}$$

For the same objective function, J_I , the controller was designed with only accessible states fed back. These states are: DW_1 , DW_2 , DP_{g1} , DP_{g2} , and DP_{ie} . The following settings were obtained:

$$C^T =$$

$$\begin{matrix} \acute{e} & 40.3228 & 31.6140 & -21.8400 & 6.5112 & 6.0167 \\ \hat{e} & -3.1097 & 0.0813 & 27.5885 & 41.7001 & -19.7625 \end{matrix} \begin{matrix} \grave{u} \\ \grave{u} \end{matrix}$$

$$a =$$

$$\begin{matrix} \acute{e} & 0.6515 & 0.2036 & 0.0035 & 0.0668 & 0.0575 \\ \hat{e} & 3.7885 & 3.0047 & 1.0090 & 0.7646 & 4.0572 \end{matrix} \begin{matrix} \grave{u} \\ \grave{u} \end{matrix}$$

ii) Objective function J_2 :

$$C_2^T =$$

$$\begin{bmatrix} 11.7584 & 12.9466 & 5.3835 & 12.0826 & 10.0748 & 4.1113 & 6.0350 & 8.2353 & 9.7144 \\ 4.7161 & 4.3873 & 3.2022 & 5.0592 & 6.1160 & 5.3830 & 2.3657 & 13.9595 & 12.5254 \end{bmatrix}$$

$$a_2 =$$

$$\begin{bmatrix} 1.3720 & 0.2571 & 0.0414 & 0.0147 & 0.0102 & 0.0755 & 1.1279 & 0.4152 & 0.8305 \\ 1.0320 & 0.4326 & 0.5690 & 0.3650 & 0.5320 & 0.0141 & 0.1074 & 0.1147 & 1.4510 \end{bmatrix}$$

The convergence of the performance indices and system response to a 0.01 p.u. load disturbance in area 1 are shown in Figure 3-19. Objective function J_1 gave the best dynamic response both in terms of undershoot and settling time. Again, this was on the expense of more chattering in the control signal. J_2 , which includes the squared value of the deviation in the control signals, provides a smooth control signal but with degradation in the dynamic behavior of the system. Furthermore, the robustness of the proposed design is tested by varying the parameters of the system by 25 % in T_g , T_b and K_p of both areas. This is illustrated in Figure 3-20. It can be seen that the proposed TS VSC controller is almost insensitive to variations in the parameters of the system.

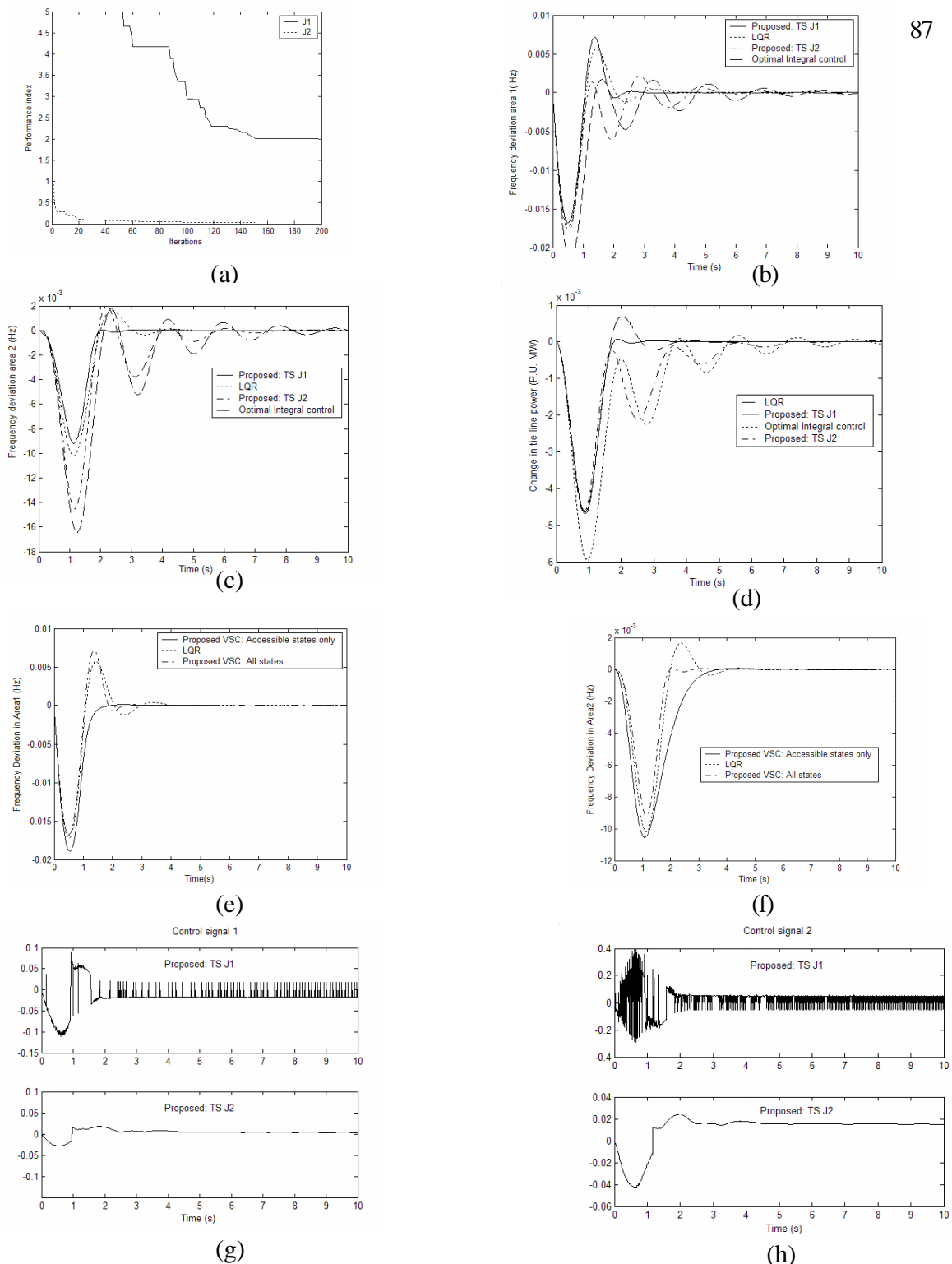


Figure 3-19: (a) Convergence of objective functions (b)-(d) Dynamic behavior when subjected to a 0.01 p.u. load disturbance in area1 (e)-(f) Frequency deviation: Accessible states VSC (g) Control effort 1 (h) Control effort 2

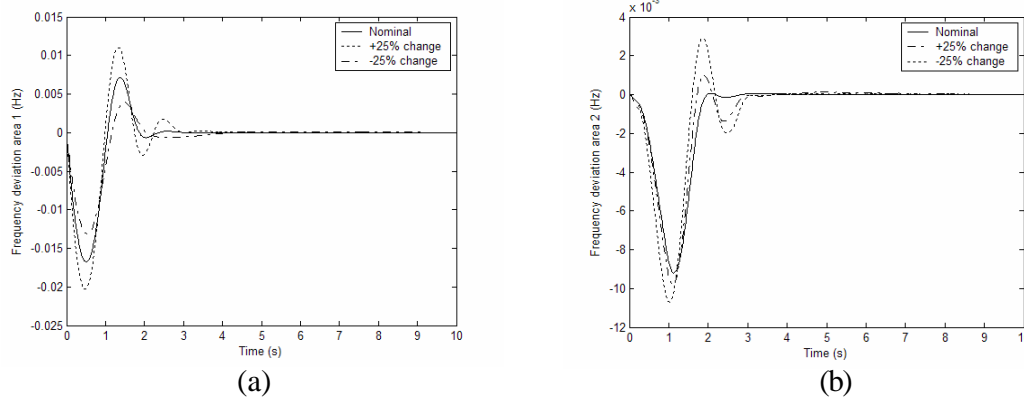


Figure 3-20: (a) Frequency deviation in area 1 (b) Frequency deviation in area 2 for a 25% change in T_g , T_b , and K_p of both areas

c) Genetic Algorithms:

The optimal settings of the VSC applied to the same interconnected two areas LFC are then obtained by GA. The optimal settings are given below:

i) Objective function J_1 :

$$C_1^T =$$

$$\begin{bmatrix} 17.0620 & 14.8945 & 4.9056 & 23.4891 & 19.9278 & -0.7254 & 8.7202 & 5.4855 & 1.1284 \\ 11.8467 & 6.1719 & 4.0573 & 15.0380 & 18.3914 & 20.6820 & 25.6712 & 17.1209 & 22.3109 \end{bmatrix} \begin{matrix} \hat{u} \\ \hat{u} \\ \hat{u} \end{matrix}$$

$$a_1 =$$

$$\begin{bmatrix} 3.5751 & 4.0484 & 1.5769 & 5.8136 & 3.2300 & 0.4441 & 5.0872 & 1.3243 & 7.4557 \\ 2.5144 & 0.2132 & 1.3909 & 0.5006 & 8.8998 & 0.7260 & 3.6326 & 5.9606 & 0.8096 \end{bmatrix} \begin{matrix} \hat{u} \\ \hat{u} \\ \hat{u} \end{matrix}$$

ii) Objective function J_2 :

$$C_2^T =$$

$$\begin{bmatrix} 29.1559 & 15.5157 & 10.9371 & 29.9919 & 17.4893 & 8.4144 & 20.9650 & 15.7446 & 15.9439 \\ 23.6313 & 2.9241 & 8.8227 & 16.0523 & -2.9328 & -0.6177 & -2.1126 & 26.8925 & 0.6376 \end{bmatrix} \begin{matrix} \hat{u} \\ \hat{u} \\ \hat{u} \end{matrix}$$

$\mathbf{a}_2 =$

$$\begin{bmatrix} 2.4164 & 0.0010 & 0.0175 & 0.0010 & 0.0010 & 0.0010 & 5.8201 & 1.2820 & 0.0010 \\ 4.0454 & 4.0643 & 0.0121 & 2.8374 & 7.0902 & 6.8646 & 0.7096 & 4.2269 & 3.5232 \end{bmatrix}$$

Figure 3-21 shows the results of the application of VSC designed by GA for controlling the disturbances of the two interconnected areas. Figure 3-21 (a) shows the convergence of the performance indices. Figure 3-21 (b)-(d) shows the dynamic response of the system for a 0.01 p.u. load disturbance in area 1. The use of objective function J_1 in finding the optimum switching vector and feedback gains of the VSC, improved the response of the system in comparison with optimal integral control and LQR design methods [105]. However, more chattering is noticed in the control signal. On the other hand, objective function J_2 reduces dramatically the chattering in the control signals, Figure 3-21(e) and (f). This enhancement of the control signal is on the expense of some degradation in the dynamic behaviour of the system. A comparison between the computational time and the minimum value of J_2 for the three algorithms applied in the VSC design for the two interconnected areas is shown in Table 3-3. In addition, a comparison between the dynamic behaviour of the system using the three optimization algorithms is shown in Figure 3-22 (a)-(c). It can be seen that the three algorithms provide almost similar dynamic behaviour. The PSO provides the best dynamic response for frequency deviation in area 1 and tie line power, Figure 3-22 (a) and (c). TS out performs the other algorithms in the dynamic response for frequency deviation in area2, Figure 3-22 (b).

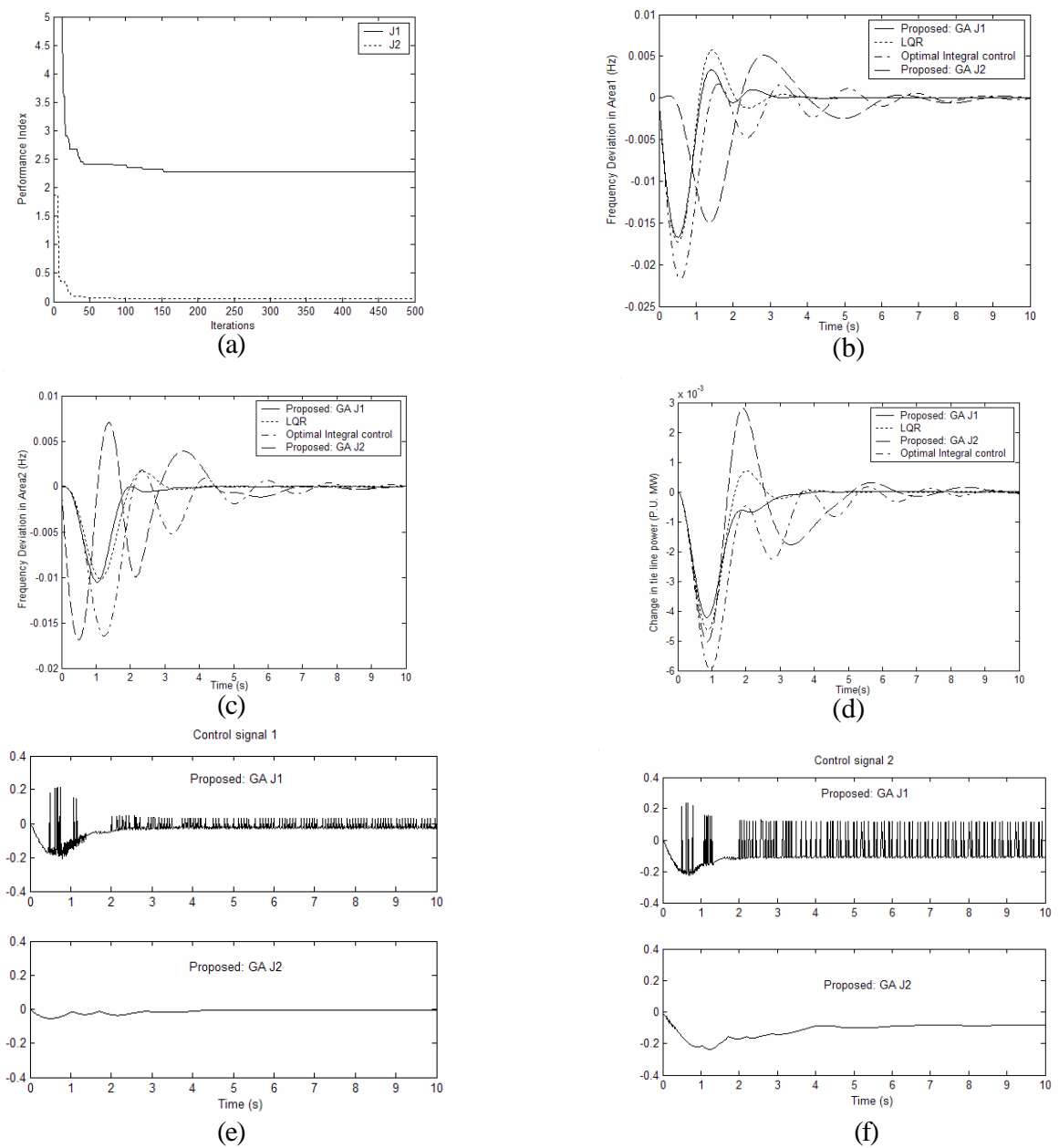


Figure 3-21: (a) Convergence of performance index (b)-(d) Dynamic response of the after a 0.01 p.u. load disturbance (e) Control 1 (f) Control 2

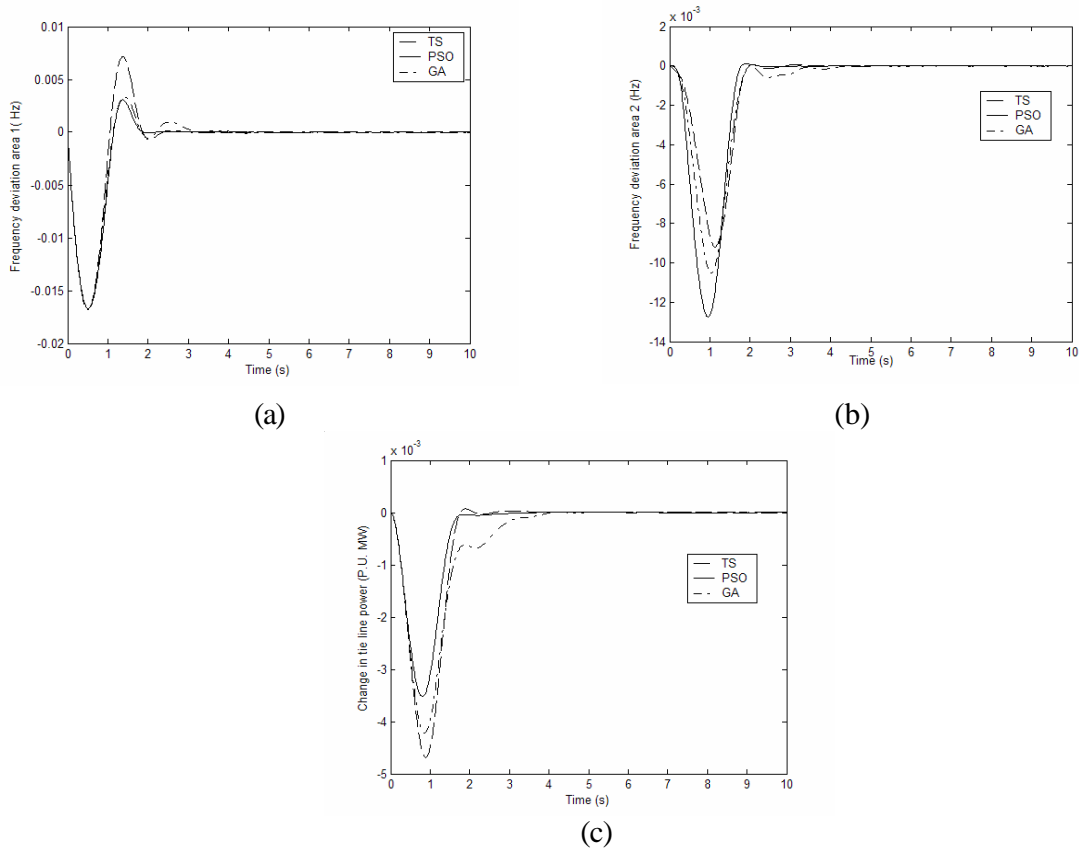


Figure 3-22: (a)-(c) Comparison between the dynamical behavior of the system designed with different heuristic algorithms. Objective function, J_1 , is considered in this case

Table 3-3: Comparison of the three algorithms for VSC design applied to two interconnected LFC areas with nonlinearities

Algorithm	Computation time (Mins)	Minimum value (J_2)
PSO	29.6608	0.0596
TS	129.2050	0.0385
GA	301.7208	0.0488

From the results of this section, the following can be concluded:

1- The iterative heuristic optimization algorithms can provide optimal settings for the variable structure controllers of interconnected two areas LFC systems that include nonlinearities. With these controllers, the dynamic behavior is improved. This is clear from Figures 3-18 (b)-(d), 3-19 (b)-(d), and 3-21 (b)-(d). This improvement was also achieved even with only the accessible states feedback, Figure 3-19 (e) and (f).

2- The chattering in the control signal can be reduced significantly by the inclusion of the deviation of the control effort in the objective function of the search process. This is also depicted in Figures 3-18 (e)-(f), 3-19 (g)-(h), and 3-21 (e)-(f). However, this causes acceptable degradation in the dynamic behavior of the system.

It is worth mentioning that it is desirable to obtain a VSC that will improve the dynamic behavior of the system and, at the same time, have a smooth control signal. This encouraged the exploration of other methods to improve the behavior of the VSC in the coming sections.

3.3.2.2 Proposed VSC controller with scaled feedback gains

In order to reduce the chattering and, at the same time, maintain an improved dynamic behavior, the following criteria for the feedback gains is proposed:

For the optimum values of feedback gains and switching vector values:

if
 $\Delta J < \varepsilon$
then
 $\mathbf{a}_{new} = m \cdot \mathbf{a}$
where
 $0 < m < 1$

and is selected by empirical trial and error procedure.

J = Objective function being minimized; For example $\int_0^{\infty} \mathbf{D}\mathbf{w}^2 dt$

ε = a small constant

\mathbf{a} = Optimum switching feedback gain

For demonstration purposes, this method is applied to the Tabu search design of section 3.3.2.1. The design proposed in section 3.3.2.1 showed an improved dynamic performance when using J_1 as the objective function to be minimized. This improvement is on the expense of having high undesired chattering in the control signal u . Therefore, a tradeoff between the two objectives i.e. having improved dynamic performance and low chattering can be achieved by applying the proposed scaling method to the optimum feedback gains found in section 3.3.2.1 as follows:

$$J = \int_0^{\infty} \mathbf{D}\mathbf{w}_1^2 + \mathbf{D}\mathbf{w}_2^2 + \mathbf{D}P_{ie}^2 dt \quad (3-14)$$

$\varepsilon = 1 \times 10^{-9}$

The scaling factors are:

m_1 (scaling factors for the first row of the feedback gains) =

[0.005 0.3 0.2 0.2 0.01 0.01 0.2 0.05 0.01]

m_2 (scaling factors for the second row of the feedback gains) =

[0.001 0.012 0.05 0.031 0.001 0.001 0.001 0.001 0.001]

The effect of this scaling on the dynamics of the system and control signal is shown in Figure 3-23. Figure 3-23(a) shows the convergence of the objective function and the time at which scaling of the feedback gains takes place. It can be seen that the system dynamics performance is very much satisfactory with an elimination of the control signal chattering after a certain time.

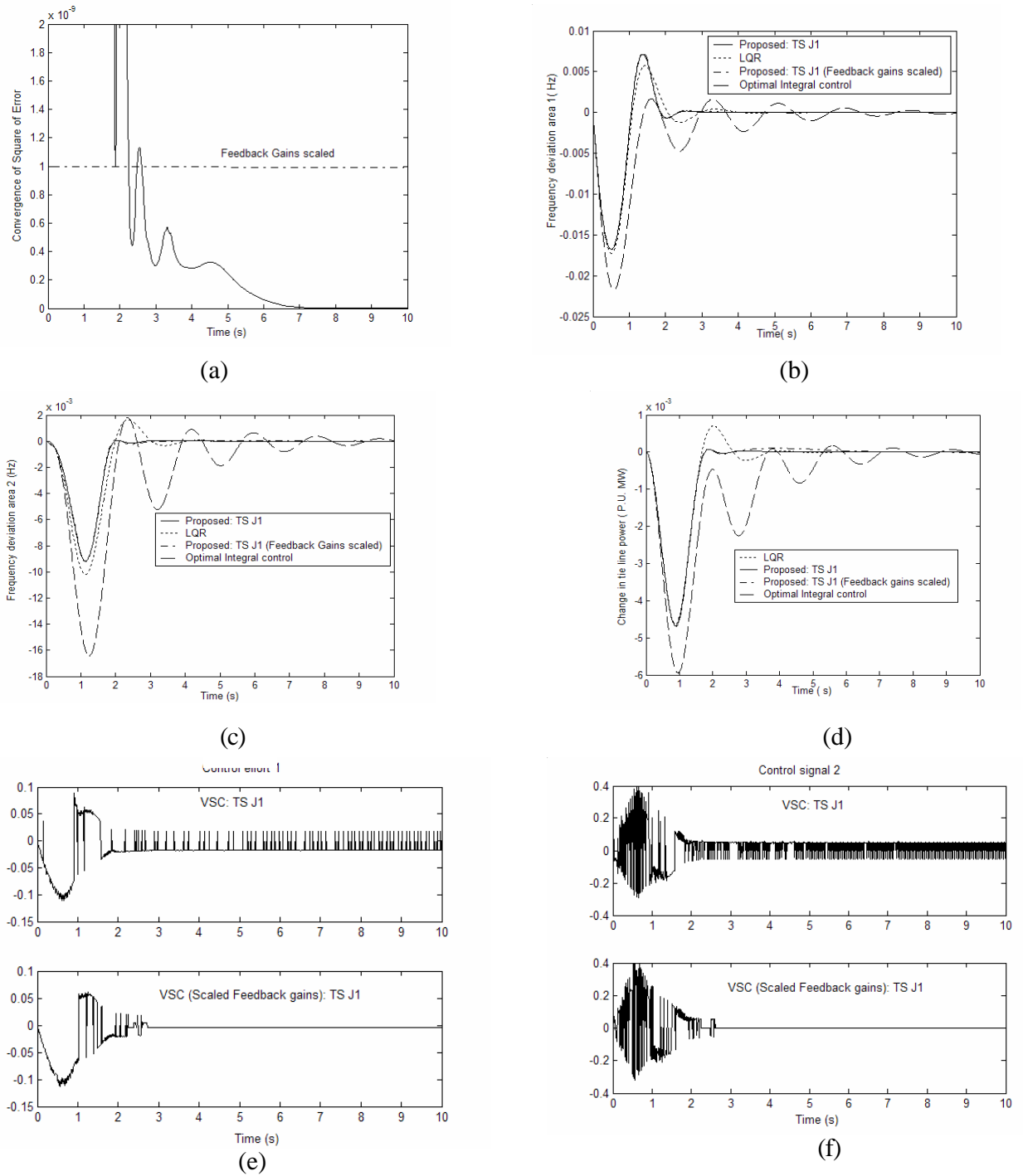


Figure 3-23: Scaled feedback gains design: (a) Convergence of the performance index (b)-(d) Dynamical behavior of the system after a 0.01 p.u. load disturbance; comparison of different designs (e) Control signals for area 1 (f) Control signals for area 2

3.3.2.3 Proposed Decentralized VSC controller

Figure 3-24 illustrates the idea of using decentralized VSC for each area. X_i represents the internal states of the i th area. U_i is the supplementary control signal going to the i th area.

The decentralized VSC is applied to the two area system of [105]. PSO and TS were used in obtaining the optimal settings of the controller.

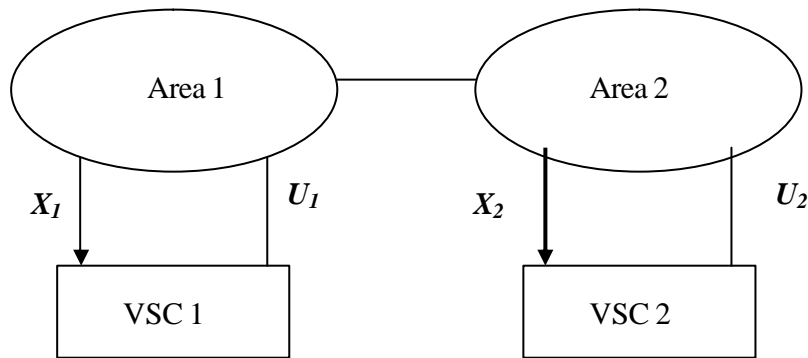


Figure 3-24: Proposed decentralized VSC controllers applied to interconnected LFC areas

The following objective function was used in optimizing the controller parameters:

$$J = \int_0^{\infty} 0.25 \cdot Dw_1^2 + 0.25 \cdot Dw_2^2 + 0.1 \cdot DP_{tie}^2 + 0.2 Du_1^2 dt \quad (3-15)$$

This objective function aims to reduce the oscillations in frequency deviation in all areas and reduce the deviation of tie line power. Furthermore, inclusion of the deviation in the control signal of area 1 into the objective function will reduce the chattering of the control effort.

$$X_i = [Dw_i \ DP_{gi} \ DP_{ti} \ DP_{ci}]$$

Where

DP_{ti} - is output of the turbine of the i th area.

DP_{ci} - signal from the integral control of the i th area.

The following are the optimal setting of the VSC found by each algorithm:

a) Particle Swarm Optimization

VSC for area 1

$$C_1^T = [15.1186 \ 17.0898 \ 1.1822 \ 22.6078]$$

$$a_1 = [10.0000 \ 0.0010 \ 0.0010 \ 8.8155]$$

VSC for area 2

$$C_2^T = [17.7402 \ 17.2089 \ 16.4721 \ 0.2903]$$

$$a_2 = [6.1308 \ 4.3529 \ 6.2699 \ 0.0010]$$

b) Tabu Search Algorithm :

VSC for area 1

$$C_1^T = [17.1758 \ 14.2153 \ 3.1950 \ 22.1597]$$

$$a_1 = [7.4323 \ 0.1771 \ 0.0980 \ 0.2550]$$

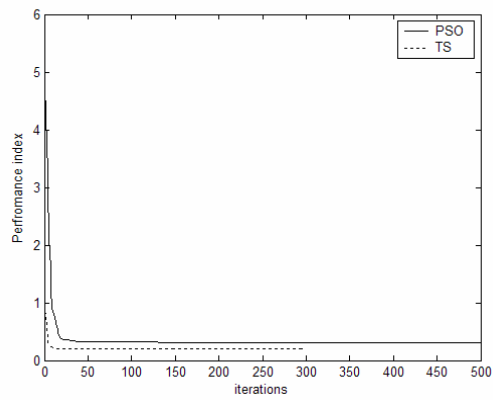
VSC for area 2

$$C_2^T = [18.4669 \ 20.7982 \ 9.8367 \ 19.3742]$$

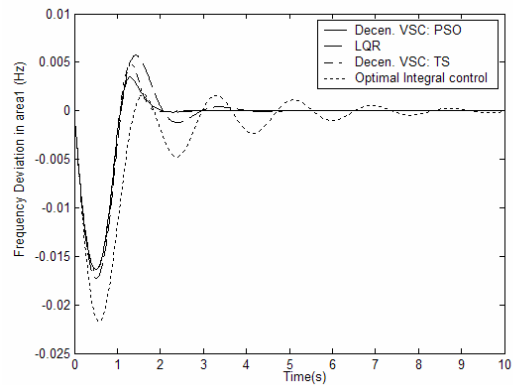
$$\mathbf{a}_2 = [5.2812 \quad 2.5351 \quad 9.5301 \quad 9.6993]$$

Figure 3-25 shows dynamical behaviour of the two areas when selecting the decentralized VSC controller parameters by PSO and TS. The following can be concluded from the results of Figures 3-25 and 3-26:

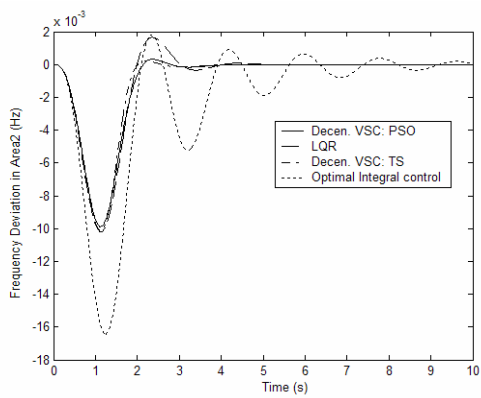
- a- The decentralized VSC designed by iterative heuristic algorithms improves the dynamic response of the two area LFC system, Figure 3-25 (a)-(c).
- b- The control signal of the controller is smooth and the fluctuations are minimized, Figure 3-25 (e) and (f).
- c- The decentralized and centralized VSC designs for PSO show similar dynamical behavior in the frequency deviation of area 1. However, the decentralized VSC design using TS is slightly better than the centralized one in terms of reduced overshoot, Figure 3-26(a) and (b).



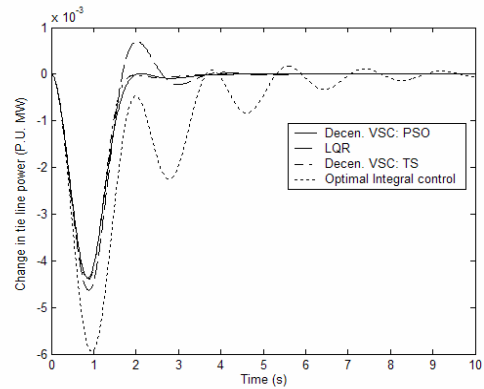
(a)



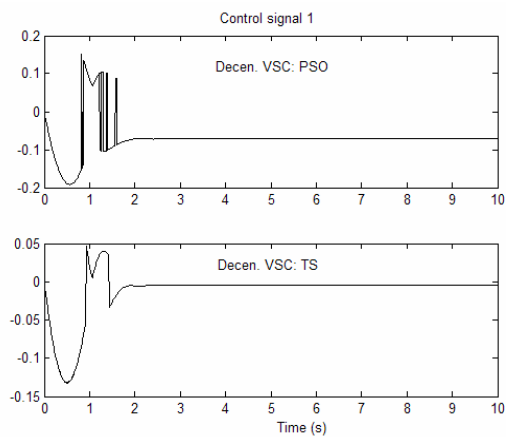
(b)



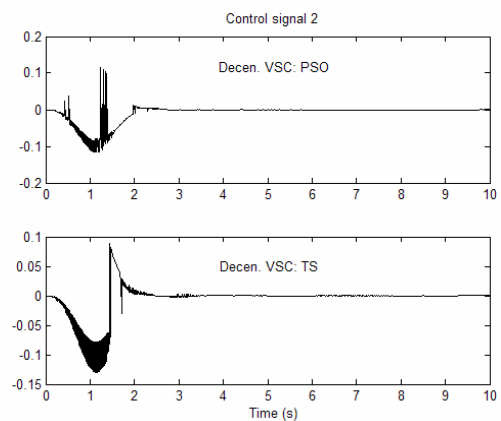
(c)



(d)



(e)



(f)

Figure 3-25: (a) Convergence of performance index (b)-(d) Dynamical behavior of the system with decentralized VSC (e) Control signal 1 (f) Control signal 2

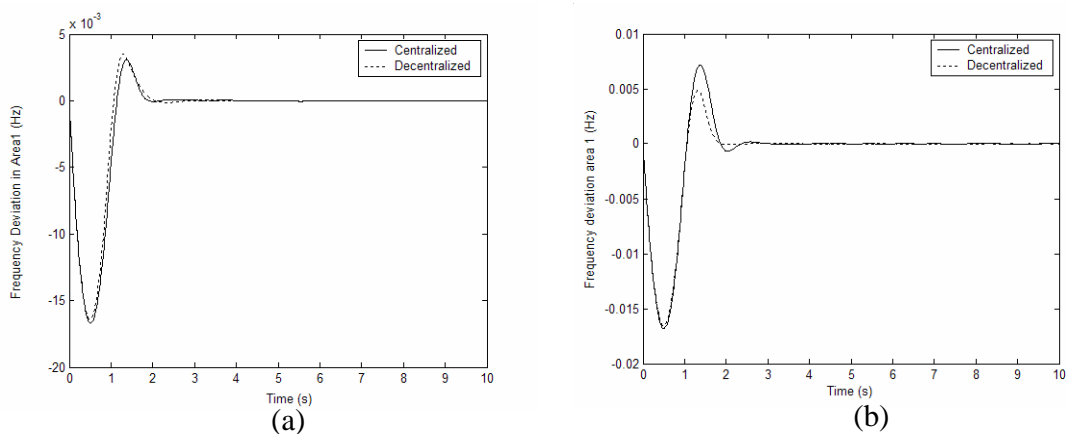


Figure 3-26: (a) PSO: Comparison between centralized and decentralized VSC designs (b) TS: Comparison between centralized and decentralized VSC designs

The following table shows a comparison between the proposed designs and LQR design of [105].

Table 3-4: Comparison between the performances of different controllers. The VSC controllers designed by TS are chosen for this comparison

Performance index	Parameter	LQR	Conventional VSC	VSC: Scaled gains	Decentralized VSC
I.S.E	Dw_1	0.0178	0.0171	0.0173	0.0154
	Dw_2	0.0077	0.0054	0.0054	0.0069
	DP_{tie}	0.0015	0.0014	0.0015	0.0013
I.A.E.T	Dw_1	1.4157	1.1520	1.2867	0.8756
	Dw_2	1.4773	0.9420	1.0432	1.0728
	DP_{tie}	0.5074	0.3893	0.5576	0.3625

From this table, it can be seen that the proposed VSC designs improve the integral square error and the integral of the absolute time error (IAET) of frequency deviation and tie line power of a two area interconnected areas of an LFC system. The best overall performance is provided by the decentralized VSC.

3.3.2.4 The effect of governor dead band on the design of decentralized VSC

In the previous designs, the governor dead band backlash was not considered for the purpose of comparison with other design methods. A 0.06% dead band for the governor is a typical value [106]. The dynamical effect of including this nonlinearity on the LQR design method ([106], [105]) is shown in Figure 3-27.

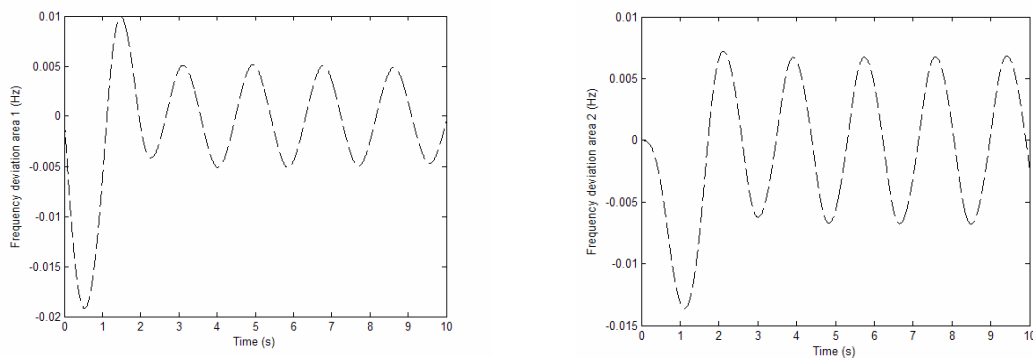


Figure 3-27: The effect of governor dead band backlash on the dynamical behavior of the LQR design [105]

As shown in Figure 3-27, the governor dead band causes more fluctuations in the frequency deviation of both areas. Therefore, a new setting is required for the VSC when governor dead band is considered.

The same design method of section 3.3.2.3 with objective function J is applied to the two area LFC system with governor dead band of 0.06% in both areas and a generation rate constraint of 0.015. The optimal settings of the decentralized VSC found by TS are given below:

VSC area 1

$$C_1^T = [17.5910 \quad 14.1432 \quad 2.0868 \quad 16.1251]$$

$$a_1 = [4.8252 \quad 0.0941 \quad 0.7711 \quad 2.0783]$$

VSC area 2

$$C_2^T = [17.0478 \quad 22.8479 \quad 0.6071 \quad 0.0228]$$

$$a_2 = [6.6656 \quad 4.7574 \quad 7.7410 \quad 9.5594]$$

The dynamical behaviour of the two area interconnected system under governor dead band and generation rate constraints is shown in Figure 3-28 when using the proposed VSC designed by TS method. The results show clearly that the proposed controller damps the frequency oscillations with a smooth control signal (effort).

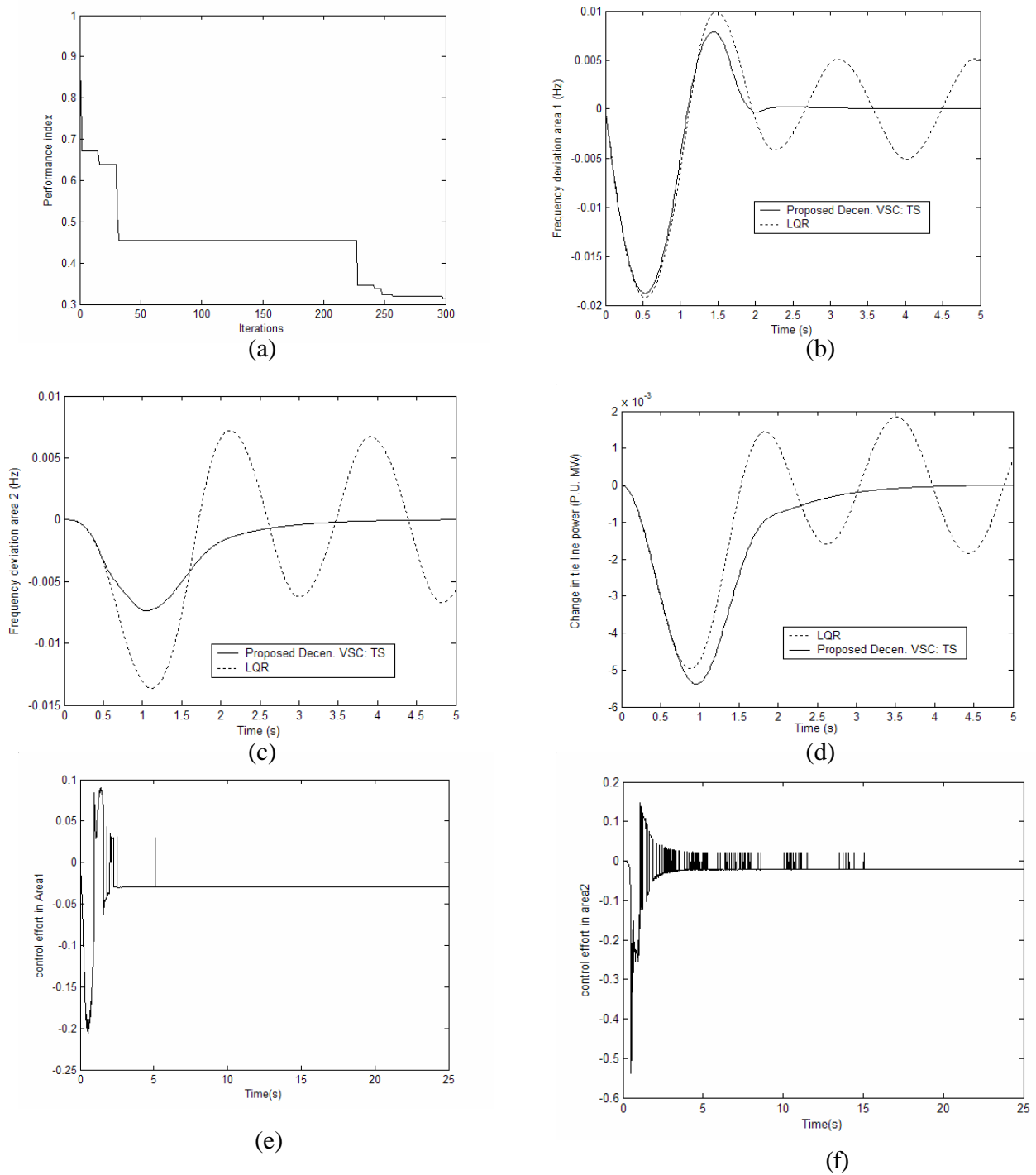


Figure 3-28: (a) Convergence of performance index (b)-(d) Dynamic behavior of the interconnected system after a 0.01 load disturbance (e) and (f) Control signal for areas 1 and 2

3.4 Three area interconnected power systems:

The schematic diagram of a three area interconnected load frequency control system is shown in Figure 3-29 [107]. It consists of two reheat turbine type thermal units and a hydro unit. Each area supplies its user region, and tie-lines allow electric power to flow between areas. Therefore, a load perturbation in one of the areas affects the output frequencies of other areas as well as the power flows on tie-lines.

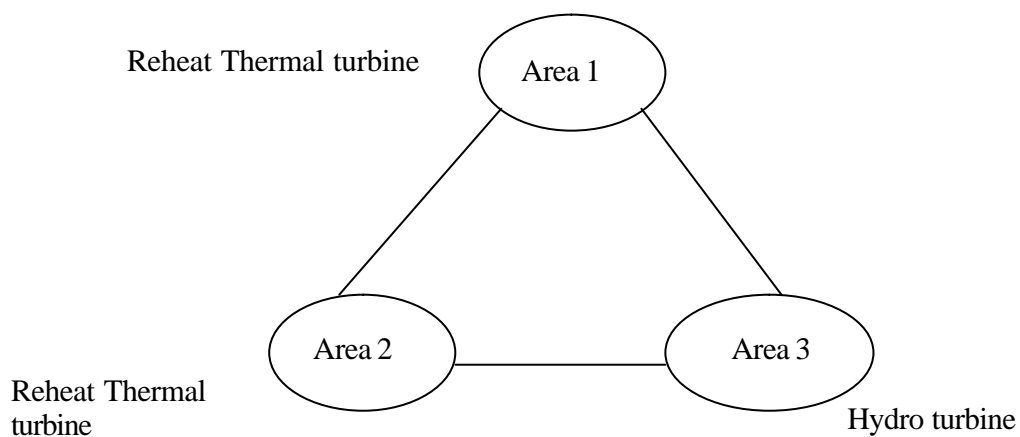


Figure 3-29: Schematic diagram of power system with three areas

A detailed block diagram of the interconnected power system is shown in Figure 3-30. The data of the system is given in Table 3-5

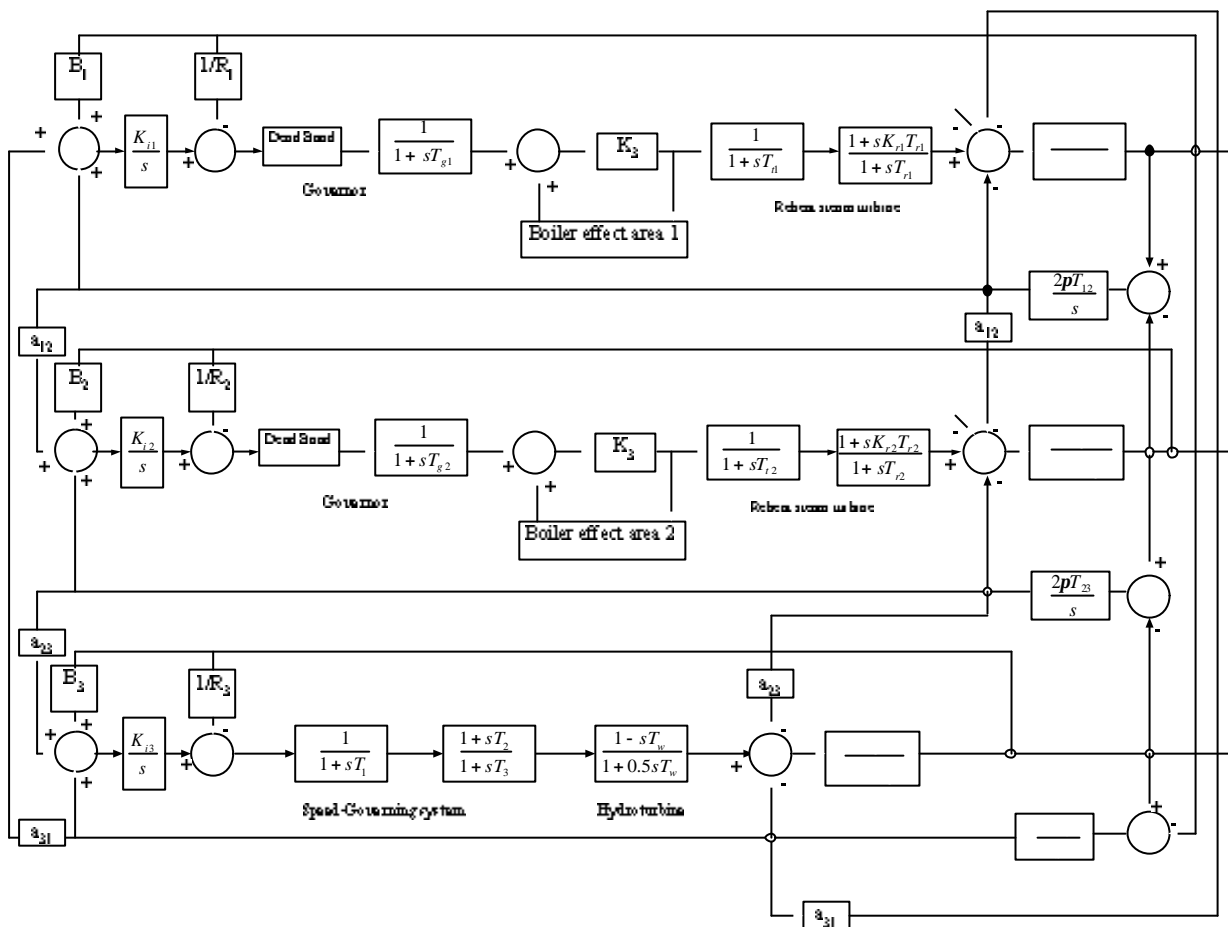


Figure 3-30: Three area interconnected LFC system

The studied system includes a reheat stage in the steam turbines. Furthermore, a dead band of 0.06% is included in the governors of the thermal areas [105]. In this example, the effect of the boiler at the thermal units is also considered. Figure 3-31 shows a block diagram for representing the boiler dynamics [108]. The long term dynamics of fuel and steam flow on boiler drum pressure are included. Representations for combustion controls are also considered. The model is basically for a drum type boiler. However, similar responses have been observed for once-

through boilers and pressurized water reactors [108]. The model can be used to study the responses of different types of boilers such as coal fired units with poorly tuned (oscillatory) combustion controls, coal fired units with well tuned controls and well tuned oil or gas fired units. In this study, a gas/oil fired unit is considered. In conventional steam units, the boiler controls respond with the necessary action upon sensing changes in steam flow and deviations in pressure due to the opening or closing of turbine steam valves following a variation in generation. Furthermore, a generation rate constraint of 0.0017 p.u. MW/s is applied for thermal units and 4.5%/s for hydro units. The system is tested for a 0.01 p.u. load disturbance in area 1.

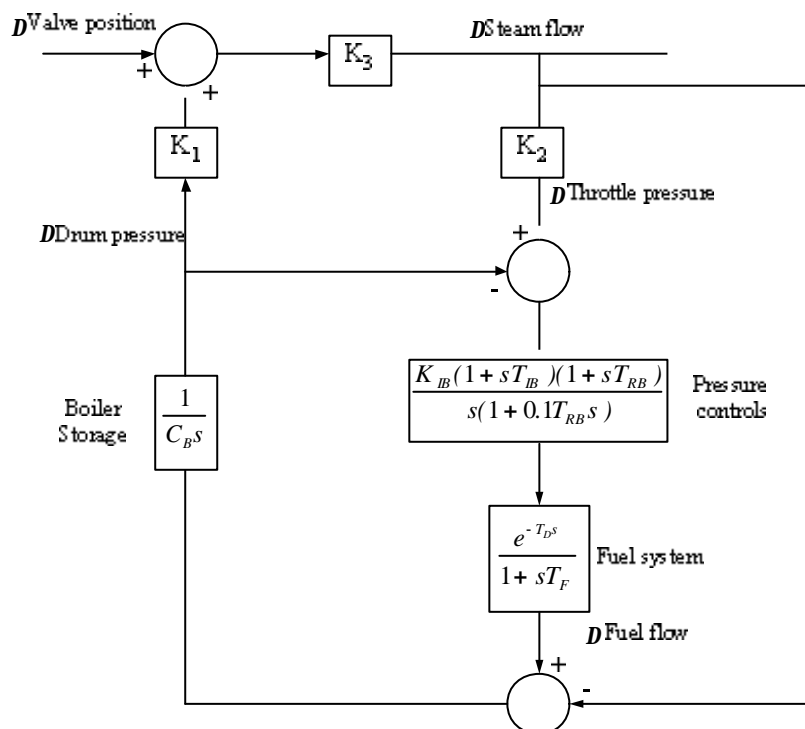


Figure 3-31: Block diagram representing Boiler dynamics

The values of the parameters for the three area power system are given below in Table 3-5 [107].

Table 3-5: Data of the three area power system

$K_{p1,2} = 120 \text{ p.u. MW}^{-1}, K_{p3} = 80 \text{ p.u. MW}^{-1}$	$2pT_{12} = 2pT_{23} = 2pT_{31} = 0.545$
$T_{p1,2} = 20 \text{ s}, T_{p3} = 13 \text{ s}$	$K_{i1,2,3} = 0.001$
$T_{g1,2} = 0.2 \text{ s}$	$R_{1,2,3} = 2.4 \text{ Hz p.u. MW}^{-1}$
$T_{i1,2} = 0.3 \text{ s}$	$K_{r1,2} = 0.333 \text{ s}$
$B_{1,2,3} = 0.425 \text{ p.u. MW/Hz}$	$T_{r1,2} = 10 \text{ s}$
$T_1 = 48.7 \text{ s}, T_2 = 0.513 \text{ s}, T_3 = 10 \text{ s}, T_w = 1 \text{ s}$	$a_{12} = a_{23} = a_{31} = -1$

VSC controllers are designed for each area. The states used for the i th VSC connected to the i th area are : $X_i = [Dw_i DP_{gi} DP_{ti} DP_{ci} DP_{ij}]$. Where j are the areas connected to i th area. PSO is utilized in the proposed design of VSC. The following objective function was optimized to guarantee minimizing the variations in frequency and tie line power between the areas:

$$J = \int_0^{\infty} (|Dw_1| + |Dw_2| + |Dw_3| + |DP_{12}| + |DP_{23}| + |DP_{31}|) dt \quad (3-16)$$

The following are settings of the controllers found by PSO :

a) **VSC area 1 :**

$$C_1^T = [11.3817 \quad 0 \quad 0.5672 \quad 17.0356 \quad 20.0 \quad 15.2477]$$

$$a_1 = [5.2801 \quad 4.2877 \quad 4.4212 \quad 3.3020] \text{ (only area states)}$$

b) **VSC area 2 :**

$$C_2^T = [1.7159 \quad 4.4657 \quad 7.9044 \quad 1.5243 \quad 14.9250 \quad 0]$$

$$a_2 = [4.1514 \quad 6.3526 \quad 6.6787 \quad 4.7101]$$

c) **VSC area 3 :**

$$C_3^T = [17.9764 \quad 12.1756 \quad 15.5068 \quad 14.1550 \quad 20.0000 \quad 4.8043]$$

$$a_3 = [0 \quad 0 \quad 9.3714 \quad 4.9867]$$

The dynamical response of the system with the designed VSC to a 0.01 p.u. disturbance in area 1 is shown in Figure 3-32.

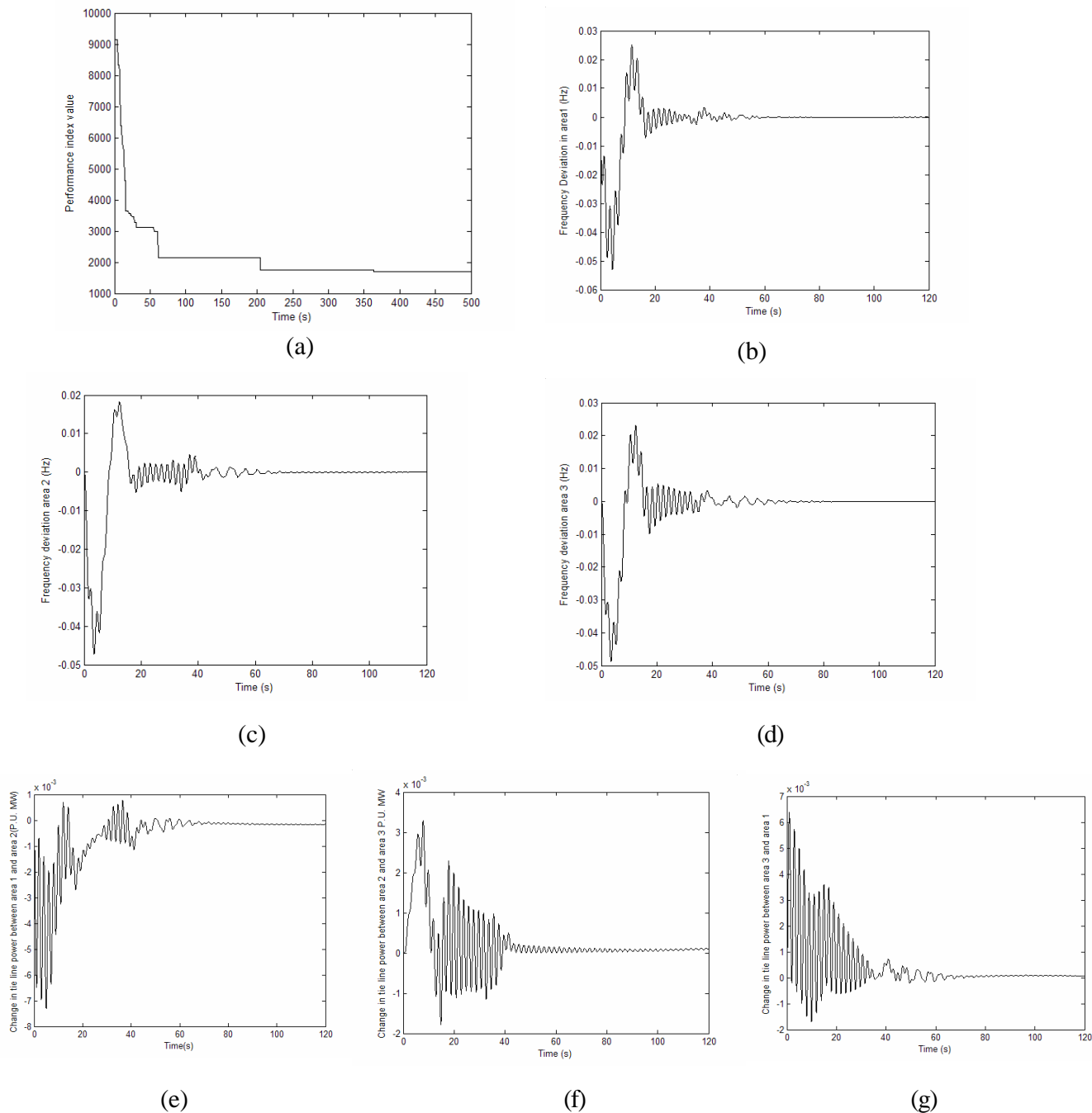


Figure 3-32: (a) Convergence of objective function (b) Frequency deviation area 1 (c) Frequency deviation area 2 (d) Frequency deviation area 3 (e)-(g) Tie line power between: (e) areas 1 and 2 (f) areas 2 and 3 (g) areas 3 and 1

It can be seen that the designed VSC was able to damp oscillations of the local frequency deviations of each area and the tie line power between the areas efficiently. The fluctuations in the parameters of the systems are mainly due to the nonlinearities present in the system. In [107], the system was equipped with SMES unit in each area to reduce these fluctuations in the signal. The time scale used for their simulation was in iterations.

Concluding remarks

The VSC designed by iterative heuristic optimization algorithms was applied to single area and interconnected LFC areas. The proposed VSC was effective in damping out the frequency oscillations of the system. The effect of nonlinearities in the form of generation rate constraint and governor dead band was also included in the studied models. The proposed VSC method proved to be efficient and reliable in improving the dynamical behavior of the studied systems.

CHAPTER 4

POWER SYSTEM STABILITY OF SINGLE MACHINE

4.1 Introduction

Power systems are usually equipped with power system stabilizers (PSS) to damp out low frequency oscillations. These oscillations are mainly caused by disturbances in the system. Various approaches were proposed for the design of PSS that include optimal control [109], classical control theory [110], adaptive control [111], and variable structure control [112] and intelligent control [113]. The power systems are usually nonlinear. The conventional method of design involves linearizing the model of synchronous machine around a suitable operation point and then linear control theory is used in designing a fixed parameter conventional PSS. Therefore some authors suggested using adaptive control methods ([114], [115]). In this chapter, VSC designed by iterative heuristics is applied to the famous linearized single machine model and compared with conventional PSS (CPSS). Furthermore, a nonlinear model of synchronous machine [116] was studied and a VSC was designed for it. In

conventional design methods, nonlinear transformation techniques are used before linear system theory is applied to the system. The new design method utilizing iterative heuristic optimization techniques provides a simpler and more systematic method with no need for complex transformations. The proposed VSC design allows the direct application of the VSC controller to the nonlinear model.

4.2 Comparison with Conventional PSS

In this section, the proposed VSC design will be compared with the conventional PSS design of [26]. PSO and TS are utilized in finding the optimum settings of the VSC controller applied to a single machine infinite bus system, Figure 4-1 (a). The linearized model is shown in Figure 4-1 (b).

The data of the studied system is given below [26]:

Generator	$M = 9.26 \quad T'_{do} = 7.76 \quad D = 0 \quad x_d = 0.973$ $x'_d = 0.190 \quad x_q = 0.550$
Excitation	$K_A = 50 \quad T_A = 0.05$
Line and Load	$R = -0.034 \quad X = 0.997 \quad G = 0.249 \quad B = 0.262$
Initial state	$P_e = 1 \quad Q_e = 0.015 \quad v_t = 1.05$

Calculation of the K's ($K1-K6$) of the linearized model can be found in Appendix A.

Figure 4-1 (c) shows a block diagram of the conventional power system stabilizer.

The values of the parameters of the CPSS are given below [26]:

$K_c=7.09$, $T = 3$ s, $T_1 = 0.6851$ s, $T_2 = 0.1$ s.

To find the optimal settings of the VSC using iterative heuristic algorithms, the following objective function is minimized:

$$J = \int_0^{\infty} |\dot{\mathbf{D}}\mathbf{w}|_t dt \quad (4-1)$$

This objective function emphasizes on damping oscillations of the speed deviation using the absolute of the speed deviation multiplied by time.

The states used in the VSC design are: $X = [\mathbf{D}\mathbf{w}(t) \ \mathbf{D}\mathbf{d}(t) \ \mathbf{D}e'_q(t) \ \mathbf{D}e_{fd}(t)]^T$. The system is simulated for a 0.01 p.u. increase in the mechanical input torque input.

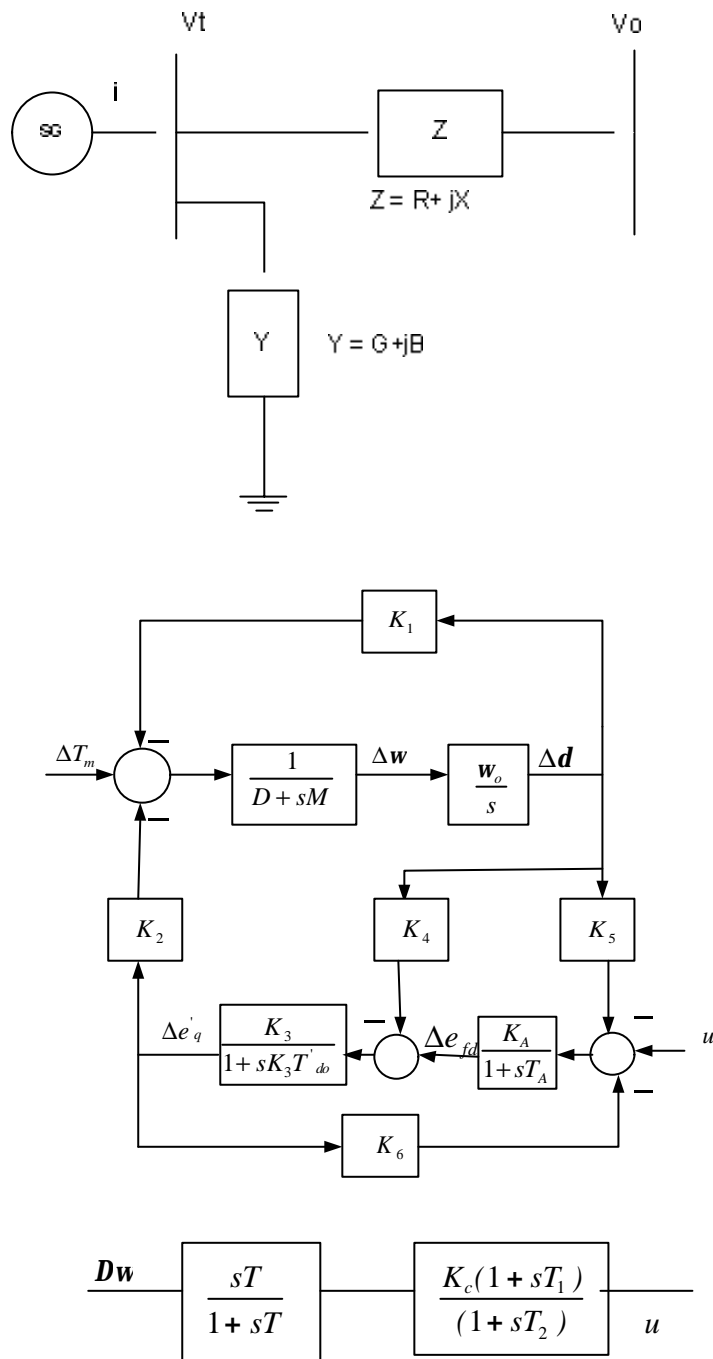


Figure 4-1: (a) Single machine infinite bus power system [26] (b) Linearized model (c) Conventional PSS

Tabu search with tabu list size of 7 and PSO with $n = 15$, maximum number of iterations = 500, $w_{max} = 0.9$, $w_{min} = 0.4$, and the maximum velocity constant factor $k = 0.1$ are used. The optimal settings found by each algorithm are given below:

a) For **PSO** design:

$\mathbf{a} = [13.8750 \quad 7.6826]$ (only x_1 and x_2 are used for switching feedback gains)

$\mathbf{C}^T = [-40000 \quad -272.7106 \quad 150 \quad 1]$

b) For **TS** design:

$\mathbf{a} = [12.3653 \quad 9.8362]$ (only x_1 and x_2 are used for switching feedback gains)

$\mathbf{C}^T = [-45763 \quad -324.1422 \quad 149.7396 \quad 1.0071]$

Figure 4-2 shows the dynamical response of the synchronous machine when applying the proposed design. Comparison is made with conventional PSS of [26]. Furthermore, the robustness of the proposed design is investigated by varying the operating point (P and Q). A comparison between the minimum value of J and computation time for the two algorithms is shown in Table 4-1.

Table 4-1: Comparison between the algorithms used in the proposed VSC design applied to a single machine infinite bus system

Algorithm	Computation Time (Mins.)	Minimum value of J
PSO	2.4210	0.0047
TS	96.3233	0.0023

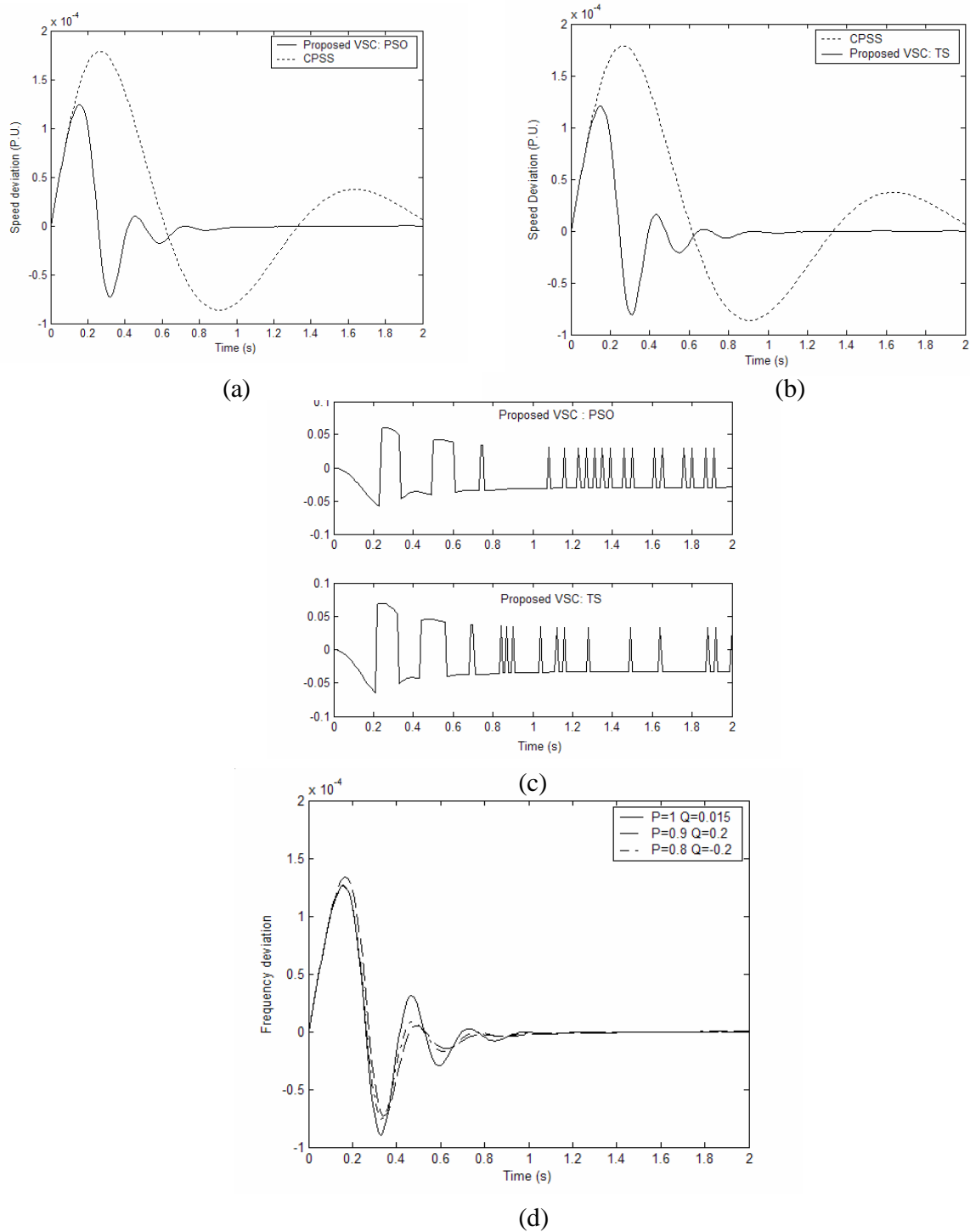


Figure 4-2: (a)-(b) Damping of frequency oscillation (c) Control signal (d) Frequency deviation of the system with the proposed VSC when operating point is changed for PSO design. Nominal operating point: $P = 1$ p.u. $Q = 0.015$ p.u.

From the above results the following can be concluded:

- 1- The new VSC design improves the damping of oscillations after the system is subjected to sudden changes in its parameters, Figure 4-2(a) and (b).
- 2- The controller shows robust behavior even when the operating point is changed, Figure 4-2(d).
- 3- The only draw back of the proposed design is an increased fluctuation in the control signal, Figure 4-2(c).
- 4- TS was able to provide a smaller value for J . However, this was on the expense of larger computation time.

The third point can be solved by the following:

- 1- Including a scaled value of the deviation of the control signal in the objective function as was done in previous problems and designs of this thesis.
- 2- Scaling the feedback gains of VSC on convergence of the integral of the square error or the integral of the deviation in frequency.

The second approach is adopted here where: for the optimum switching vector value and feedback gains found by the PSO method:

if $\Delta J < \varepsilon$
then $\mathbf{a}_{new} = m \cdot \mathbf{a}$
where $0 < m < 1$

where J is the objective function being minimized. ϵ is a small number. For this example, and using the optimum settings of VSC found by PSO, the following values were chosen: $m = 0.3$ and $\epsilon = 1 \times 10^{-13}$. The dynamical behaviour of the single machine infinite bus system when this approach is used for the controller design is shown in Figure 4-3. The following can be concluded from the results:

- 1- Scaling of the feedback gains caused negligible degradation in the performance of the VSC. This is clear from Figure 4-3 (a).
- 2- The chattering in the control effort is almost eliminated by the proposed scaling method as seen in Figure 4-3 (b).

In this way, both improvement in the performance of the VSC and smooth control signal is provided by the new method.

In addition, the robustness of the controller under variation of the system operating point is investigated. Figure 4-3 (c) shows that the designed controller is almost insensitive to the change in operating point.

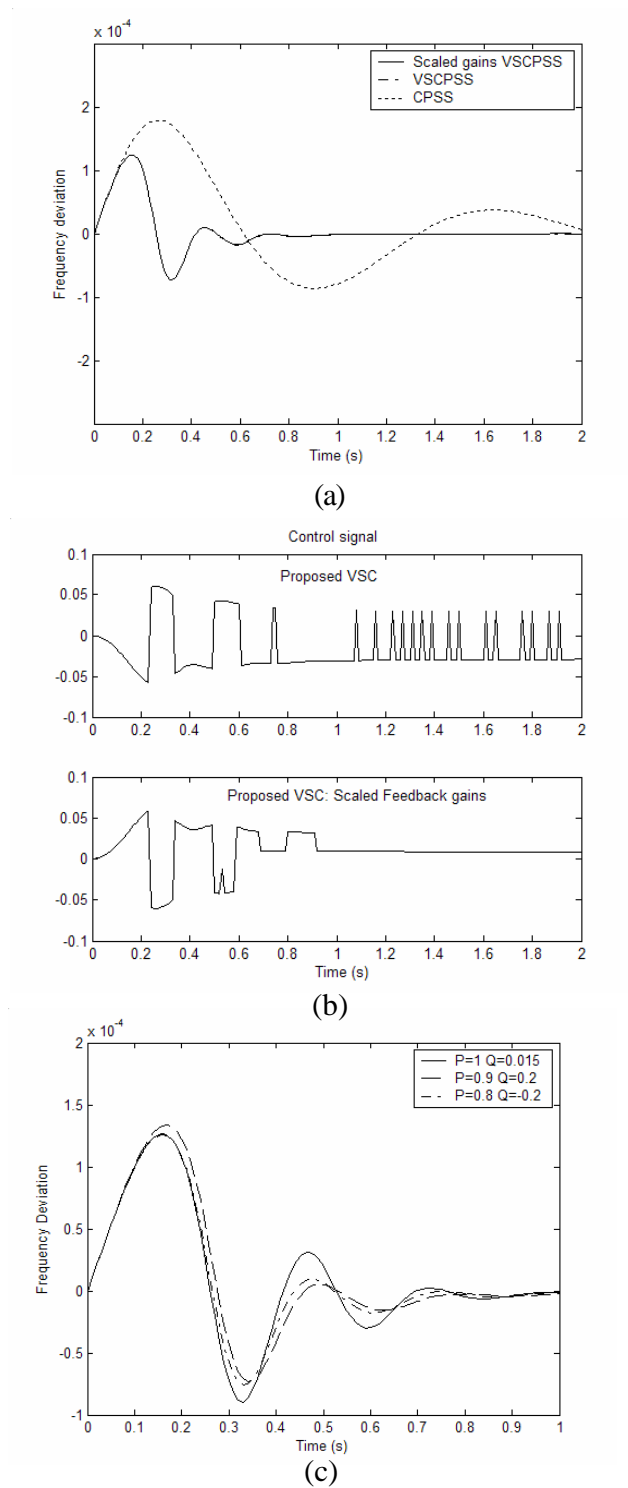


Figure 4-3: (a) Damping of frequency oscillations (b) Control signal (c) Robustness of the system with the proposed scaled gains VSC when operating point is varied. Nominal operating point: $P=1$ p.u. $Q=0.015$ p.u.

4.3 Comparison with other VSC methods

In this section a comparison is made with the design method proposed by Lee et. al in [117]. The proposed objective function optimized is given below:

$$J = \int_0^{\infty} q_1 \cdot \mathbf{Dw}^2 + q_2 \cdot \mathbf{Du}^2 dt \quad (4-2)$$

This objective function includes the square of the deviation in frequency to damp out its oscillations. It also includes the square of the change in the control signal to reduce chattering.

$q_1 = 1 \times 10^4$ and $q_2=1$ were chosen for the design. The setting of the controllers given by different iterative heuristic optimization algorithms are given below:

a) For **GA** :

$$\mathbf{C}^T = [-9240.7 \ -11.2506 \ 125 \ 1]$$

$$\mathbf{a} = [2.9989 \ 0.0109 \ 0.0021 \ 0.0711]$$

b) For **PSO** :

$$\mathbf{C}^T = [-20000 \ -1.7211 \ 297.7160 \ 2.2218]$$

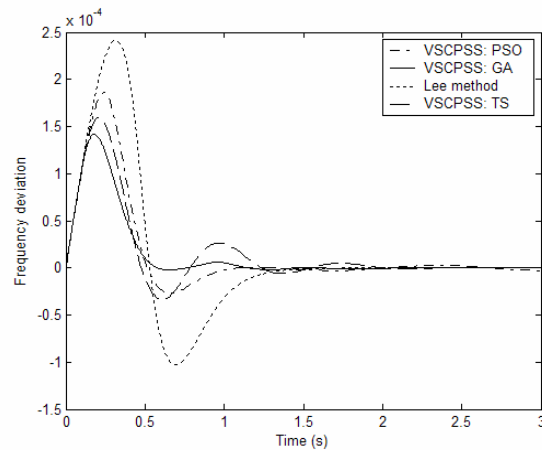
$$\mathbf{a} = [3.2166 \ 0 \ 0.7602 \ 0.0355]$$

c) For **TS** :

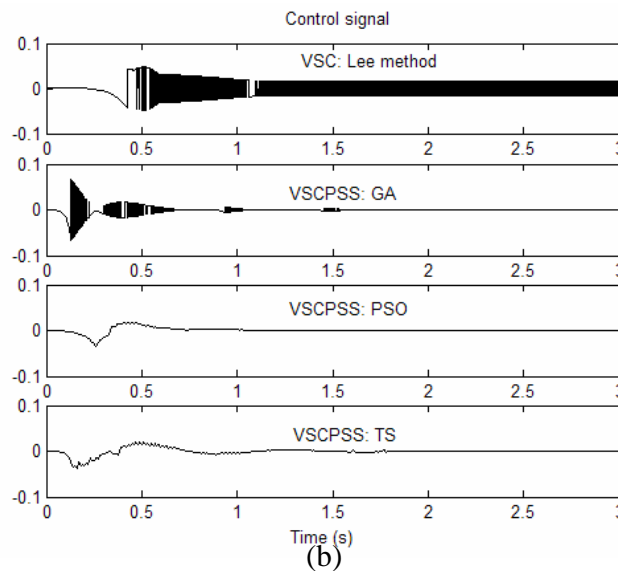
$$\mathbf{C}^T = [-1.9398 \times 10^4 \ -4.5008 \ 213.1303 \ 3.5382]$$

$$\mathbf{a} = [1.7112 \ 0.0206 \ 0.0234 \ 0.0648]$$

The parameters of the system used in this design [117] are: $K_1 = 0.5698$, $K_2 = 0.9709$, $K_3 = 0.6584$, $K_4 = 0.5233$, $K_5 = -0.0500$, $K_6 = 0.8454$, $M = 9.26$, $D = 0$, $T'_{do} = 7.76$, $K_A = 50$, $T_A = 0.05$. The system is subjected to a 0.01 p.u. increase in the input mechanical torque. Figure 4-4 shows that the proposed VSC design applied to single machine infinite bus improves the damping the oscillations in the frequency of the machine compared with the method proposed by Lee. Both reduced over shoot and faster settling of the frequency deviation can be seen in Figure 4-4(a). Furthermore, the fluctuations in the control signal are minimized. For the algorithms used, GA tuned VSC was able to provide the best dynamic response for the system. However, PSO tuned VSC had the smoothest control signal.



(a)



(b)

Figure 4-4: (a) Damping of frequency oscillations (b) Control effort

4.4 Nonlinear model of the synchronous machine

In [116], a nonlinear model of a synchronous machine connected to an infinite bus is investigated. In order to design the VSC for this system, various nonlinear transformations were required before applying linear control theory to develop a

switched control law that drives the machine from an unstable state to a desired equilibrium point and maintain it there. The system studied is shown in Figure 4-5. To develop the mathematical model that describes the dominant dynamics of the nonlinear single machine, the following assumptions were made by the author:

- 1) the voltage behind the transient reactance of the machine is constant
- 2) governor/turbine dynamics are represented by a slow first-order system
- 3) swing equations are used to describe the mechanical motion of the synchronous machine.

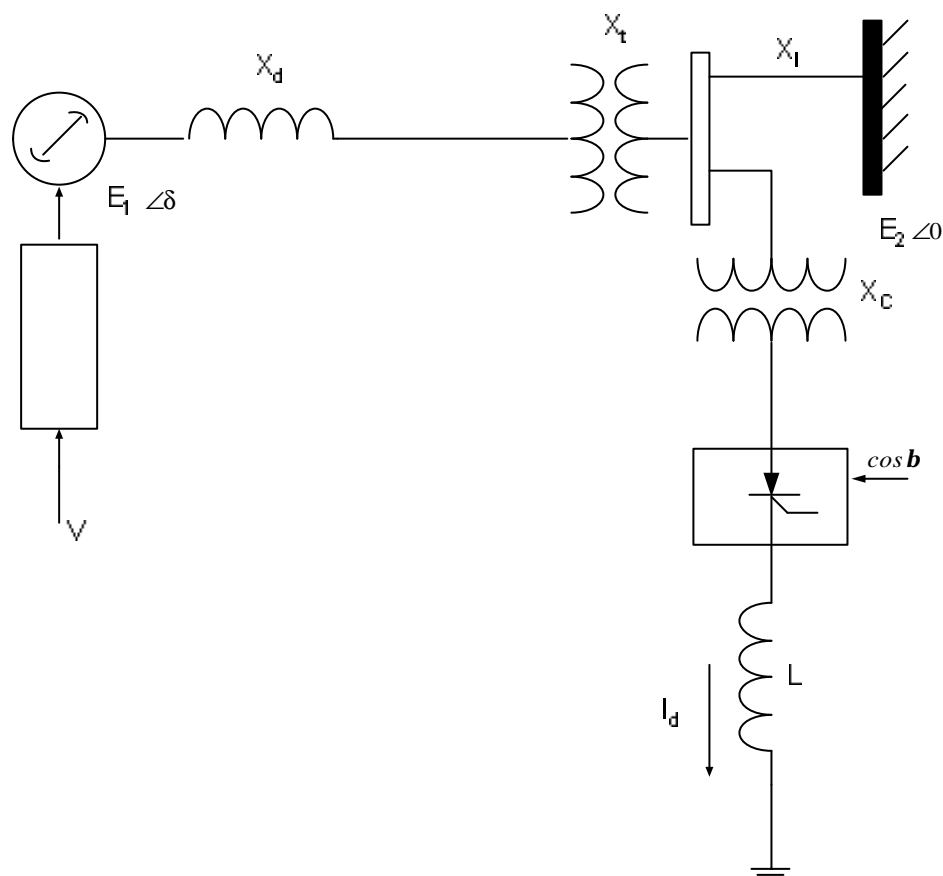


Figure 4-5: Synchronous machine infinite bus power system

The dynamics of the system are described by the following equations:

$$\dot{\mathbf{d}} = \mathbf{w} \quad (4-3)$$

$$\dot{\mathbf{w}} = \frac{\mathbf{w}_B}{2H} [P_m - P_{ac} - KP_{dc}] - D \cdot \mathbf{w} \quad (4-4)$$

$$P_{dc} = (\cos(\mathbf{b}) - R_c I_d) I_d \quad (4-5)$$

$$\dot{I}_d = 1/L(\cos(\mathbf{b}) - R_c I_d) \quad (4-6)$$

$$\dot{P}_m = -\mathbf{a}P_m + v \quad (4-7)$$

where

\mathbf{d} : rotor angle of the machine in electrical radians relative to the center of mass.

\mathbf{w} : rotor angular velocity in radians per second with respect to synchronous speed.

H : inertia constant in seconds.

D : damping coefficient in seconds⁻¹.

P_m : per unit mechanical power.

P_{ac} : per unit AC power.

P_{dc} : per unit power stored in the converter.

$\mathbf{w}_B = 377$ rad/s $K = 1$

\mathbf{a} : time constant of governor/turbine or mechanical power actuator

v : the corresponding input

I_d : Dc current through converter

R_c : per unit commutating resistance

$$X = X_d + X_t + X_l, P_{ac} = (E_1 E_2 / X) \sin d$$

The dynamic equations can be put into state form by the following definitions:

$x_1 = d$, $x_2 = I_d$, $x_3 = \omega$, $x_4 = P_m$. The two control inputs are $u_1 = \cos(\beta)$ and $u_2 = v$.

The state space model is given as follows:

$$\begin{aligned} \dot{\hat{x}}_1 &= \hat{u} & \hat{x}_3 & & \dot{\hat{u}} &= 0 & 0 \\ \dot{\hat{x}}_2 &= \hat{e} & -k_1 x_2 & & \dot{\hat{u}} &= \hat{e} k_4 & 0 \\ \dot{\hat{x}}_3 &= \hat{e} - k_2 \sin(x_1) + k_3 x_2^2 - D x_3 + k_5 x_4 & & & \dot{\hat{u}} &= \hat{e} u_1 & \hat{u} \\ \dot{\hat{x}}_4 &= \hat{e} & -a x_4 & & \dot{\hat{u}} &= \hat{e} u_2 & \hat{u} \\ \dot{\hat{u}} & & & & \dot{\hat{u}} &= 0 & 1 \end{aligned} \quad (4-8)$$

where

$$k_1 = \frac{R_c}{L}, k_2 = \frac{w_B E_1 E_2}{2HX}, k_3 = \frac{w_B R_c}{2H}, k_4 = \frac{1}{L}, k_5 = \frac{w_B}{2H}$$

The parameters of the system are [116]: DC converter rated at 80 MW, 230KV system, Machine rating 800 MVA. On a 800 MVA base: $X = 0.2$ p.u., $R_c = 0.3$ p.u., $L = 0.015$ p.u., $H = 7$ s, $D = 0.5$ s⁻¹, and $a = -0.1$ s⁻¹. This gives: $k_1 = 20$, $k_2 = 177.72857$, $k_3 = 8.078571$, $k_4 = 66.667$, and $k_5 = 26.928571$.

The control objective in [116] is to derive the machine from a perturbed state to a desired equilibrium point and maintain it there. This objective involves the following goals: 1) Operating the machine at the rated frequency, i.e. x_3 must be zero at

equilibrium 2) keeping the dc current (x_2) at zero 3) Delivering a specified amount of AC power to the bus and this defines a *desired load angle* \mathbf{g} of x_1 . The design procedure proposed in [116] involves:

- 1- Transforming the system state space model into a Luenberger canonical form.
- 2- Construction of a suitable sliding surface.

The first step is complicated and involves many manipulations.

In the present work, iterative heuristic optimization algorithms in the following way:

- 1- The control signals, u_1 and u_2 of state space equation 4-1, are of VSC type and are given as follows:

$$X = [\mathbf{w} \quad I_d \quad P_{me} \quad \mathbf{d}_e \quad]$$

$$P_{me} = P_m - P_{mdesired} \quad (4-9)$$

$$\mathbf{d}_e = \mathbf{d} - \mathbf{g} \quad (4-10)$$

$$u_1 = -\mathbf{y}_1 \cdot x_1 \quad (4-11)$$

where

$$\mathbf{y}_1 = \begin{cases} \hat{\mathbf{1}} \cdot \mathbf{a}_1 & \text{if } \mathbf{s}_1 \cdot x_1 > 0 \\ \hat{\mathbf{1}} - \mathbf{a}_1 & \text{if } \mathbf{s}_1 \cdot x_1 < 0 \end{cases} \quad (4-12)$$

and

$$\mathbf{s}_1 = C_1 \cdot x_1 = 0 \quad (4-13)$$

Also,

$$u_2 = -\mathbf{y}^T \cdot X \quad (4-14)$$

where

$$\mathbf{y}_{2j} = \begin{cases} \hat{1} \cdot \mathbf{a}_{2j} & \text{if } x_j \mathbf{s}_2 > 0 \\ \hat{1} - \mathbf{a}_{2j} & \text{if } x_j \mathbf{s}_2 < 0 \end{cases} \quad j = 1, \dots, 4 \quad (4-15)$$

and

$$\mathbf{s}_2 = C_2^T \cdot X = 0 \quad (4-16)$$

2- The optimum values of the VSC are found by an iterative heuristic algorithm. The following objective function is minimized:

$$J = \int_0^{\infty} \mathbf{d}_e^2 + \mathbf{w}^2 + P_{me}^2 dt \quad (4-17)$$

The above objective function includes the square of the frequency deviation, the square of the error in angle, and the square of the error in mechanical power. By minimizing such an objective function the desired angle and mechanical power will be reached and the frequency deviation will be minimized and thus the control objectives will be satisfied. The system (4-1) was simulated with the following initial conditions [116]:

$$x_1 = 0.0522, \quad x_2 = 0.1, \quad x_3 = 0.1, \quad x_4 = 6.6 \sin(x_1(0))$$

The three heuristic (PSO, GA, and TS) algorithms were used to find the optimal settings of the controller. The settings of the VSC found by each algorithm are given below:

a) For **GA (cross over =1 Mutation = 0.001):**

$$C_1^T = -7.7146$$

$$a_1 = 1$$

$$C_2^T = [15.9418 \quad -3.1396 \quad 15.5786 \quad 7.3765]$$

$$a_2 = [4.0306 \quad 3.5430 \quad 5.0000 \quad 5.0000]$$

b) **PSO ($n = 15$ $w_{max} = 0.9$, $w_{min} = 0.4$, and the maximum velocity constant factor $k = 0.1$)**

$$C_1^T = 5.2149$$

$$a_1 = 1$$

$$C_2^T = [12.6720 \quad 20.0000 \quad 12.5277 \quad 4.9987]$$

$$a_2 = [5.0000 \quad 5.6522 \quad 5.0000 \quad 5.0000]$$

c) **TS (tabu list size =7)**

$$C_1^T = 5.0987$$

$$a_1 = 0.9767$$

$$C_2^T = [6.3733 \quad 7.4961 \quad 6.2283 \quad 5.5775]$$

$$a_2 = [4.4706 \quad 5.0689 \quad 4.9972 \quad 4.9997]$$

The dynamic behaviour of the system with the proposed VSC controller is shown in Figures 4-6, 4-7, and 4-8 for each algorithm respectively. A comparison between the minimum value of J and computation time for the three algorithms is shown in Table 4-2.

Table 4-2: Comparison between the three algorithms used in the proposed VSC design applied to a nonlinear model of a synchronous machine infinite bus system

Algorithm	Computation Time (Mins.)	Minimum value of J
GA	72.1765	9.3031
PSO	6.8405	9.3045
TS	74.7293	9.3067

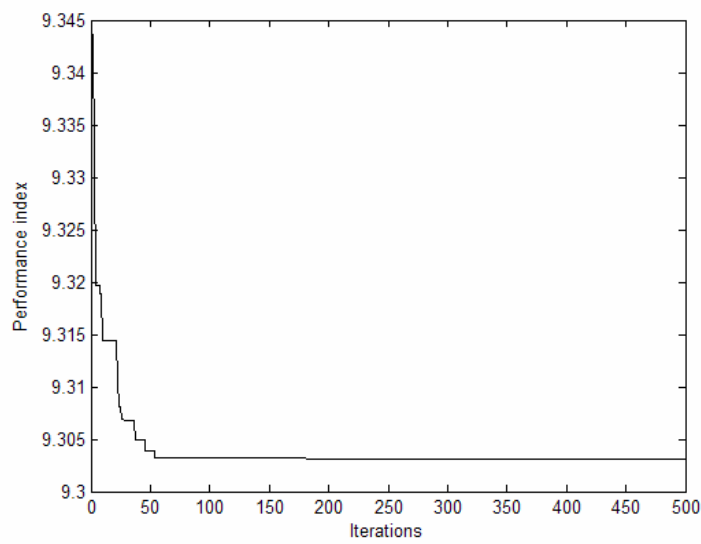
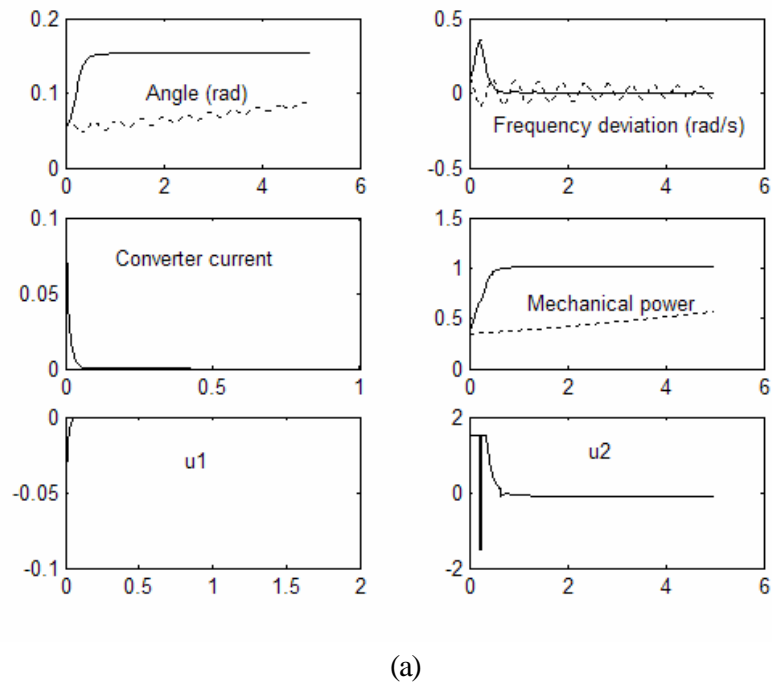
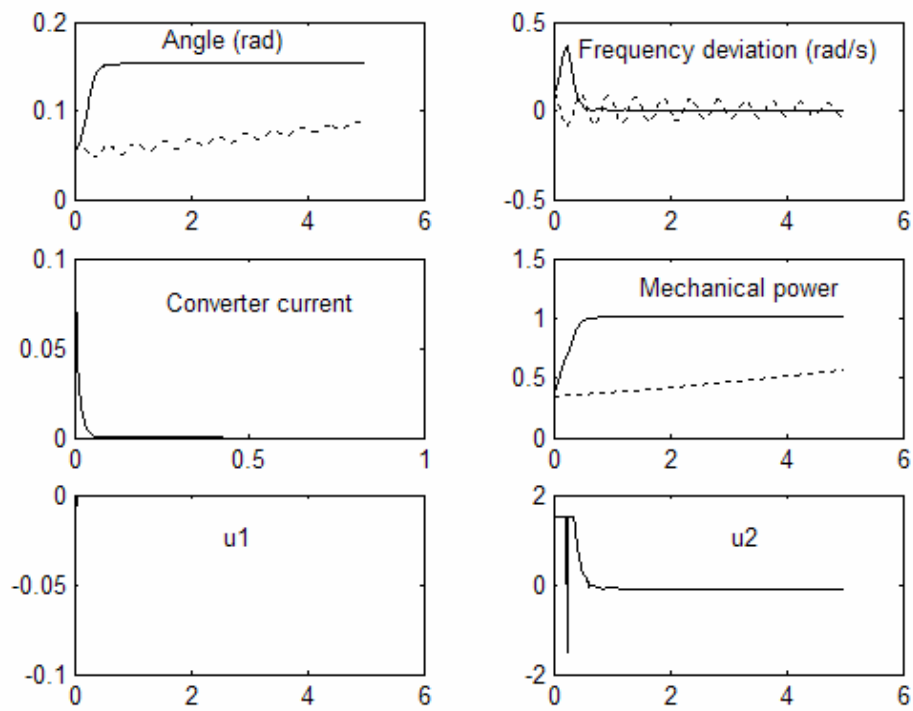
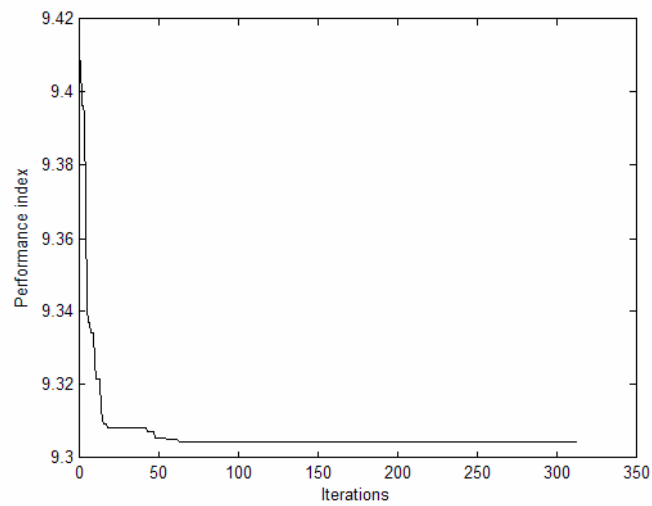


Figure 4-6: GA design: (a) Performance of system with the proposed VSC (--without controller) (b) Convergence of performance index

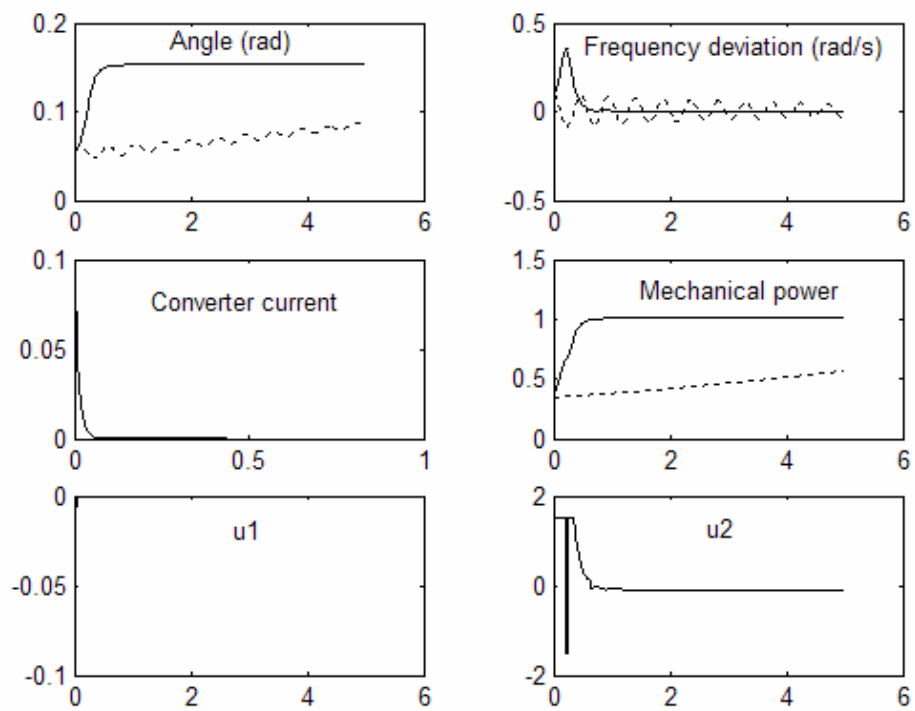


(a)

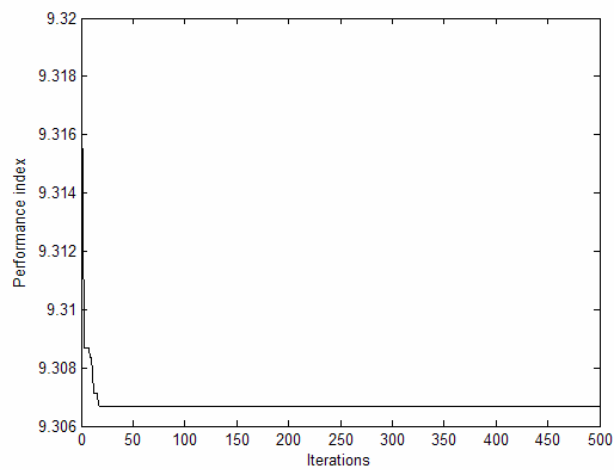


(b)

Figure 4-7: PSO design (a) Dynamical performance of the system (--without controller) (b) Convergence of the performance index



(a)



(b)

Figure 4-8: TS design: (a) Dynamical behavior of the system and control signals (--- without controller) (b) Convergence of performance index

From the above results it can be concluded that the proposed design method of VSC can be applied successfully to nonlinear systems. The proposed method requires no nonlinear transformation or linearization of the model. Thus, a systematic simple way of designing VSC controller is achieved. The control objectives of minimizing the frequency deviation and following a desired angle were satisfied, Figures 4-6(a), 4-7(a), and 4-8(a). Furthermore, the algorithms used for the design showed similar behavior. The GA algorithm was able to find the smallest value of the objective function. Compared with the results of the design method proposed [116], the dynamical behavior of the method proposed is very similar in terms of both the overshoot and settling time. However, the proposed method is much simpler and does not require any nonlinear transformations to arrive at the optimal values for both switching vector and feedback gains.

Concluding remarks

The VSC designed by iterative heuristic optimization algorithms was applied to single machine systems. Both linear and nonlinear models of a synchronous machine connected to an infinite bus were studied. The proposed method was applied successfully to both.

CHAPTER 5

CONCLUSIONS AND FUTURE DIRECTIONS

The design of suitable controllers for enhancing the dynamic performance of power systems is one of the most important subjects concerning power engineers. This thesis addressed the design of robust optimal variable structure controllers applied to important power system problems such as LFC of single, two, and three areas interconnected, and single machine infinite bus system. The new proposed design method utilizes iterative heuristic optimization algorithms to find the optimum switching vector and feed back gains of the VSC. The following can be considered as the contributions of this thesis:

- 1- A new simple and systematic way of designing optimal variable structure controllers applied to power system dynamic problems is introduced in this thesis. The new method formulates the design of VSC as an optimization problem and uses iterative heuristic optimization algorithms in the design procedure.

- 2- Linear and nonlinear models of the investigated systems were considered.
- 3- Reduction of the chattering in the control signal by two methods:
 - a- Including a scaled value of the deviation of the control signal into the objective function of the optimization process.
 - b- Scaling the feedback gains of the controller on convergence of the objective function
- 4- Enhancing the dynamic performance of power systems problems studied, namely the load frequency control problem and stability of a single machine connected to an infinite bus. The new method improved the dynamic behavior of the systems studied in comparison with other control and VSC methods reported in the literature.
- 5- The proposed controllers were designed using either all states or only the accessible states of the system. The results obtained in the later case are very much promising while the complexity of the controller is highly reduced.
- 6- The new method can incorporate nonlinearities with ease into the models being studied. This requires no coordinate or nonlinear transformations and hence simplifies the design procedure.

7- The robustness of the proposed controllers was investigated. It has been found that the three proposed controllers (PSO, GA, and TS) are almost insensitive to system parameters variations.

Recommendations for future research directions

The research in this subject can be further advanced in the following suggested directions:

1- Adaptation of the feedback gains in accordance with the integral of square of error or objective function. This method might further reduce the chattering in the control signal. Fuzzy logic can be used for this purpose. But this adaptation might reduce the robustness of the controller.

2- Using control laws different from the discontinuous law used in this thesis. Some of these laws are included in section 2.4 of this thesis. These control laws can further help in reducing the chattering in the control signal.

3- Combining VSC with other types of controllers in a way that might overcome some of the demerits of the VSC.

4- Exploring other power systems problems. The problems investigated in this thesis are mainly that of load frequency control and stability of single machine connected to infinite bus. There are other numerous power system control problems on which the new proposed VSC can be applied. For example, the proposed VSC design can be applied to the stability of a multi-machine power system.

Appendix A

Calculation of constants K_1, K_2, \dots, K_6 [26]

For the calculation of constant K_1, K_2, \dots, K_6 of Figure 4-1(a), the armature current components i_d and i_q must be known. Figure 4-1 (b) shows the one machine infinite-bus model of a power system with a synchronous generator SG, an armature current I , a terminal voltage v_t , an infinite-bus voltage v_o , a series transmission impedance Z , and a shunt load admittance Y . The armature current, terminal voltage, torque angle \mathbf{d} defined as the angle between the infinite-bus voltage v_o , and the internal voltage e'_q can be written as follows:

$$i = i_d + j i_q, \quad v_t = v_d + j v_q \quad (\text{A-1})$$

$$[\text{Phasor } v_o] = v_o (\sin \mathbf{d} + j \cos \mathbf{d})$$

where

$$\mathbf{d} = \mathfrak{D}(e'_q, v_o) \quad (\text{A-2})$$

To simplify the calculations, the following constants and parameters are introduced:

$$1 + ZY = C_1 + jC_2$$

$$R_1 = R - C_2x'_d \quad X_1 = X + C_1x_q \quad R_2 = R - C_2x_q \quad X_2 = X + C_1x'_d \quad (A-3)$$

$$Z_e^2 = R_1R_2 + X_1X_2$$

$$Y_d = (C_1X_1 - C_2R_2)/Z_e^2 \quad Y_q = (C_1R_1 + C_2X_2)/Z_e^2$$

From Figure 4-1 (a), the following can be written:

$$i = Yv_t + Z^{-1}(v_t - v_o) \quad \text{or} \quad Zi = (1 + ZY)v_t - v_o \quad (A-4)$$

The last equation can be separated into real and imaginary parts, the results can be written in matrix form in real numbers as follows:

$$\begin{bmatrix} \hat{e}R \\ \hat{e}X \end{bmatrix} - \begin{bmatrix} X \\ R \end{bmatrix} \begin{bmatrix} \hat{u}i_d \\ \hat{u}i_q \end{bmatrix} = \begin{bmatrix} \hat{e}C_1 \\ \hat{e}C_3 \end{bmatrix} - \begin{bmatrix} C_2 \\ C_1 \end{bmatrix} \begin{bmatrix} \hat{u}v_d \\ \hat{u}v_q \end{bmatrix} - v_o \begin{bmatrix} \hat{e} \sin d \\ \hat{e} \cos d \end{bmatrix} \quad (A-5)$$

Where

$$C_1 = 1 + RG - XB, \quad C_2 = XG + RB \quad (A-5a)$$

The magnitudes of v_d and v_q can be written as follows:

$$\begin{bmatrix} \hat{e}v_d \\ \hat{e}v_q \end{bmatrix} = \begin{bmatrix} \hat{e}0 \\ \hat{e}1 \end{bmatrix} \begin{bmatrix} \hat{u}e'q \\ \hat{u}e'q \end{bmatrix} - \begin{bmatrix} \hat{e}0 \\ \hat{e}x'd \end{bmatrix} \begin{bmatrix} \hat{u}i_d \\ \hat{u}i_q \end{bmatrix} \quad (A-6)$$

Substituting (A-6) into (A-5) and solving for i_d and i_q gives:

$$\begin{bmatrix} \hat{e}i_d \\ \hat{e}i_q \end{bmatrix} = \begin{bmatrix} \hat{e}Y_d \\ \hat{e}Y_q \end{bmatrix} \begin{bmatrix} \hat{u}e'q \\ \hat{u}e'q \end{bmatrix} - \frac{v_o}{Z_e^2} \begin{bmatrix} \hat{e}R_2 \\ \hat{e}X_2 \end{bmatrix} - \begin{bmatrix} X_1 \\ R_1 \end{bmatrix} \begin{bmatrix} \hat{u} \sin d \\ \hat{u} \cos d \end{bmatrix} \quad (A-7)$$

Linearization of (A-7) results in

$$\begin{bmatrix} \hat{e}Dj_d \\ \hat{e}Dj_q \end{bmatrix} \hat{u} = \begin{bmatrix} \hat{e}Y_d \\ \hat{e}Y_q \end{bmatrix} \hat{u} D e'q + \begin{bmatrix} \hat{e}F_d \\ \hat{e}F_q \end{bmatrix} \hat{u} D d \quad (A-8)$$

Where Y_d and Y_q are given in (A-3),

$$\begin{aligned} \hat{e}F_d \hat{u} &= \frac{v_o}{Z_e^2} \hat{e} - R_2 X_1 \hat{u} \hat{e} \cos d_o \hat{u} \\ \hat{e}F_q \hat{u} &= \hat{e} X_2 R_1 \hat{u} \hat{e} \sin d_o \hat{u} \end{aligned} \quad (\text{A-9})$$

and d_o is the initial angle.

Now, the constants K_s are calculated as follows:

K_1 and K_2 from Electric Torque. The electric torque of a synchronous machine near the synchronous speed can be approximated by:

$$T_e \approx P_e = i_d v_d + i_q v_q \text{ per unit} \quad (\text{A-10})$$

Substituting v_d and v_q from (A-6) into (A-10) yields:

$$T_e = i_q e'_{q'} + (x_q - x'_d) \dot{i}_d i_q \quad (\text{A-11})$$

Substituting \mathbf{Di}_d and \mathbf{Di}_q of (A-8) into the linearized results of (A-11) yields:

$$\mathbf{DT}_e = K_1 \mathbf{Dd} + K_2 \mathbf{De}'_q \quad (\text{A-12})$$

Where

$$\begin{aligned} \hat{e}K_1 \hat{u} &= \hat{e} 0 \hat{u} + \hat{e}F_d F_q \hat{u} \hat{e} (x_q - x'_d) \dot{i}_{qo} \hat{u} \\ \hat{e}K_2 \hat{u} &= \hat{e} \dot{i}_{qo} \hat{u} + \hat{e} Y_d Y_q \hat{u} \hat{e} e'_{qo} + (x_q - x'_d) \dot{i}_{do} \hat{u} \end{aligned} \quad (\text{A-13})$$

K_3 and K_4 from the field voltage equation. The field winding voltage equation can be written as follows (Linearized):

$$(1 + sT'_{do}) \mathbf{De}'_q = \mathbf{DE}_{FD} - (x_d - x'_d) \mathbf{Di}_d \quad (\text{A-14})$$

Substituting \mathbf{Di}_d of (A-8) into (A-14) results in

$$(1 + sT'_{do} K_3) \mathbf{De}'_q = K_3 [\mathbf{DE}_{FD} - K_4 \mathbf{Dd}] \quad (\text{A-15})$$

Where

$$\begin{aligned} K_3 &= 1 / [1 + (x_d - x'_d) Y_d] \\ K_4 &= (x_d - x'_d) F_d \end{aligned} \quad (\text{A-16})$$

K_5 and K_6 from the terminal voltage magnitude. The magnitude of the generator terminal voltage can be expressed in terms of its d and q components as:

$$v_t^2 = v_d^2 + v_q^2 \quad (\text{A-17a})$$

and the deviation as

$$Dv_t = (v_{do} / v_{to}) Dv_d + (v_{qo} / v_{to}) Dv_q \quad (\text{A-17b})$$

Substituting (A-8) into the linearized results of (A-6) and Dv_d and Dv_q thus obtained into (A-17b) gives

$$Dv_t = K_5 Dd + K_6 De_q \quad (\text{A-18})$$

Where

$$\begin{aligned} \hat{K}_5 \hat{u} &= \hat{e} \quad 0 \quad \hat{u} \quad \hat{e} F_d \quad F_q \hat{u} \hat{e} - x_d' v_{qo} / v_{to} \hat{u} \\ \hat{K}_6 \hat{u} &= \hat{e} v_{qo} / v_{to} \hat{u} + \hat{e} Y_d \quad Y_q \hat{u} \hat{e} \quad x_q v_{do} / v_{to} \hat{u} \end{aligned} \quad (\text{A-19})$$

In (A-19), F_d and F_q are given in (A-9) and Y_d and Y_q in (A-3).

References

- [1] Prahba Kundur., *Power System Stability and Control*, McGraw-Hill, USA, 1994.
- [2] O. I. Elgerd and C. E. Fosha, "Optimum megawatt frequency control of multiarea electric energy systems," *IEEE Trans. Power Appar. and Syst.*, vol 89, pp. 556-563, 1970.
- [3] J. Nanda and B. L. Kaul, "Automatic generation control of an interconnected power system," *Proc. IEE*, vol. 125, No. 5, pp. 385-390, 1978.
- [4] Young-Hyun Moon, Heon-Su Ryu, Byoung-Kon Choi, Hyung-Jong Kook, "Improvement of system damping by using differential feedback in the load frequency control," *Proc. of the IEEE PES 1999 Winter Meeting*, vol. 1, pp. 683-688, 1999.
- [5] J. D. Glover and F. C. Schweppa, "Advanced Load Frequency Control," *IEEE Trans. Power Appar. and Syst.*, vol. 91, pp. 2095-2103, 1972.
- [6] N. N. Bengiamin and W. C. Chan, "Multilevel Load-Frequency of interconnected power systems", *Proc. IEE*, vol. 125, No. 6, pp. 521-526, 1978.
- [7] W. C. Chan and Y. Y. Hsu, "Automatic generation control of interconnected power system using variable structure controllers," *Proc. IEE Part C*, vol. 128, No. 5, pp. 269-279, 1981.

- [8] C. T. Pan and C. M. Lian, "An adaptive controller for power system load frequency control," *IEEE Trans. on Power systems*, vol. 4, No. 1, pp. 122-128, 1989.
- [9] F. Beaufays, Y. A. Magid, and B. Widrow, "Applications of Neural Networks to load frequency control in power systems," *Neural Networks*, vol. 7, No. 1, pp. 183-194, 1994.
- [10] A. Demiroren, N. S. Sengor, and H. L. Zeynelgil, "Automatic generation control by using ANN technique," *Electric Power Components and Systems*, vol. 29, No. 10, pp. 883-896, 2001.
- [11] A. Demiroren, H. L. Zeynelgil, N. S. Sengor, "Automatic generation control for power system with SMES by using Neural Network controller," *Electric Power Components and Systems*, vol 31, pp. 1-25, 2003.
- [12] D. Rerkpreedapong, A. Feliachi, "PI gain scheduler for Load frequency control using spline techniques," *Proc. of the 35th south eastern symposium on system theory*, pp. 259-263, 2003.
- [13] W. C. Chan and Y. Y. Hsu, "Automatic generation control of interconnected power system using variable structure controller," *IEE Proc. Part C*, vol. 128, No.5, pp. 269-279, 1981.
- [14] A. Y. Sivarmakrishnan, M. V. Hariharan, and M. C. Srisailam, "Design of variable structure load frequency controller using pole assignment technique," *Int. Journal Control*, vol. 40, No.3, pp. 487-498, 1984.
- [15] A. Kumar, O. P. Malik, and G. S. Hope, "Variable structure system control applied to AGC of interconnected power system," *IEE Proc. Part C*, vol. 132, No. 1, pp. 23-29, 1985.

- [16] D. Das, M. L. Kothari, D. P. Kothari, and J. Nanda, "Variable structure control strategy to automatic generation control of interconnected reheat thermal system", *IEE Proc. Part D*, vol. 138, No. 6, 1991.
- [17] Z. Al-Hamouz and Y. Abdel-Magid, "Variable structure load frequency controllers for multiarea power systems," *International Journal of Electric Power and Energy Systems*, vol. 15, No. 5, pp. 293-300, 1993.
- [18] Yang Ming-Sheng, "Load frequency scheme for power systems using smoothed switching structure theory," *Proc. IEEE International symposium on Industrial electronics*, vol. 1, pp. 191-195, 2000.
- [19] Q. P. Ha, A fuzzy sliding mode controller for power system load frequency control, *Second international conference on knowledge-based intelligent electronic systems*, vol. 1, pp. 149-154, 1998.
- [20] Z. Al-Hamouz and H. N. Al-Duwaish, "A new load frequency variable structure controller using Genetic algorithms," *Electric Power Systems Research*, vol. 55, pp. 1-6, 2000.
- [21] Naji A. Al-Musabi, Z. M. Al-Hamouz, H. N. Al-Duwaish, Samir Al-Baiyat, Variable structure load frequency controller using the particle swarm optimization technique," *Proc. of the 10th IEEE International Conference on Electronics, Circuits and Systems*, pp. 380-383, 2003.
- [22] IEEE Standard 122-1991, *Recommended practice for functional and performance characteristics of control systems for steam turbine-generator units*, 1992.

- [23] A. Kumar, O. P. Malik, and G. S. Hope, "Variable structure system control applied to AGC of interconnected power system," *IEE Proceedings Part C*, vol. 132, No. 1, pp. 23-29, 1985.
- [24] D. Das, M. L. Kothari, D. P. Kothari, and J. Nanda, "Variable structure control strategy to automatic generation control of interconnected reheat thermal system," *IEE Proceedings Part D*, vol. 138, No. 6, 1991.
- [25] W. Peter Sauer and M. A. Pai, *Power System Dynamics and Stability*, Prentice Hall Inc., New Jersey, USA, 1998.
- [26] Y. N. YU, *Electric power system dynamics*, Academic press, 1983.
- [27] Y. H. Song, "Emerging techniques for power system dynamics stabilisation", *IEE colloquium on power system dynamics stabilisation*, London, pp. 12/1 -12/5, 1998.
- [28] J. W. Chapman, M. D. Ilic, C. C. King, L. Eng, H. Kanfman, "Stabilizing a multimachine power system via decentralized feedback linearizing excitation control," *IEEE Trans. Power Syst.*, vol. 8, No. 3, pp. 830-838, 1993.
- [29] X. Y. Li, Y. H. Song, X. C. Liu, J. Y. Liu, "A nonlinear optimal-variable-aim strategy for improving multimachine power system transient stability," *IEE Proceedings- Generation, Transmission, and Distribution*, vol. 143, No. 3, pp. 249-252, 1996.
- [30] Q. Lu and Y. Sun, "Decentralized nonlinear optimal excitation control," *IEEE Transactions on Power Systems*, vol. 11, No. 4, pp. 1957-1962, 1996.

- [31] Y. Z. Sun, X. Li, S. Yan, Y. H. Song, M. M. Farsangi, "Novel Decentralized Robust Excitation control for Power System Stability Improvement," *IEEE International Conference on Electric Utility Deregulation and Restructuring and Power Technologies*, pp. 443-449, 2000.
- [32] Q. Lu and Y. Z. Sun, *Nonlinear control of power system*, Science publishing house, 1993.
- [33] Y. Hsu and C. Cheng, "Tunning of power system stabilizers using an artificial neural network," *IEEE Transactions on Energy Conversion*, vol. 6, pp. 612-619, 1991.
- [34] Y. Park, S. Hyum, J. Lee, "A synchronous generator stabilizer design using neuro inverse controller and error reduction network," *IEEE Transactions on Power Systems*, vol. 11, No. 4, pp. 1969-1975, 1996.
- [35] D. Kennedy and V. Quitana, "Neural network regulator for synchronous machines," *Proceedings of the IFAC world congress*, vol. 5, pp. 131-136, 1993.
- [36] M. Hassan, O. P. Malik, G. S. Hope, "A fuzzy logic based stabilizer for a synchronous machine," *IEEE Transactions on Energy conversion*, vol 6, No. 3, pp. 407-413, 1992.
- [37] A. Elshafei and K. El-Metwally, "Power system stabilization via adaptive fuzzy logic control," *Proceedings of the 12th IEEE International symposium on intelligent control*, pp. 89-94, 1997.

- [38] V. Samarasinghe and N. Pahalawaththa, "Damping of multimodal oscillations in power systems using variable structure control techniques," *IEE Proceeding- Generation, Transmission, and Distribution*, vol. 144, No. 3, pp. 323-331, 1997.
- [39] H. N. Al-Duwaish and Z. Al-Hamouz, "Adaptive Variable structure controller using neural networks," *Conference Record of the 2000 IEEE Industry Applications*, vol. 2, pp. 954-958, 2000.
- [40] K. Ohtsuka, T. Taniguchi, T. Sato, S. Yokokawa, Y. Ueki, "A H_∞ optimal theory-based generator control system," *IEEE Transactions on EC*, vol. 7, No.1, pp.108-113, 1992.
- [41] R. Marino, "An example of a nonlinear regulator," *IEEE Transactions on Automatic Control*, vol. AC-29, No. 2, pp. 276-279, 1984.
- [42] M. D. Ilic and F. K. Mak, "A new class of fast voltage controllers and their impact on improved transmission capacity," *Proceedings of 1989 American Control Conference*, Pittsburgh, PA, vol. 2, pp. 1246-1251, 1989.
- [43] Y. Wang, L. Xie, D. J. Hill, R. H. Middleton, "Robust nonlinear controller design for transient stability enhancement of power systems," *Proceedings of 31st Conference of Decision Control*, Tucson, AZ., pp. 1117-1122, 1992.
- [44] J. W. Chapman and M. D. Ilic, "Some robustness results for feedback linearizing control of generator excitation," *Proceedings of 31st Conference Decision Control*, Tucson, AZ, pp. 1123-1128, 1992.
- [45] Sandeep Jain, Farshad, Khorrami, B. Fardanesh, "Adaptive nonlinear excitation control of power systems with unknown Interconnections," *IEEE Transactions on Control Systems Technology*, vol. 2, No. 4, 1994.

- [46] Y. Y. Wang, D. J. Hill, "Transient stabilization of power systems with an adaptive control law," *Automatica*, vol. 30, No. 6, pp.1409-1413, 1994.
- [47] T. Lahdhiri and A. T. Abuani, "Design of nonlinear excitation controller for a synchronous generator using the concept of exact stochastic feedback linearization," *Proceedings of American Control conference*, Albuquerque, NM, USA, pp. 1963-1967, 1997.
- [48] Y. J. Cao, L. Jiang, S. J. Cheng, O. P. Malik, "A nonlinear variable structure stabiliser for power system stability," *IEEE Transactions Energy conversion*, vol. 9, No. 3, pp.489-496, 1994.
- [49] W. Mielczarski and A. M. Zajackowski, "Nonlinear field voltage control of a synchronous generator using feedback linearization," *Automatica*, vol. 30, No. 10, pp.1625-1630, 1994.
- [50] J. T. Moura, H. Elmali, N. Olgac, "Sliding mode control with sliding perturbation observer," *Journal of Dynamics Systems, Measurement, and Control*, vol. 119, No. 4, pp. 657-665, 1997.
- [51] L. Jiang, Q. H. Wu, J. Wang, C. Zhang, X. Y. Zhou, "Robust observer-based nonlinear control of multimachine power systems," *IEE Proceedings-Generation, Transmission, Distribution*, vol. 148, No. 6, 2001.
- [52] K. Fregene and D. Kennedy, "Stabilizing control of a high-order generator model by adaptive feedback linearization," *IEEE Transactions on Energy Conversion*, vol. 18, No.1, 2003.
- [53] W. C. Chan and Y. Y. Hsu, "Optimal control of electric power generation using variable structure controllers," *Electric power system research*, No. 6, pp. 269-278, 1983.

- [54] W. C. Chan and Y. Y. Hsu, "An optimal variable structure stabilizer for power system stabilization," *IEEE Transactions on Power apparatus and systems*, vol. PAS-102, No. 6, pp. 1738-1746, 1983.
- [55] Y. Y. Hsu and W. C. Chan, "Stabilization of power systems using variable structure stabilizer," *Electric power systems research*, No. 6, pp. 129-139, 1983.
- [56] N. N. Bengiamin and W. C. Chan, "Variable structure control of electric power generation," *IEEE Transactions on Power apparatus and systems*, vol. PAS-101, No. 2, pp.376-380, 1982.
- [57] R. J. Fleming and Jun Sun, "An optimal variable structure stabilizer for a synchronous generator," *International Journal of Power and Energy systems*, vol. 12, No. 1, 1992.
- [58] Bhattacharya, M. Kothari, and J. Nanda, "Design of discrete mode variable structure power system stabilizers," *International Journal Electric Power and Energy Systems*, vol. 17, No. 6, pp. 399-406, 1995.
- [59] Kumar, O. P. Malik and G. S. Hope, "Discrete variable structure for load frequency control of multiarea interconnected power systems," *IEE Proceedings- Generation, Transmission, and Distribution*, vol. 134, No. 2, pp. 116-122, 1987.
- [60] Abdel-Magid, Z. Al-Hamouz and J. Bakhawain, "A variable-structure stabilizer for wind turbine generators," *Electric Power Systems Research*, vol. 33, pp. 41-48, 1995.

- [61] Samarasinghe and N. Pahalawatha, "Damping of multimodal oscillations in power systems using variable structure control technique," *IEE Proceedings-, Generation, Transmission, and Distribution*, vol. 144, No. 3, pp. 323-331, 1997.
- [62] T-L Chern, J. Chang, G-K. Chang, "DSP-based integral variable structure model following control for brushless DC motor drivers," *IEEE Transactions Power Systems*, vol. 12, No.1, pp. 53-63, 1997.
- [63] T-L Chern, C-S Liu, C-F Jong and G-M Yan, "Discrete integral variable structure model following control for induction motor drivers," *IEE Proceedings- Electric Power Applications*, vol. 143, No. 6, pp. 467-474, 1996.
- [64] Murty, S. Parameswaran, K. Ramar, "Design of decentralized variable structure stabilizers for multimachine power systems," *International Journal Electric Power and Energy Systems*, vol.18, No. 8, pp. 535-546, 1996.
- [65] X.-Y. Lu, S. Spurgeon, I. Postlethwaite, "Robust variable structure control of a PVTOL aircraft," *International Journal of Systems Science*, vol. 28, No. 6, pp. 547-558, 1997.
- [66] Innocenti and A. Thukral, "Robustness of a variable structure control system for maneuverable flight vehicles," *Journal of Guidance, Control, and Dynamics*, vol. 20, No. 2, pp. 377-383, 1997.
- [67] M. Steinberg Singh and R. DiGirolamo, "Variable structure robust flight control system for the F-14," *IEEE Transactions Aerospace and Electronic Systems*, vol. 33, No. 1, pp. 77-84, 1997.
- [68] Zribi, L. Huang and S. Chan, "Variable structure control of two manipulators handling a constrained object," *Cybernetics and Systems*, vol. 28, No. 4, pp. 263-286, 1997.

- [69] Lee, S. Coates and V. Coverstone-Carroll, "Variable structure control applied to underactuated robots," *Robotica*, vol. 15, No. 3, pp. 313-318, 1997.
- [70] Itkis, *Control systems of variable structure*, Keter Publishing House, Jerusalem, 1976.
- [71] Utkin and K. Yang, "Methods for constructing discontinuity planes in multidimensional variable structure systems", *Automatic and Remote Control*, vol. 39, pp. 1466-1470, 1978.
- [72] Utkin I. V., "Variable Structure systems with sliding modes: Survey Paper," *IEEE Transactions on Automatic control*, vol .AC-22, No. 2, pp. 212-222, 1977.
- [73] V. I. Utkin, "Sliding Modes and Their Applications in Variable Structure Systems," *MIR*, Moscow, 1978.
- [74] Chung Se-Kyo, "Integral Variable Structure Controller for Current Control of PWM Inverter-Fed AC Drives," *Electric Machines and Power Systems*, vol. 27, pp. 753-769, 1999.
- [75] T. L. Chern and Y. C. Wu, "Design of brushless DC position servo systems using integral variable structure approach," *IEE Proceedings Part B*, vol. 140, No. 1, pp. 27-34, 1993.
- [76] S. K. Chung, J. H. Lee, and M. J. Youn, "A robust speed control of brushless direct drive motor using integral variable structure control with sliding mode observer," *Conference Records of IEEE IAS Annual Meeting*, pp.393-400, 1994.

- [77] Raymond A. DeCarlo, Stanislaw H. Zak, and Gregory P. Matthews, "Variable Structure Control of Nonlinear Multivariable Systems: A Tutorial," *Proceedings of the IEEE*, vol. 76, No. 3, 1988.
- [78] R. S. Ortega, M. D. Espana, and J. J. Espino, "Variable Structure systems with chattering reduction: a microprocessor based design," *Automatica*, vol. 20, No.1, pp. 133-134, 1984.
- [79] M. J. Corless and G. Leitmann, "Continuous state feedback guaranteeing uniform ultimate boundedness for uncertain dynamic systems," *IEEE Transactions Automatic Control*, vol. AC-26, No. 5, pp. 1139-1144, 1981.
- [80] Shaikh Khasimul Mukarram, Variable Structure Control of Nonlinear Systems, *M. Sc. Thesis*, 1998.
- [81] G. Celentano, G. Ambrosino, F. Garofalo, "Variable structure model reference adaptive control systems," *International Journal of Control*, vol. 39, No. 6, 1984.
- [82] R. S. Ortega, M. D. Espana, J. J. Epsino, "Variable Structure systems with chattering reduction: a microprocessor based design," *Automatica*, vol. 20, No.1, pp. 122-134, 1984.
- [83] F. H. F. Leung, L. K. Wong, P. K. S. Tam, "Algorithm for eliminating chattering in sliding mode control," *IEE Electronics Letters*, vol. 32, No. 6, pp. 599-601, 1996.
- [84] G. P. Matthews, R. A. Decarlo, P. Hawley, S. Lefebvre, "Toward a feasible variable structure control design for a synchronous machine connected to an infinite bus," *IEEE Transactions on Automatic control*, vol. AC-31, No. 12, 1986.

- [85] John Y. Hung, Weibing Gao, and James C. Hung, "Variable structure control: A survey," *IEEE Transactions on Industrial Electronics*, vol. 40, No. 1, 1993.
- [86] Sadiq M. Sait and Habib Youssef, *Iterative Computer Algorithms with Applications in Engineering (Solving Combinational Optimization Problems)*, IEEE Computer Society Press, Los Alamitos, California, 1999.
- [87] J. H. Holland, *Adaptation in Natural and Artificial Systems*, University of Michigan Press, Ann Arbor, Michigan, 1975.
- [88] D. Goldberg, *Genetic Algorithms in Search Optimization and Machine Learning*, Addison-Wesley, 1989.
- [89] D. C. Walters and G. B. Sheble, "Genetic algorithm solution of economic dispatch with valve point loading," *IEEE Transactions on PWRs*, vol. 8, no. 3, pp. 1325–1332, 1993.
- [90] P. H. Chen and H. C. Chang, "Large-scale economic dispatch by genetic algorithm," *IEEE Transactions on PWRs*, vol. 10, no. 4, pp. 1919–1926, 1995.
- [91] D. Dasgupta and D. R. McGregor, "Thermal unit commitment using genetic algorithms," *IEE Proceedings—Generation, Transmission, and Distribution*, vol. 141, no. 5, pp. 459–465, 1994.
- [92] K. Iba, "Reactive power optimization by genetic algorithm," *IEEE Transactions on PWRs*, vol. 9, no. 2, pp. 685–692, 1994.

- [93] K. Y. Lee and F. F. Yang, "Optimal reactive power planning using evolutionary algorithms: A comparative study for evolutionary programming, evolutionary strategy, genetic algorithm, and linear programming," *IEEE Transactions on PWRs*, vol 13, no. 1, pp. 101–108, 1998.
- [94] R. Dimeo and K. Y. Lee, "Boiler–Turbine control system design using a genetic algorithm," *IEEE Transactions on Energy Conversion*, vol. 10, no. 4, pp. 752–759, 1995.
- [95] Y. Zhao, R. M. Edwards, and K. Y. Lee, "Hybrid feedforward and feedback controller design for nuclear steam generators over wide range operation using genetic algorithm," *IEEE Transactions on Energy Conversion*, vol 12, no. 1, pp. 100–106, 1997.
- [96] Yoshikazu Fukuyama and Hsaio -Dang Chang, "A Parallel Genetic Algorithm for Generation Expansion Planning," *International Conference on Intelligent System Application on Power System: ISAP'94*, Montpellier, France, September, 1994.
- [97] Kennedy J. and Eberhart R., "Particle Swarm Optimization," *IEEE International Conference on Neural Networks*, vol 4, pp. 1942 -1948, 1995.
- [98] Eberhat and Yuhui Shi, "Particle Swarm Optimization: developments, applications, and resources," *Proceedings of the 2001 Congress on Evolutionary Computation*, vol. 1, pp. 81-86, 2001.
- [99] F. Glover, "Tabu Search-Part I," *ORSA Journal on Computing*, vol. 1, No. 3, pp. 190-206, 1989.
- [100] F. Glover, "Tabu Search-Part II," *ORSA Journal on Computing*, vol 2, No.1, pp. 4-32, 1990.

- [101] F. Glover and M. Laguna, *Tabu Search*, Kluwer Academic Publisher, Boston, 1997.
- [102] John J. Grainger, Jr. William D. Stevenson, *Power system analysis*, McGraw-Hill Inc., International Edition, Singapore, 1994.
- [103] IEEE Standard 122-1991, *Recommended practice for functional and performance characteristics of control systems for steam turbine-generator units*, 1992.
- [104] L. Hari, M. L. Kothari, J. Nanda, "Optimum selection of speed regulation parameters for automatic generation control in discrete mode considering generation rate constraints," *IEE proceedings-Part C*, vol 138, No. 5, pp. 401-406, 1991.
- [105] T. C. Yang and H. Cimen, "Applying structured singular values and a new LQR design to robust decentralized power system load frequency control," *Proceedings of the IEEE international conference on industrial technology*, pp. 880-884, 1996.
- [106] C. Concordia, L. K. Kirchmayer, E. A. Szymanski, "Effect of speed-governor dead band on tie-line power and frequency control performance," *American Institute of Electrical Engineers Transactions*, vol 76, pp. 429-435, 1957.
- [107] A. Demiroren and E. Yesil, "Automatic generation control with fuzzy logic controllers in the power system including SMES units," *Electrical Power and Energy Systems*, vol 26, pp. 291-305, 2004.
- [108] S. C. Tripathy, R. Balasubramanian, P. S. Chandramohan Nair, "Effect of superconducting magnetic energy storage on Automatic generation control considering governor dead band and boiler dynamics," *IEEE Transactions on Power systems*, vol 7, No. 3, 1992.

- [109] Y.N. Yu and H. A. M. Moussa, "Optimal stabilization of a multimachine system," *IEEE Transactions on Power Apparatus and Systems*, PAS-91, pp. 1174-1182, 1972.
- [110] F. P. Demello and C. Concordia, "Concepts of synchronous machine stability as affected by excitation control," *IEEE Transactions on Power Apparatus and Systems*, PAS-88, pp. 316-329, 1969.
- [111] N. C. Pahalawaththa, G. C. Hope, O. P. Malik, "Multivariable self-tuning power system stabilizer, simulation and implementation studies," *IEEE Transactions*, EC-6, pp.310-319, 1991.
- [112] Y. Cao, L. Jiang, S. Cheng, D. Chen, O. P. Malik, G. S. Hope, "A nonlinear variable structure stabilizer for power system stability," *IEEE Transactions on Energy Conversion*, vol 9, pp.489-495, 1994.
- [113] T. Hiyama and T. Sameshima, "Fuzzy logic control scheme for on-line stabilization of multimachine power system," *Fuzzy sets systems*, vol 39, pp. 181-194, 1991.
- [114] D. A. Pierre, "A perspective of adaptive control of power system," *Electric power system and research*, vol.2, pp.423-426, 1987.
- [115] A. Ghosh, G. Ledwich, O. P. Malik, G. S. Hope, "Power system stabilizer based on adaptive control techniques," *IEEE Transactions on Power Apparatus and Systems*, vol. PAS-103, pp. 1983-1989, 1984.
- [116] G. P. Matthews, R. A. Decarlo, P. Hawley, S. Lefebvre, "Toward a feasible variable structure control design for a synchronous machine connected to an infinite bus," *IEEE Transactions on Automatic Control*, vol. AC-31, No. 12, pp. 1159-1163, 1986.

- [117] S. Lee and J. Park, "Design of power system stabilizer using observer/sliding mode, observer/sliding mode model following and H_{∞} / sliding mode controllers for small signal stability study," *Electrical Power and Energy Systems*, vol 20, No. 8, pp. 543-553, 1998.
- [118] Y. Wang, R. Zhou, and C. Wen, "Robust load-frequency controller design for power systems," *IEE. Proc. C*, vol. 140, pp. 11-16, 1993.

Vita

- Naji A. AlMusabi
- Born in Abu Dhabi, United Arab Emirates
- Received Bachelor's degree in Electrical and Electronics Engineering from the American University of Sharjah in May 2001
- Completed Master's degree requirements at King Fahd University of Petroleum and Minerals in June 2004